2010

Recent advances in glylons science

Cornelia Rosu
Louisiana State University and Agricultural and Mechanical College, crosu1@tigers.lsu.edu

RECENT ADVANCES IN GLYLONS SCIENCE

A Thesis

Submitted to the Graduate Faculty of the
Louisiana State University and
Agricultural and Mechanical College
in partial fulfillment of the
requirements for the degree of
Master of Science

in

The Department of Chemistry

by
Cornelia Rosu
B.S., University ”Al. I. Cuza”, Iasi, Romania, 1996
May 2010

ACKNOWLEDGMENTS

There are many people whom I would like to thank and to express my gratitude for support and assistance during the first two years of doctoral program at Louisiana State University. I would especially like to begin with Professor Paul S. Russo, William H. Daly and Ioan I. Negulescu for their generous time and enthusiasm. Throughout this time they encouraged me to refine my research skills necessary to complete this project for the master thesis. Dr. Mathew Brown deserves my special thanks for assisting me in Socolofsky lab (Life Science Building) to use the microscopes and to do the measurements. To Drs. Rafael Cueto and Ionela Glover I address infinitely appreciation for their time spent to train me different techniques necessary to complete this thesis. I would like also to thank Professor Roger Laine and Professor John Pojman for their time and encouragement.

I am grateful to Center for Advanced Microstructure & Devices for allowing me to use their equipment in order to conduct a part of my investigations.

I especially appreciate Louisiana State University for allowing me to be a part of the first class research community.

I infinitely value the moral support and encouragement of my family and friends: my mother Leontina and my father Pavel, my uncle Simioan Petrovan and his dear wife Daniela Petrovan (Knoxville, USA), my cousins Simona and Ovidiu Romanoschi (New Jersey, USA), my dear friends Daniela and George Slevoaca (Lyon, France), and Luminita Damian (Quebec, Canada).

Finally, I would like to thank all of the professors, colleagues from both group research, all my friends and family members who assisted me along to complete this work and this dissertation. Their contribution is too complex and diverse to describe in a few short paragraphs.

TABLE OF CONTENTS

LIST OF TABLES

LIST OF FIGURES

LIST OF SCHEMES

LIST OF ABBREVIATIONS AND SYMBOLS

Å	Angstrom
BMIMCl	1-butyl-3-methyl-imidazolium chloride
°C	Celsius degree
COSY	Correlation Spectroscopy
DDSC	Derivative of heat flow
DEX	Diethyl xylarate
DMSO	Dimethylsulfoxide
DMT	Dimethyl tartrate
DP	Degree of polymerization
DPA	1,3-propylene diamine
DRI	Detector response intensity
DSC	Differential Scanning Calorimetry
DTG	Derivative of weight loss
EG	Ethylene glycol
Equiv	Equivalent
Exo	Exothermic
FTIR	Fourier Transformer Infrared Spectroscopy
GalEt_hexa	*P*oly(2,3:4,5-bis-O-isopropylidene-1,3-propylidene-galactamide)
GalEt_hexaunpr	*P*oly(hexamethylene galactamide)
GalEt_prop	Poly(2,3;4,5-bis-O-isopropylidene-1,3-propylidene-galactamide)
GalEt_propunpr	Poly(propylene galactamide)
GC/MS	Gas Chromatography Mass Spectometry
GluEt_hexa	Poly(3,4-mono-O-isopropylidene-1,3-propylidene-D-glucaramide)
GluEt_prop	Poly(3,4-mono-O-isopropylidene-1,3-propylidene-D-glucaramide)

Gly	Glylon
GPC	Gel Permeation Chromatography
h	Hour
HMDA	*H*examethylene diamine
hMw	High molecular weight
Hz	Hertz
I	Intensity
IAA	Indolacrylic acid
Iso-PrOH	Isopropylene alcohol
J	Joule
k	Rate constant
KDa	Kilo dalton
Lac	Lactone
Log	Logarithm (10 base)
[M]	Mass unit
MALDI-TOF	Matrix Assisted Laser Desorption/Ionization Time of Flight
Me_2SO-d_6	*D*euterated dimethylsulfoxide
MeOH	Methanol
MHz	Megahertz
Min	Minute
Mol	Molar
mW	Miliwatt
n, x	Number of repeating units
nm	Nanometer
NMMO	N-morpholine-N-oxide

NMR	Nuclear Magnetic Resonance
PF	Pullulan
PHPA	Polyhydroxypolyamides
ppm	Part per million
PVA	Polyvinyl alcohol
PVP	Polyvinyl pyrolidone
q	Magnitude of scattering vector
ROH	Aliphatic alcohol
s	Second
SAXRD	Small Angle X-ray Diffraction
SAXS	Small Angle X-ray Scattering
SEC	Size Exclusion Chromatography
t	Time
t-butyl	Tert butyl
T_c	Temperature of crystalline transition
TFK	1,1,1-trifluroacetone
T_g	Temperature of glass transition
TGA	Thermogravimetric Analysis
THF	Tetrahydrofuran
T_m	Temperature of melting transition
u	Unit
V_e	Elution volume
WAXS	Wide Angle X-ray Scattering
δ	Chemical shift
μm	Micron

ABSTRACT

A variety of sugar- based polyamides called *glylons* were synthesized by using different pathways. The sugar- units were derived from D- glucaric acid and D-galactaric acid. Glylons D-glucaric- based with pendant free hydroxyl groups showed a low solubility in organic solvents, due to hydroxyl preference to form strong intra- and intermolecular H- bonding. To minimize these interactions an acetalation reaction was performed. Monoacetalated D-glucaric-based polymers exhibited a better solubility in a broader range of solvents but the residual hydroxyl groups favored aggregation. Completely blocked bis-acetalated galactaric-based glylons are soluble in a broad range of solvents including toluene/methanol mixtures. Deprotection reaction performed with hydrofluoric acid led to the initial problem of solubility.

A combination of techniques such as FTIR, ^{1}H, ^{13}C, COSY NMR, MALDI-TOF, GPC, DSC and TGA were employed to characterize the synthesized glylons. The course of the polymerization reaction was monitored with FTIR and NMR. Cyclic and linear species were identified with MALDI-TOF mass spectrometry. The cyclization leads to premature termination and only low molecular weight glylons can be isolated. The ratio linear to cyclic varies for glylons with both odd-carbon numbered and even-carbon numbered diamines. Glylons bearing propylene diamine units have a higher ratio of linear species when compared with glylons having hexamethylene diamine units. These conformers were identified also by GPC, DSC and TGA. Furthermore, GPC technique suggests the existence of a higher molecular weight polymer fraction. Thermal analysis pointed out that glylons are low crystalline polymers.

Organized patterns resembling *tree-rings* were found to form in solutions of deprotected glylons (gly-6, 6 and GalEt_unpr) in NMMO monohydrate and BMIMCl. The investigation of their morphologies was performed with optical, polarized light and confocal microscopy,small/wide angle light scattering as well. The thickness of the rings was noted to be

highly influenced by the concentration, temperature, viscosity and the surface available for growth.

In dimethylsulfoxide deprotected galactaric glylons were found to form gels.

CHAPTER 1 INTRODUCTION

1.1 General Aspects

The need for development of new industrial processes that involves monosaccharides is one of the reasons of this work. Monosaccharides, oligosaccharides and polysaccharides are available from agriculture resources. The compounds of primary commercial interest are D-glucose, D-xylose and D-galactose. Hydrolysis of starch or sucrose (sugar) is the main source of these compounds. Annually billions of pounds of "liquid dextrose" are produced particularly in United States. Yet dextrose remains a largely untapped chemical reservoir for novel, major scale industrial synthetic processes generating new and useful biodegradable materials.

1.2 Synthesis of Classic Nylons

Synthetic polyamides or nylons are polyamides obtained either by condensation of diamines with organic diacids or by polymerization of lactames. The basic sources for nylon monomers are petrochemicals. Classic polyamides have good tenacity and abrasion resistance. Yet, due to absence of hydrophilic groups in their chemical composition (e.g. hydroxyl group, -OH) and hence low water absorbency, nylons are rather low comfort materials. Furthermore the lack of hydrophilic units makes nylons non-biodegradable.

Nylon-6, 6 is synthesized by condensation of adipic acid ($HOOC\text{-}(CH_2)_4\text{-}COOH$) with hexamethylene diamine [$H_2N\text{-}(CH_2)_6\text{-}NH_2$] (Scheme 1.1). Even though the polymer has good qualities in terms of durability and strength, it still has limited water absorbency properties as expected.

1.3 Synthesis of Polyhydroxylated Nylons-*Glylons*

A new class of nylon-like materials can be obtained by substituting the diacids from nylons with aldaric acids. Aldaric acids are obtained by oxidation of sugars. Oxidation of D-glucose gives glucaric acid ($HOOC\text{-}(CH\text{-}OH)_4\text{-}COOH$) (Scheme 1.2**)**.[1]

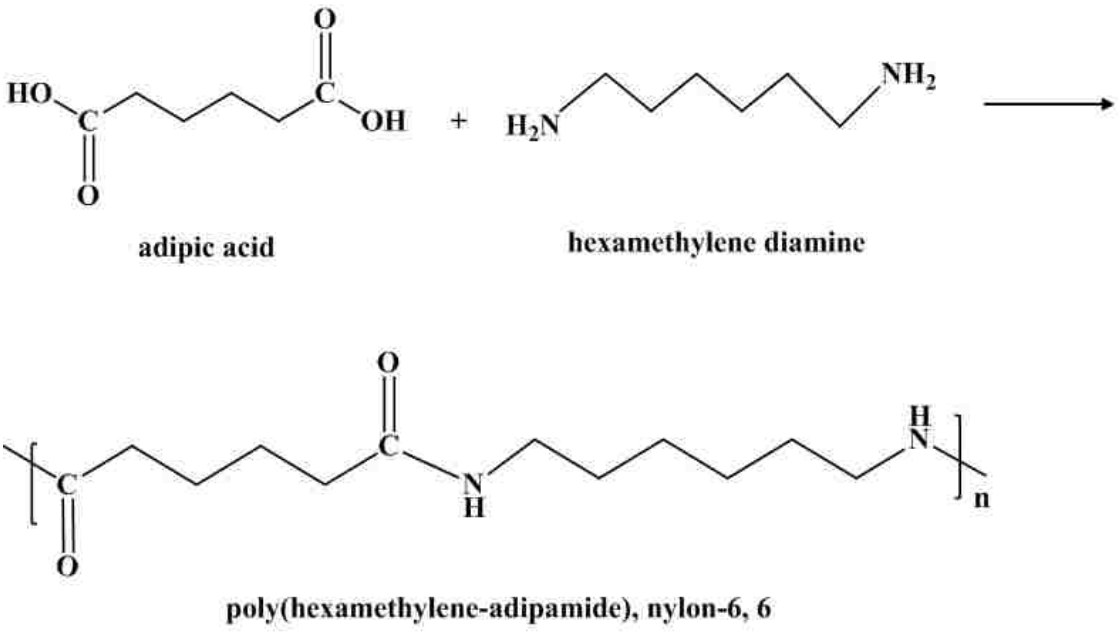

Scheme 1.1 Synthesis of Nylon-6, 6

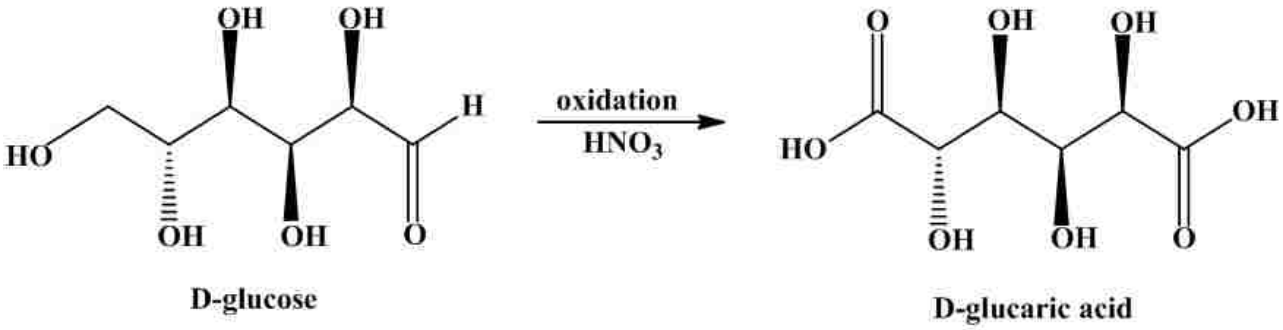

Scheme 1.2 Preparation of D-glucaric acid from D-glucose

Further glucaric acid is used as monomer precursor capable to polymerize with diamines. The new type of polyamide has four hydroxyl groups. By similarity with classic nylons this class of polymers is called *Glylons*.[2] Glylons would be expected to have the strength of nylons. Plus, the new polymers will be environmentally friendly, biodegradable.

First studies performed on monosaccharides were reported by Ogata and coworkers.[3-10]

The pioneer study was performed on L-tartarate. Dimethyl L-tartarate underwent polymerization reaction with hexamethylene diamine in solutions under mild conditions (30ºC) to form polyamides having pendant hydroxyl groups.[10] Diethyl esters of mucic (galactaric) acid were found to have high reactivity toward condensation with diamines but the obtained polyamides had low molecular weights.[11] More studies were focused on the influence of the solvent and polymer matrices such as poly(vinyl pyrolidone) (PVP), Pullulan (polysaccharide) (PF) and poly(vinyl alcohol) (PVA) on the rate of polycondensation. The rate enhancement was found to be directly proportional with the molecular weight of the polymer matrix.[11] However it was not clear how matrices influence the molecular weight of the polyamides. These polyamides with pendant groups were partially soluble in dimethylsulfoxide (DMSO). The reaction of dimethyl tartrate (DMT) with hexamethylene diamine (HMDA) in the presence of poly(vinyl alcohol) (PVA) caused gelation within 4 h[11] (Figure 1.1). Dilute solutions of L-tartaramides in addition to PVA

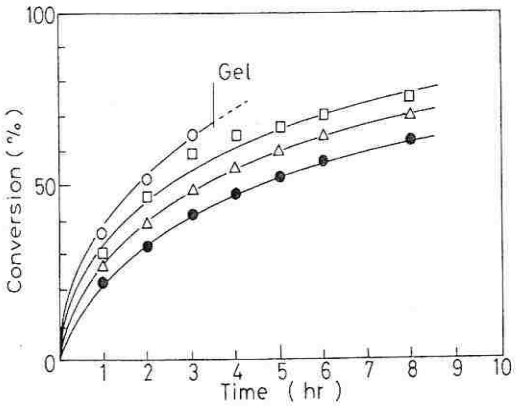

Figure 1.1 Polycondensation of DMT with HMDA in the presence of PVA in DMSO at 60ºC: monomer concentration: 0.5 mole/dm^3; concentration of PVA unit: 1.0 mole/dm^3; (●) none, (◘) PVA-2 (22 KDa), (○) PVA-7 (66 KDa), PVA-9 (88 KDa), (△) iso-PrOH, EG (ethylene glycol), glycerol.[11]

didn't exhibit such phenomena due to poor solubility in DMSO. It was concluded that the polycondensation of DMT with HMDA in the presence of polymer matrices gave increased molecular weight polymers. When polymerization was performed in DMSO and PVA as matrix,

gelation phenomenon occurred due to polymer complex formation.[11]

Similar studies on sugars were performed by Hoagland *et al.*[12-15] Their main interest was to investigate the intermediate γ-lactones found to form during aminolysis of diethyl galactarate. They were able to establish the reaction sequence for the competitive, second- order kinetics (k_1= k_2 can be applied) (Figure 1.2) by ^{13}C NMR spectroscopy (Table 1-1).

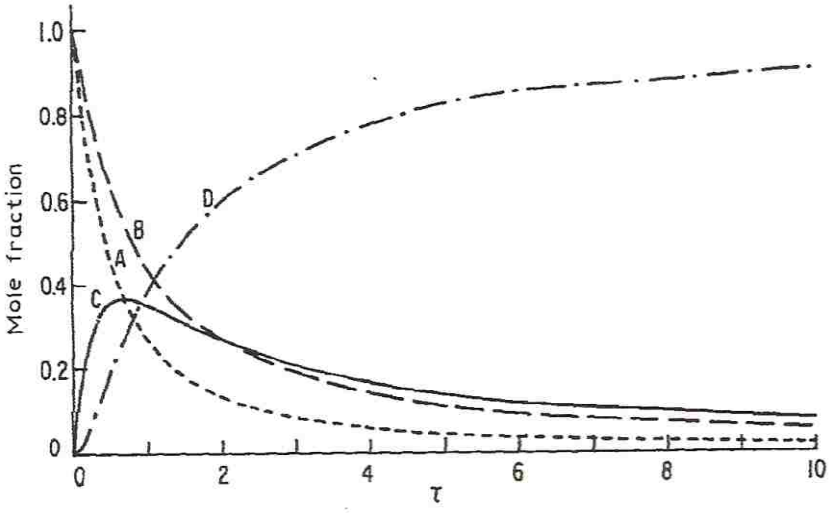

Figure 1.2 Theoretical plots for reactants in a competitive, consecutive, second-order reaction [A= 2-aminoethanol (A/A_0); B= 6- ethyl galactarate-(1,4-lactone) (B/B_0); C= galactaric 1-amide-6,3-lactone (C/B_0) and D= galactaric 1,6-diamide (D/B_0), where A_0- initial concentration of 2-aminoethanol (A_0= $2B_0$) and B_0- initial concentration of 6-ethyl galactarate-1,4-lactone (B_0=0.13 M)], $\tau = kB_0t$ and $k= k_1= k_2$ the rate constants for aminolysis of lactones[13]

It was apparent that the aminolysis of diethyl galactarate is carried out through intermediate species, lactones, previously reported by Ogata for diethyl L-tartrate or diethyl adipate. Both studies concluded that lactones are capable to react readily with diamines. However their statement is based on the observation made on the polymerizations performed when hydroxyl groups are free or protected with isopropylidene groups (the rate of reaction is lower due to the diester incapacity to form lactones. The same behavior was found for the diethyl xylarate (DEX) although the aminolysis differs: for DEX the reaction is complete within 4 h whereas diethyl galactarate requires 18 h for completition under the same conditions.[13]

Table 1-1 Relative intensities of ^{13}C resonances of reaction species during the 2-aminoethanolysis of diethyl galactarate in Me_2SO-d_6 at 31ºC.[12] To the original drawing from Reference 12, the chemical structures drawn with ChemDraw software were added.

Compound	Species	δ (p.p.m.)	Time (min) 1	10	22	52	112	174	367	360	540	780	1080	1500
1	C-1 (6)	173.67	35	0										
	C-2 (5)	71.25	50	13	0									
	C-3 (4)	70.15	56	18	0									
	C-7 (9)	60.15	60	20	0									
2	C-6	174.13	0	14	11	11	0							
	C-1	171.46	0	16	16	12	0							
	C-4	80.48	0	30	30	23	13	12	0					
	C-2	73.59	0	32	34	24	17	0						
	C-3	72.29	0	32	29	23	14	9	0					
	C-5	67.36	0	29	31	20	13	11	0					
	C-7	60.86	0	36	34	22	15	10	0					
4	C-1	174.32				0	9	14	13	13	9	0		
	C-6	171.14				0	9	12	11	11	8	0		
	C-3	80.22				0	14	17	17	15	12	13	9	0
	C-5	73.72				0	17	18	21	15	14	12	10	0
	C-4	72.49				0	12	16	16	14	13	13	10	0
	C-2	68.07				0	13	14	18	15	10	12	8	0
	C-8	59.69			0	9	16	18	20	18	17	17	14	0
5	C-1 (6)	173.54					0	16	26	31	41	49	53	49	46
	C-2 (3) (4) (5)	70.73				0	12	26	41	51	59	73	80	80	86
	C-7 (9)	41.18				0	20	27	33	38	50	58	53	52	60
	C-8 (10)	59.95					0	19	27	27	43	55	55	59	56
c	C-1	63.33	62	48	53	40	34	30	25	25	21	16	15	10
	C-2	44.17	54	52	56	46	35	35	31	24	20	19	15	0

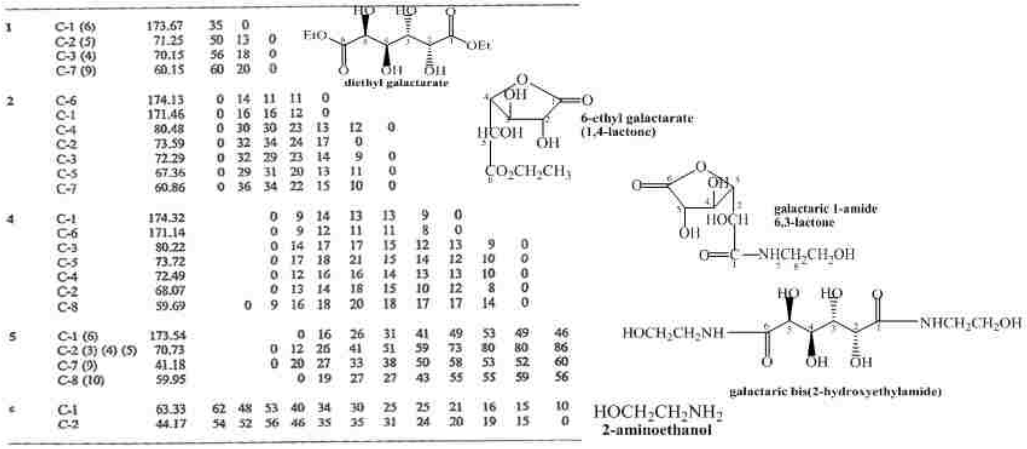

Kiely *et al.* came with further understanding of the polymerization mechanism.[16-21] They described the condensation of aldaric acids with different diamines including mostly with an even number of carbons. The synthesis follows two major steps: formation of dialkyl ester and aminolysis of activated five- or six-carbon aldaric acid diesters (mono and dilactones). First a mixture of linear and cyclic esters (lactones) is prepared by direct acidification/esterification of potassium D-glucarate in alcohol solution. This step was conducted under anhydrous conditions. To remove KCl formed, the solution was filtered and the filtrate concentrated to syrup. The syrup was dissolved in fresh methanol and the pH of the D-glucaric acid diester and lactone mixture was adjusted from acidic to basic with triethylamine. The basic solution was then used for direct polymerization with diamines. To the alcoholic solution of activated D-glucaric acid monomers a stoichiometric amount of alkyledene diamine was added and the mixture refluxed several hours. The polymer, which began to precipitate within 15 minutes, was separated by filtration and washed with alcohol (methanol) (Scheme 1.3**)**. The lactones and dilactone were considered

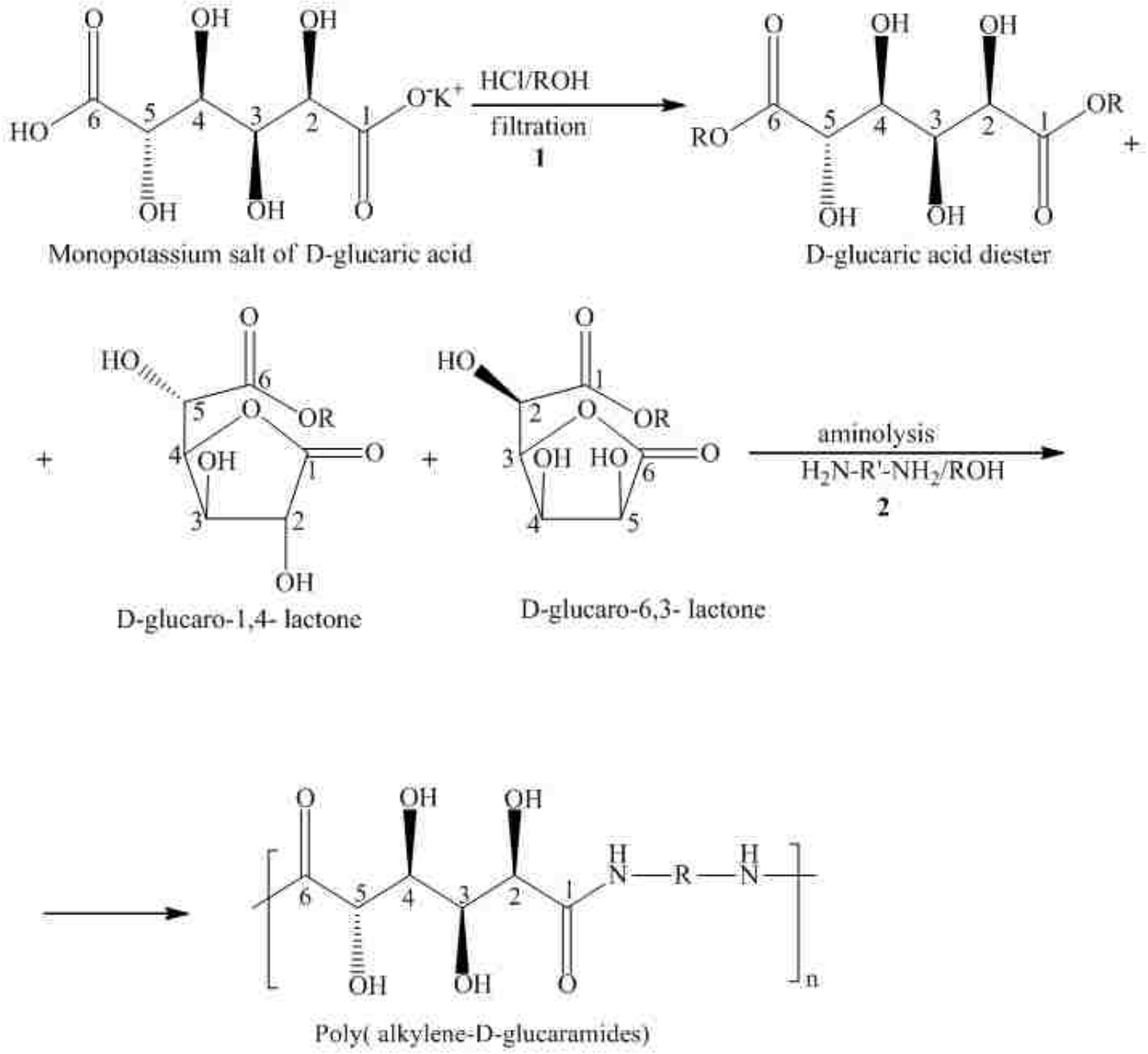

Scheme1.3 General mechanism of poly (alkylene-D-glucaramide) synthesis

suitable alternative monomer to the linear one. For example, dilactone was prepared by melting the monolactones/ester at reduced pressure while removing the alcohol. Then the dilactone was crystallized from a concentrated acetone solution (Scheme 1.4).

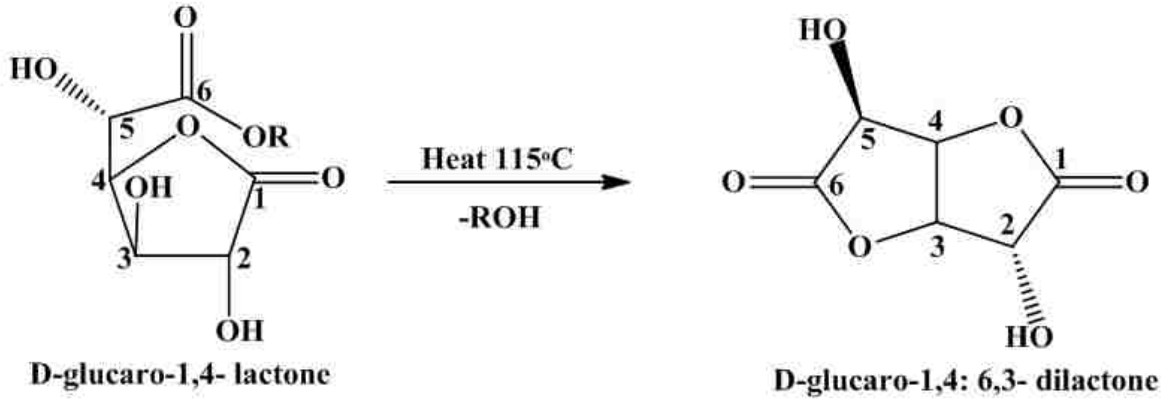

Scheme 1.4 Preparation of D-glucaro-1, 4:6, 3-dilactone

This compound is a new activated D-glucaric acid monomer suitable for polymerization condensation with diamines to yield poly (alkylene-D-glucaramide).

The isolated polyhydroxypolyamides (PHPA) exhibited low number average molecular weights as estimated by ^{1}H, ^{13}C NMR end group analysis.[22] Size Exclusion Chromatography (SEC), a method used as a simple and convenient tool to evaluate the polymers polydispersity did not yield useful results. The low molecular weights were attributed to competitive reactions that interrupt the stoichiometry and terminated the reaction. A relationship between the size of the fragments and the monomer's configuration used during polymerization was observed. In order to push the reaction to completition and to form homogeneous compositions Kiely et *al*. synthesized more complex precursors, diamido-diacid monomers targeted to react with diamines.[23-25] DMSO and methanol were used as solvents. Once solubilized, reactants failed to yield high molecular weight polymers due to the zwitterion phenomenon occurrence. Several stereoregular glicomers, *head, tail-tail, head*-poly(alkylene D-glucaramide) were synthesized by

condensation polymerization. Basic properties such as melting point and solubility were comparable with random counterparts.

All the studies previously performed reported the occurrence of lactonization during synthesis of PHPAs. It is suspected that for D-glucaric derivatives, the methyl D-glucarate 6,3-lactone, methyl D-glucarate 1,4-lactone and D-glucaro-1,4: 6,3-dilactone (Figure 1.3) coexist with the linear species and dictate the complication of polymerization mechanism NMR analyses indicated the presence of these cyclic species.[26]

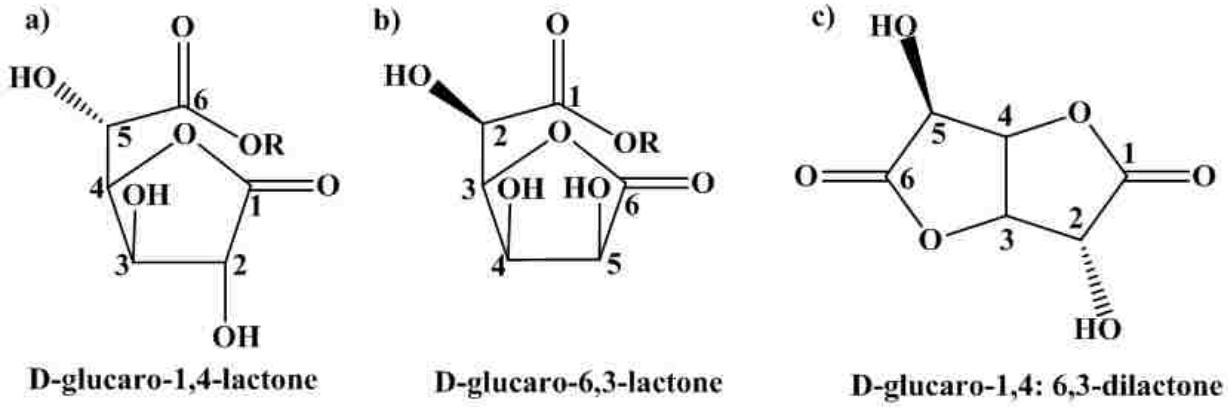

Figure 1.3 Cyclic and acyclic forms of diethyl D-glucaric acid identified in the mixture of an acidic methanol solution

Based on these observations Kiely et *al.* investigated the esterification of D-glucaric acid in acidic methanol solution. The analysis of the mixture using ^{1}H NMR, ^{13}C NMR and GC/MS determined the existence of cyclic and acyclic structures.[26] It was concluded that the activated forms (mono and dilactones) are present in the system from the beginning before aminolysis is performed and are useful for the condensation with diamines to obtain PHPA. In order to overcome the difficulties of such a low solubility manifested by these polymers several literature reports focused on protection of hydroxyl groups attached to the sugar backbone. The most suitable and convenient method to do the modification on the backbone was found to be acetyla-

tion reaction.[27-32] Another method regarded the preparation of deoxyfluoro sugars.[33-34]

More recent studies on polyhydroxypolyamides were reported by I.I. Negulescu and M. Cucu.[35] A suitable solvent was found for PHPA, N-morpholine-N-oxide monohydrate (NMMO x H_2O). Solutions of preformed poly(hexamethylene glucaramide) and blends with cellulose in NMMO x H_2O were prepared and characterized by thermogravimetric methods (Figure 1.4) and rheology.

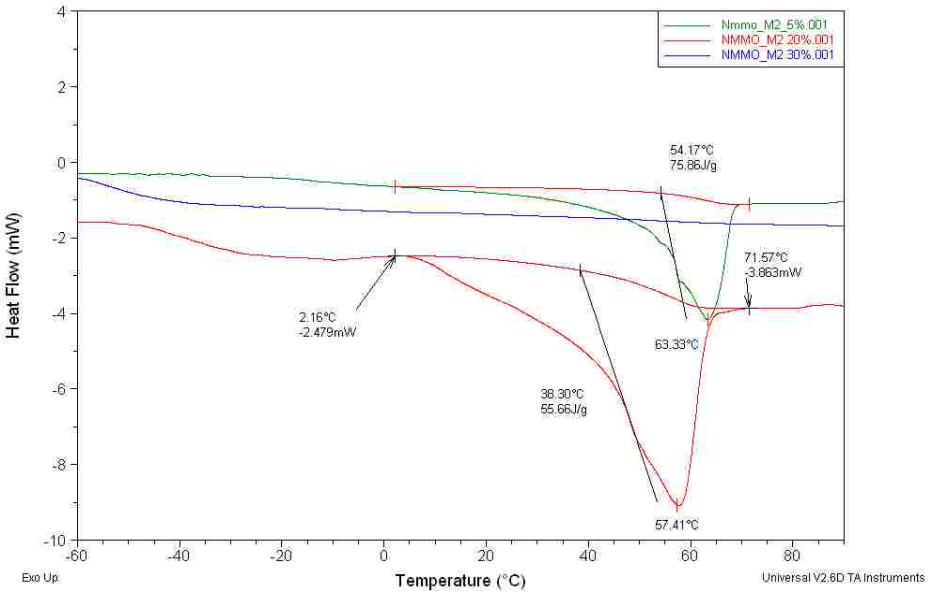

Figure 1.4 DSC curve of glylons 6, 6 solutions in NMMO x H_2O[2]

A 20% composite solution (1:1, glylons: cellulose) in NMMO x H_2O exhibited isotropization at 100°C (heating mode, Figure 1.5) and anisotropization at 75°C (cooling mode, Figure 1.6).

Solutions of 5 and 20% glylons 6, 6 in NMMO x H_2O showed a depressed crystalline melting temperature. The 30% solution seemed to be amorphous (no crystalline melting). Glylons solutions in NMMO x H_2O form ordered patterns called *spherulites* (Figures 1.7 and 1.8) by the investigators.

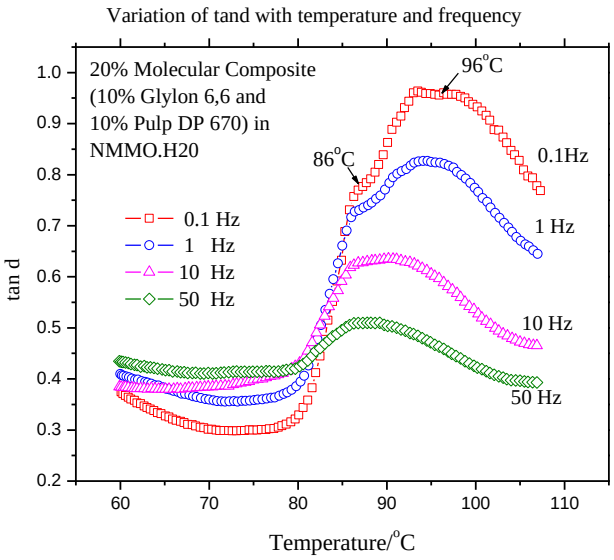

Figure 1.5 Izotropization temperature for 20% composite solution (1:1 glylon: cellulose) in NMMO monohydrate (heating mode).[2]

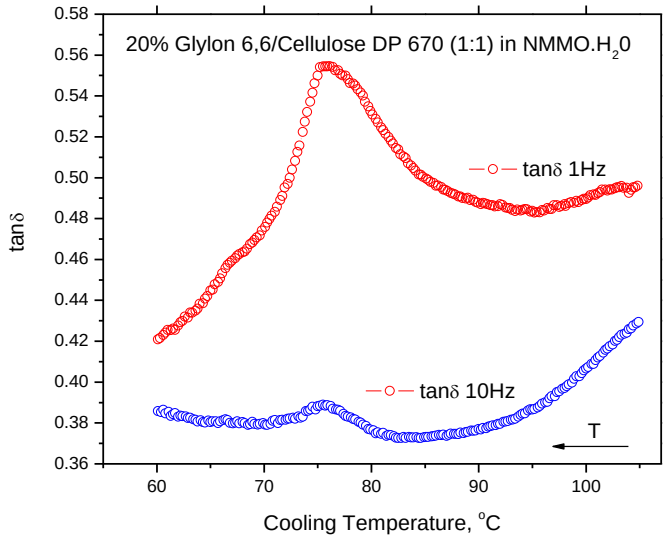

Figure 1.6 Anizotropization temperature for 20% composite solution (1:1 glylon: cellulose) in NMMO monohydrate (cooling mode).[2]

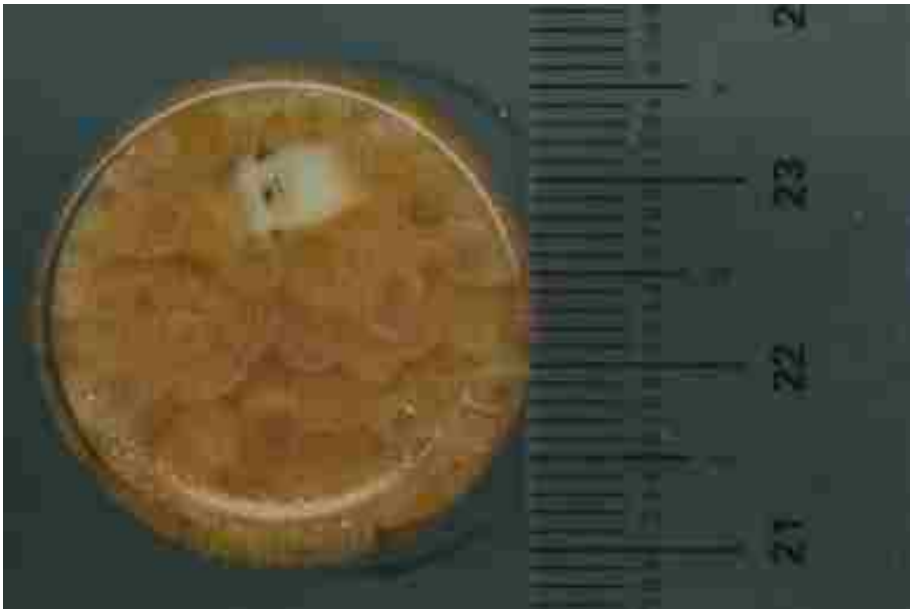

Figure 1.7 Patterns of 15% solution of glylons 6, 6 in NMMO x H2O[2]

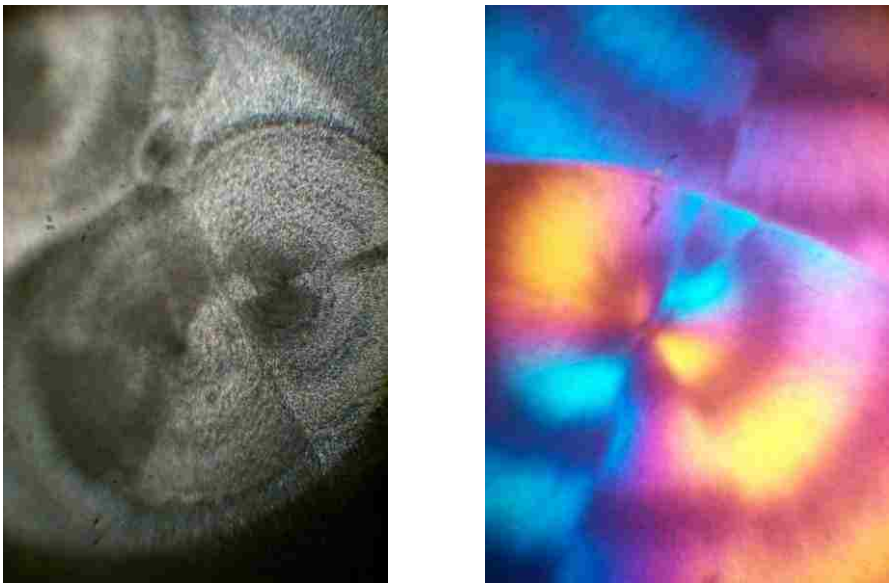

Figure 1.8 Microscopic structures of 15% glylons 6, 6 solution in NMMO x H_2O^2

Microscopic analysis and small X-ray diffraction, SAXRD (Figure 1.9) (ring facilities from Stanford University of California) data of these solutions were collected.

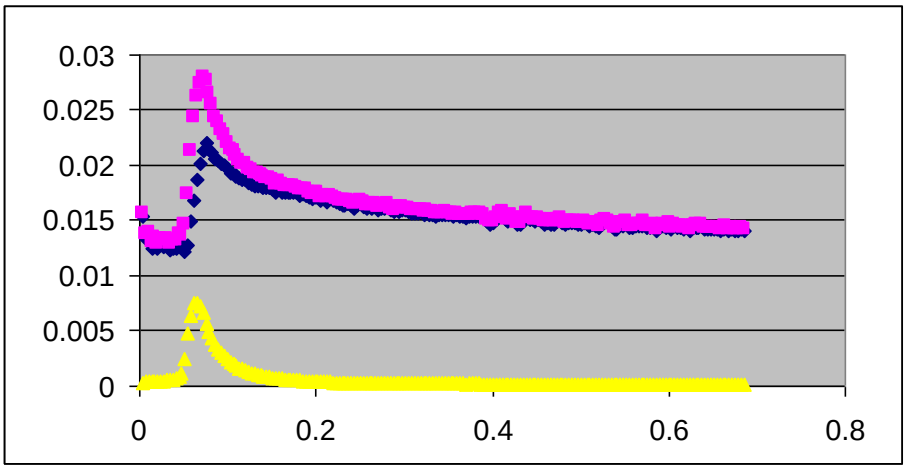

Figure 1.9 SAXRD data obtained at 30°C for a 20% solution of glylons 6, 6 in NMMO x H_2O[2]

1.4 Applications of Polyhydroxylated Nylons- *Glylons*

The environmental attributes of being annually renewable and biodegradable in contrast with the current petroleum based plastics will be a major driver for entry of biodegradable plastics and other biodegradable materials based on agricultural feed stocks into the market place. Markets for biodegradable plastics are not restricted to packaging alone. The area of disposable nonwovens like diapers, personal and feminine hygiene products and certain medical plastics like masks, gowns, gloves, etc., are excellent candidates for replacement with biodegradable plastics.

1.5 Objectives

The objectives of this research are:

- To reproduce the synthesis of the polyhexamethylene glucaramides according with Kiely's work.[26]
- To design new ways to obtain higher molecular weight polyhexamethylene glucaramide

- To understand the role of the D-glucose's free hydroxyl groups
- To propose a procedure to synthesize D-glucaric acid-based glylons with blocked hydroxyl groups.
- To perform parallel studies on D-glucaric acid and galactaric acid-based glylons to understand the mechanisms that govern the polymerization reaction.
- To control the stoichiometry of the condensation reaction in order to achieve the optimum parameters to obtain a high yield.
- To investigate the solutions of glylons in NMMO x H_2O, DMSO and anionic liquids.

CHAPTER 2 SYNTHESIS

2.1 Materials

Cation-exchange resin (DOWEX), monopotassium D-glucarate, sodium acetate, acetylchloride, hydrochloric acid, trifluoroacetic acid, triethylamine, N-morpholine N-oxide monohydrate, methyl-D-gluconate (lactone), hexamethyldisilizane, trimethylchlorosilane, 2,2-dimethoxy propane, *p*-toluene sulfonic acid, molecular sieves (4Å, 8-12 mesh), mucic acid, sodium carbonate, benzaldehide, 1-propyl galate, 1-methylimidazole, 1-chlorobutane, acetone, dimethylsulfoxide, chloroform, methylene chloride, ethyl ether high grade purity (98, 99%) were purchased by Sigma-Aldrich and used as received. Anhydrous solvents: methanol, tetrahydrofuran, dimethylformamide, pyridine, ethanol and toluene were purchased from the same vendor, Sigma-Aldrich. Hexamethylene diamine and 1,3-diamino propane were distilled before use. Liquid compounds were measured with digital pipets and for solids a 4-digits balance was used.

2.2 D-Glucaric Acid-Based Glylons

2.2.1 D-Glucaro-6, 3-Lactone[20]

The acid form of a cation-exchange resin (DOWEX) (20 ml, 40 mequiv) was prewashed with deionized water (3 x 150 ml) until the filtrate was colorless. Monopotassium D-glucarate (10.00 g; 39.89 mmol), the above treated resin (20 ml, 40 mequiv) and deionized water (100 ml) were added in a 200 ml flat-bottomed flask. The mixture was stirred at room temperature for 3h. Within 10-15 min. the white solid of potassium D-glucarate dissolved. The resin was removed by filtration, washed with water, and retained for regeneration to its acid form. The filtrate was concentrated to syrup by rotary-vaporation. The concentrated solution was placed in the fridge to crystallize. White crystals formed and were removed by filtration. The crystals were washed with acetone (15 ml) and dried under vacuum to yield D-glucaro-6,3-lactone (7.00 g, 33.9 mmol, yield 70%).

2.2.2 Na-D-Glucarate-6, 3-Lactone[20]

D-glucaro-6, 3-lactone (3.00 g, 15.62 mmol) was added to deionized water (10 ml) in a 100 ml Erlenmeyer flask. To the mixture above sodium acetate, CH_3COONa x H_2O (2.12 g, 15.62 mmol) was added. White crystals begin to form within 20 min. after scratching the wall. The solution was let aside at room temperature for 6 h. The crystalline product was removed by filtration and washed with acetone (3 x 5 ml). The filtrate, aqueous solution of acetone was kept for another 2 h at room temperature to collect additional crop of crystals formed. The two crops of product were combined and dried under vacuum to yield sodium D-glucarate-6, 3-lactone (2.7 g, 11.9 mmol., yield 86.26%).

2.2.3 Poly(Hexamethylene D-Glucaramide) from Monopotassium D- Glucarate

The method described bellow uses the procedure described by Kiely.[20] (Scheme 2.1). Different solvents were used in attempt to prepare higher molecular weight polymers.

2.2.3.1. Transesterification

Acetyl chloride (3.00 ml, 42 mmol) was added dropwise to methanol (25 ml) in a 100 ml round-bottomed flask placed in an ice bath. The reagents were left to react for 30 minutes. To the cold MeOH/HCl solution, monopotassium D-glucarate (5.00 g, 20.2 mmol) was added. The mixture was heated to reflux for 6 h and cooled to the room temperature. KCl (1.42 g, 94.80%) was removed by filtration and dried. The filtrate was rotavaporated to give a yellow concentrated solution (syrup). Methanol (15 ml) was added to dissolve the syrup and to obtain a clear solution of dimethyl glucarate (4.792 g, 94.74%) (Scheme 2.1, step 1).

2.2.3.2 Aminolysis

2.2.3.2.1 In Methanol (MeOH)

To a solution of dimethyl glucarate in methanol (20 ml) triethylamine was added until the solution became basic (pH paper).

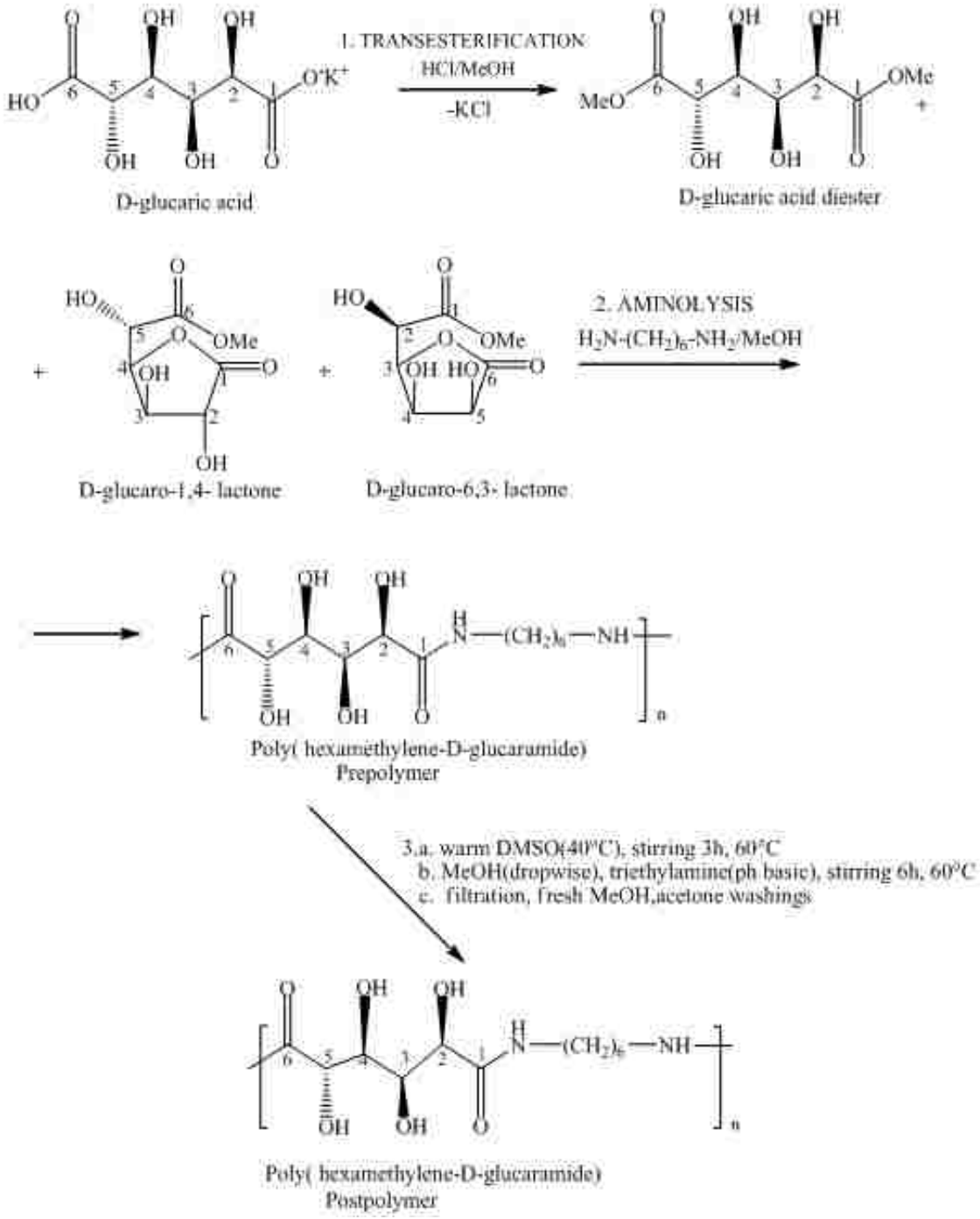

Scheme 2.1 Synthesis of high molecular weight glylons 6, 6

Additional triethylamine (1 ml) was necessary to ensure the basic pH during the condensation reaction. A methanol solution of hexamethylene diamine (17.7 ml, 20.2 mmol) was added to the above mixture. Within 15-20 min. a large amount of white solid precipitated from solution. The mixture was stirred for 3h at room temperature. The white solid was removed by filtration and washed with methanol (3 x 10 ml) and acetone (3 x 10 ml). The solid was dried under vacuum to yield poly(hexamethylene D-glucaramide), [gly-6, 6_MeOH] (4.46 g, 15.38 mmol, 91.71%) (Scheme 2.1, steps 1 and 2).

2.2.3.2.2 In Dimethylsulfoxide (DMSO)

A syrup of dimethyl D-glucarate in methanol (6 ml) was dissolved in warm DMSO (30 ml, 40 ºC). The mixture was stirred under argon for 30 minutes. Triethylamine (0.3 ml) was used to shift the pH from acidic to basic and an excess amount was added to ensure basicity. To the above mixture a methanol solution of hexamethylene diamine (5.31 ml) was added. The reaction mixture was heated from 80°C-110°C to reflux for 3-4 h to remove the methanol using a Claisen tube attached to the installation. A pale yellow solid began to form within 1h from solution. The solid was removed by filtration and washed with methanol (3 x 10 ml), acetone (3 x 10 ml) and dried to yield poly(hexamethylene D-glucaramide), [gly-6, 6_DMSO] (2.23 g, 7.71 mmol, 91.98%).

2.2.3.2.3 In N-Morpholine Oxide (NMMO x H_2O)

Triethylamine (1.5 ml) was added to a methanol solution of dimethyl D-glucarate (6 ml) to shift the solution pH onto the basic range. Additional triethylamine was necessary to ensure the basic pH. N-morpholine N-oxide monohydrate (NMMO x H_2O) (12 g, 88.88 mmol) was added and the mixture was heated under argon with stirring to a temperature low enough to maintain NMMO x H_2O liquid. A methanol solution of hexamethylene diamine (17.7 ml, 20.2 mmol) was added to the warm mixture and heated to reflux (argon atmosphere) to remove the

methanol using a Claisen tube. A very viscous solution of poly(hexamethylene D-glucaramide) in NMMO x H_2O was obtained,[gly-6, 6_NMMO]. The most difficult step was to precipitate the polymer from solution. A small portion of approximately 2mL was precipitated by adding water to the mixture. Efforts to isolate the polymer from the reaction mixture failed (Scheme 2.1, steps 1 and 2).

2.2.4 Poly(Hexamethylenediamine D-Glucaramide) from D-Gluconic Acid

2.2.4.1 Transesterification

Acetyl chloride (3.00 ml, 42 mmol) was added dropwise to methanol (25 ml) in a 100 ml round-bottomed flask placed in an ice bath. The reagents were left to react until the fuming stopped. To this cold MeOH/HCl solution D-gluconic (lactone) was added (5.00 g, 25.7 mmol). The mixture was heated to reflux for 6 h and rotavaporated to give a pale yellow concentrated solution (syrup). Methanol (15 ml) was added to dissolve the syrup and to obtain a clear solution of methyl D-gluconate (lactone) (5.95 g, 23.62 mmol, 91.66%) (Scheme 2.1, step 1).

2.2.4.2 Aminolysis

2.2.4.2.1 In Methanol (MeOH)

A syrup of methyl D-gluconate (lactone) (7.5 ml) was mixed with methanol (4.5 ml), and triethylamine (0.57 ml) was added until the solution became basic (pH paper). Additional triethylamine (1 ml) was necessary to ensure the basic pH during the condensation reaction. A methanol solution of hexamethylene diamine (10.2 ml, 9.02 mmol) was added to the above solution. Within 15-20 min. an amount of white solid precipitated from solution. The mixture was stirred for 3h at room temperature. The white solid was removed by filtration and washed with methanol (3 x 10 ml) and acetone (3 x 10 ml). The solid was dried to yield poly(hexamethylene D-glucaramide), [gly-6, 6lac_MeOH], (2.579 g, 8.9 mmol, 75.3%) (Scheme 2.1, steps 1 and 2).

2.2.4.2.2 In Dimethylsulfoxide (DMSO)

Syrup of dimethyl D-glucarate (7.5 ml) was added to warm DMSO (4.5 ml, 40 ºC). The mixture was stirred under argon for 30 minutes. Triethylamine was used to shift the pH from acidic to basic and an excess amount was added to ensure basicity. To the above mixture a methanol solution of hexamethylene diamine (10.2 ml, 9.02 mmol)) was added. The reaction mixture was heated from 80°C-110°C to reflux for 3-4 h under argon to remove the methanol using a Claisen tube attached to the installation. A pale yellow solid began to form within 1h from solution. The solid was removed by filtration and washed with methanol (3 x 10 ml), acetone (3 x 10 ml) and dried to yield poly(hexamethylene D-glucaramide), [gly-6, 6lac_DMSO] (2.64 g, 9.12 mmol, 77.22%) (Scheme 2.1, steps 1 and 2).

2.2.5. Method to Increase Molecular Weight

Poly (hexamethylene D-glucaramide) (1 g) was added to warm DMSO (10 ml, 40ºC) in a 100 ml round-bottomed flask under stirring and argon atmosphere for 3 h at 60ºC. Within 10 min. the polymer dissolved in DMSO. To the mixture above methanol (3.5 ml) was added dropwise for 5 min. Triethylamine (1 ml) was necessary to ensure a basic pH (pH paper). The mixture was heated to reflux for 6h at 60ºC and cooled at room temperature. A pale yellow solid precipitated from solution and was removed by filtration. Methanol (3 x 10 ml) and acetone (3 x 10 ml) were used to wash the solid. The precipitate was dried under reduced vacuum to yield poly- (hexamethylene D-glucaramide), [gly-6, 6_hMw], (1.32 g) (Scheme 2.1)

2.2.6 Derivatization of Poly(HexamethyleneD-Glucaramides)

2.2.6.1 Silylation

Different ratios of trimethylchlorosilane and hexamethyldisilizane (Table 2-1) were added to stirred poly (hexamethylene D-glucaramide) (0.01 g). After the addition of the pyridine (3.74 ml), the mixture was kept under stirring at room temperature for 7 days in an effort to form

Table 2-1 Different ratios of trimethychlorosilane and hexamethyldisilizane used in silylation reaction

Nr. Crt.	Glylon-6,6 (g)	Trimethylchlo--rosilane (g)	Hexamethyldi--silizane (g)	Pyridine (ml)
1.	0.01	0.10	0.20	3.70
2.	0.01	0.05	0.25	3.70
3.	0.01	0.06	0.24	3.70
4.	0.01	0.15	0.15	3.70
5.	0.01	0.20	0.10	3.70
6.	0.01	0.25	0.05	3.70

poly (hexamethylene-tetra-2,3,4,5-trimethylsiloxy-D-glucaramide).[36] The isolation of a pure compound failed.

2.2.7 Diethyl D-Glucarate- EtOH/HCl Method

The synthesis (Scheme 2.2) is an adaptation of the work published by Prömpers *et al.*[37] They synthesized polyurethanes bearing galactose units. The procedure of the acetalation reaction performed to minimize the H-bonding between free hydroxyl groups could be adapted for the purpose of this project.

D-glucaric acid potassium salt (21.00 g, 96.33 mmol) was added to ethanol (500 ml) and concentrated hydrochloric acid (10 ml). The mixture was heated 24 h to reflux to give a pale yellow mixture. KCl formed during reaction was filtered and dried under vacuum. The solvent was removed by rotary vaporation. A thick yellow oil was obtained and identified as diethyl D-glucaric acid (19.20 g, 72.19 mmol, 85.27%) (Scheme 2.2, step 1).

2.2.8 Diethyl 3,4-Mono-O-Isopropylidene D-Glucarate

The synthesis (Scheme 2.2) follows the procedure described by Prömpers *et al.*[37] Diethyl D-glucarate (15 g, 56.4 mmol) was mixed with 2,2-dimethoxy propane (5.865 g, 56,4 mmol), and *p*-toluenesulfonic acid (0.09 g, 0.54 mmol). The mixture was dissolved in acetone (187.5 ml) and heated for 13h to reflux in a Soxhlet apparatus containing molecular sieves (4Å, 8-12 mesh).

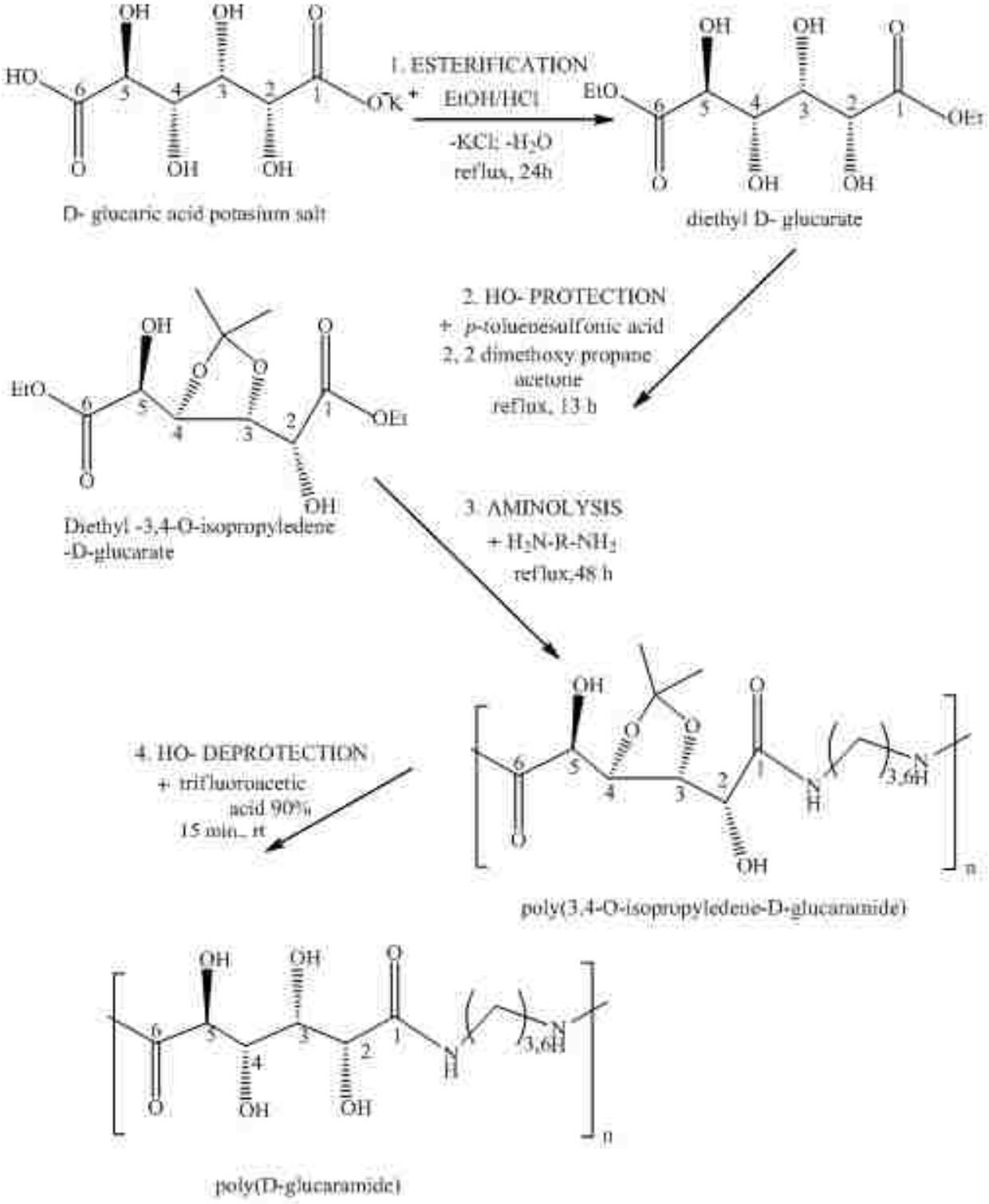

Scheme 2.2 Synthesis of OH protected and deprotected D-glucaramides

After cooling, the pale pink solution was neutralized with sodium carbonate. The inorganic salts formed were removed by filtration and the solvent was removed by rotavaporation. The residue was dissolved in ethanol (125 ml) and rotary vaporated again. The product was an yellow syrup identified as D-glucaric acid 2,3: 4,5-bis-O-isopropylidene diethylester (14.86 g, 50.20 mmol, 89.04%), (Scheme 2.2, steps1 and 2).

2.2.9 Poly(3,4-Mono-O-Isopropylidene-Alkyledene-D-Glucaramides)

2.2.9.1 Poly(3,4-Mono-O-Isopropylidene-1,3-Propyledene-D-Glucaramide)

Diethyl-2,3: 4,5-di-O-isopropyledene D-glucarate (6 g, 18.18 mmol) and 1,3-diamino-propane (1.34 g, 18,18 mmol) were added to THF (24 ml). The mixture was heated to reflux 48 h, under nitrogen. The solvent and excess reactants were removed by rotary vaporation. The product was dried under vacuum and obtained as a transparent, golden gel (Scheme 2.2, steps 1, 2 and 3), (3.85 g, 14.66 mmol., 72.07%).

2.2.9.2 Poly(3,4-Mono-O-Isopropylidene-1,6-Hexamethylene-D-Glucaramide)

Diethyl- 2,3:4,5-di-O-isopropyledene-D-glucarate (6 g, 18.18 mmol) and 1,6-hexame-thylene diamine (2.10 g, 18.18 mmol) were added to THF (24 ml). The mixture was heated to reflux 48 h, under nitrogen. The solvent and volatile byproducts were removed by rotary vapora-tion. The product, a transparent, yellow gel was dried under vacuum at room temperature (5.13 g, 16.77 mmol, 82.27%), (Scheme 2.2, steps 1, 2 and 3).

2.2.10 Poly(Alkyledene-D-Glucaramide) (Deprotection)

2.2.10.1 Poly(1,3-Propylidene-D-Glucaramide)

Poly(2,3:4.5-bis-O-isopropylidene-1,3-propylidene-D-glucaramide), [GluEt_prop], (2 g) was reacted for different reaction times (30 min. and 60 min.) at room temperature with 90% trifluoroacetic acid (10 ml), (Table 2-2). The solvent was removed by rotary vaporation. The product was precipitated in ether, filtered and dried overnight under vacuum (Scheme 2.2).

Table 2-2 Deprotection of poly(2,3: 4,5-bis-*O*-isopropylidene-D-glucaramide) with trifluoroacetic acid at different reaction time

Nr. Crt.	GluEt_prop (g)	Trifluroacetic Acid (ml)	Reaction Time (min.)	Mass of Polymer (g)	Yield %
1.	2	10	30	1.120	66.27
2.	2	10	60	1.237	75.23

2.2.10.2 Poly(Hexamethylene-D-Glucaramide)

Poly(2,3:4.5-bis-O-isopropylidene-hexamethylene-D-glucaramide), [GluEt_hexa], (2 g) was reacted for different reaction times (30 min. and 60 min.) at room temperature with 90% trifluoroacetic acid (10 ml) (Table 2-3). The solvent was removed by rotary vaporation. The residue was precipitated in ether, filtered and dried overnight under vacuum (Scheme 2.2).

Table 2-3 Deprotection of poly(2,3: 4,5-bis-*O*-isopropylidene-hexamethylene-D-glucaramide) with trifluoroacetic acid at different reaction time

Nr. Crt.	GluEt_hexa (g)	Trifluroacetic Acid (ml)	Reaction Time (min)	Mass of Polymer (g)	Yield %
1.	2	10	30	1.204	67.26
2.	2	10	60	1.362	76.08

2.3 Galactaric Acid-Based Glylons

The synthesis **(**Scheme 2.3) is an adaption of the work published by Prömpers *et al*.[37]

2.3.1 Diethyl Mucate (Diethyl Galactarate)

Galactaric acid (21.00 g, 71.43 mmol) was added to ethanol (500 ml) and concentrated hydrochloric acid (10 ml). The mixture was heated 24 h to reflux. The product crystallized from the clear pale yellow solution after the flask was placed in the fridge. The white solid, (very thin needles) was recrystallized from ethanol, separated by filtration and dried under vacuum (24.15 g, 69.79 mmol, 91%) (Scheme 2.3, step 1).

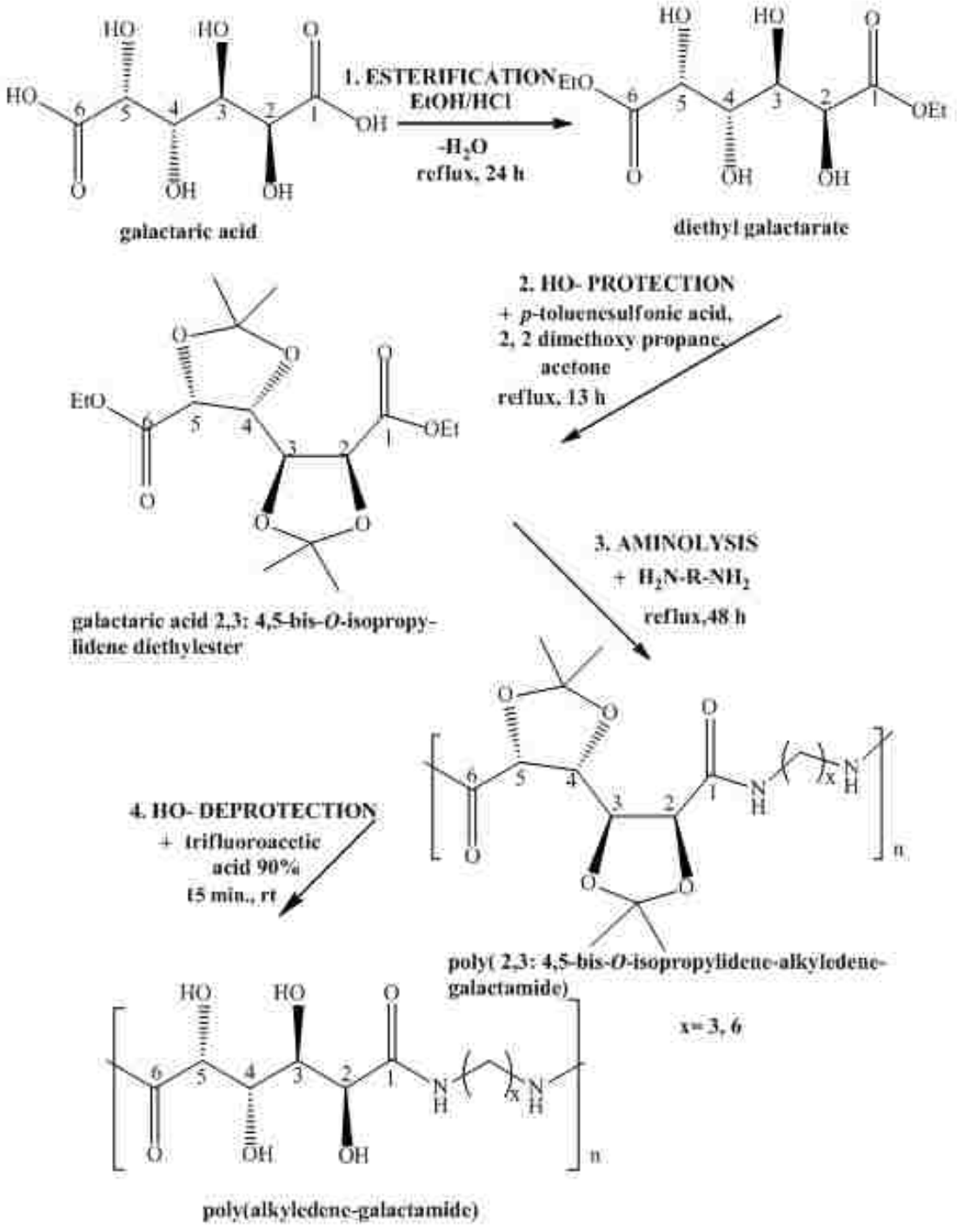

Scheme 2.3 Synthesis of galactaric acid-based derivatives. The value of x is 3 and 6.

2.3.2 Dimethyl Mucate (Dimethyl Galactarate)

Acetyl chloride (3 ml) and methanol (25 ml) were mixed in a 100 ml round bottomed flask placed in an ice bath for 30 min. Mucic acid (5.04 g, 24 mmol) was added and the mixture was heated to reflux for 24 h. The solvent was partially removed by rotary vaporation. Fresh methanol was used to recrystallize the final product that was dried under vacuum (3.02 g, 12.67 mmol, 53%).

2.3.3 Diethyl-2,3: 4,5-bis-O-Isopropylidene Galactarate

Diethyl galactarate (15 g, 56.39 mmol) was mixed with 2, 2-dimethoxy propane (12.18 g, 117.11 mmol) and *p*-toluenesulfonic acid (0.187 g, 1.08 mmol). The mixture was dissolved in acetone (187.5 ml) and heated for 13 h to reflux in a Soxhlet apparatus containing molecular sieves (4Å, 8-12 mesh). After cooling, the pale pink solution was neutralized with sodium carbonate. The inorganic salts formed were removed by filtration. The solvent was rotary vaporated. The residue, a white crystalline compound, was crystallized from ethanol (125 ml). The product was filtered and dried under vacuum (18.15 g, 52.45 mmol, 93.03%), (Scheme 2.3, step 2).

2.3.4 Diethyl-2,3: 4,5-bis-O-Benzylidene Galactarate

Diethyl galactarate (5 g, 18.79 mmol), benzaldehyde (8.28 g, 78.11 mmol), *p*-toluene sulfonic acid (0.125 g, 0.71 mmol) and toluene (62.5 mL) were mixed in a 250 ml round bottomed flask. A Soxhlet tube containing molecular sieves (4Å, 8-12 mesh) was attached to the flask to ensure water removal. The mixture was heated to reflux under stirring in nitrogen atmosphere for 13 h. Within 120 min. a pale yellow layer began to form. The resulting solution pH was very acidic, the neutralization encountered difficulties because of the solution viscosity. The final product was filtered and dried under vacuum (8.56 g, 19.36 mmol, 86.64%). The same procedure was followed using benzylic alcohol (50 mL) as solvent. The product was filtered and vacuum dried (8.12 g, 18.37 mmol, 83.09%), (Table 2-4, Scheme 2.4).

Table 2-4 Yields of galactaric acid 2,3: 4,5-bis-O-benzylidene diethylester (GalEt_benzal) obtained by using different solvents

Solvent (mL)	GalEt_benzal (g)	Molarity mmolar	Yield %
Toluene 62.5	8.56	19.36	87.54
Benzylic Alcohol 50	8.12	18.37	83.09

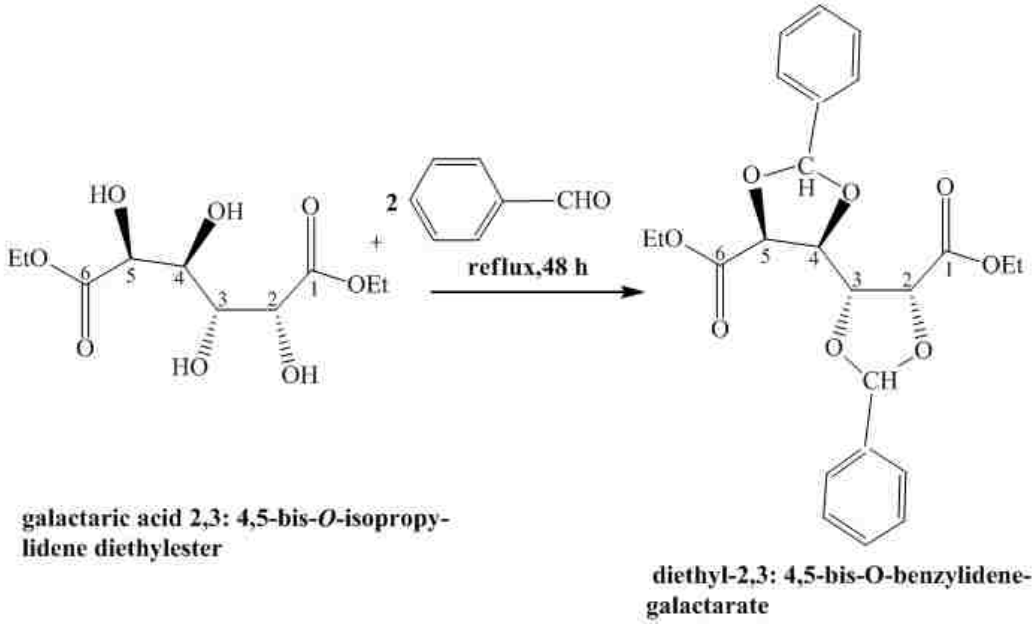

Scheme 2.4 Synthesis of diethyl-2,3: 4,5-bis-O-benzylidene galactarate

2.3.5 Poly(2,3: 4,5-bis-O-Isopropylidene-Alkyledene-Galactamides)

2.3.5.1 Poly(2,3: 4,5-bis-O-Isopropylidene-1,3-Propyledene-Galactamide)

Diethyl- 2,3:4,5-di-O-isopropyledene galactarate (6 g, 17.34 mmol) and 1,3-diaminopropane (1.28 g, 17.34 mmol) were added to THF (24 ml). The mixture was heated to reflux 48 h, under nitrogen. The solvent was removed by rotary vaporation. The residue was dissolved in dimethylformamide and precipitated in anhydrous ethyl ether. The polymer was dried overnight

under vacuum (4.892 g, 15.19 mmol, 86.1%, (Scheme 2.3), where x = 3. Different ratios of monomers, diester/1,3-diaminopropane were used (Table 2.5).

Table 2-5. Different ratio diester/DPA used in the synthesis of poly(2,3: 4,5-bis-O-isopropylidene-1,3-propyledene-galactaramide)

Nr. Crt.	Ratio Diester/DPA*	Mass of Diester (g)	Molarity molar	Mass of DPA (g)	Molarity mmolar
1.	1:1	6.00	17.34	1.28	17.34
2.	1:0.98	6.00	17.34	1.25	16.89
3.	1:0.95	6.00	17.34	1.21	16.35

*DPA-1,3-propylene diamine

2.3.5.2 Poly(2,3: 4,5-bis-O-Isopropylidene-1,6-Hexamethylene-Galactamide)

Galactaric acid 2,3: 4,5-di-O-isopropyledene diethylester (6 g, 17.34 mmol) and 1,6-hexamethylene diamine (1.84 g,17.34 mmol) were added to THF (24 ml). The mixture was heated to reflux 48 h, under nitrogen. The solvent was removed by rotary vaporation. The transparent, pale yellow gel like product was dissolved in dimethylformamide and precipitated in ethyl ether anhydrous. The polymer was dried overnight at reduced pressure (5.875 g, 15.87 mmol, 89.9%, (Scheme 2.3 steps 1, 2 and 3), where x = 6. Table 2-6 reflects the ratios of monomers used during polymerization.

Table 2-6 Different ratio diester/HMDA used in the synthesis of poly(2,3: 4,5-bis-O-isopropylidene-1,6-hexamethylene-galactarate amide)

Nr. Crt.	Ratio Diester/HMDA*	Mass of diester (g)	Molarity mmolar	Mass of HMDA (g)	Molarity mmolar
1.	1:1	6.00	17.34	2.01	17.34
2.	1:0.98	6.00	17.34	1.97	16.98
3.	1:0.95	6.00	17.34	1.90	16.46
4.	1:0.90	6.00	17.34	1.81	15.59
5.	1:0.89	6.00	17.34	1.78	15.42

*HMDA-hexamethylene diamine

2.3.5.3 2,3: 4,5-bis-O-Isopropylidene-N,N-bis-*t*-Butyl-Galactamide

Galactaric acid 2,3: 4,5-di-O-isopropyledene diethylester (3.8 g, 11.11 mmol) and *t*-butyl amine (0.92 g, 11.11 mmol) were added to THF (16 ml). The mixture was heated to reflux for 48h. A yellow product precipitated within 90 min. The solid was filtered, washed with fresh methanol (2 x 5 ml) and acetone (2 x 5 mL) and dried overnight under reduced vacuum (1,342 g, 4.34 mmol, 38.86%), (Scheme 2.5).

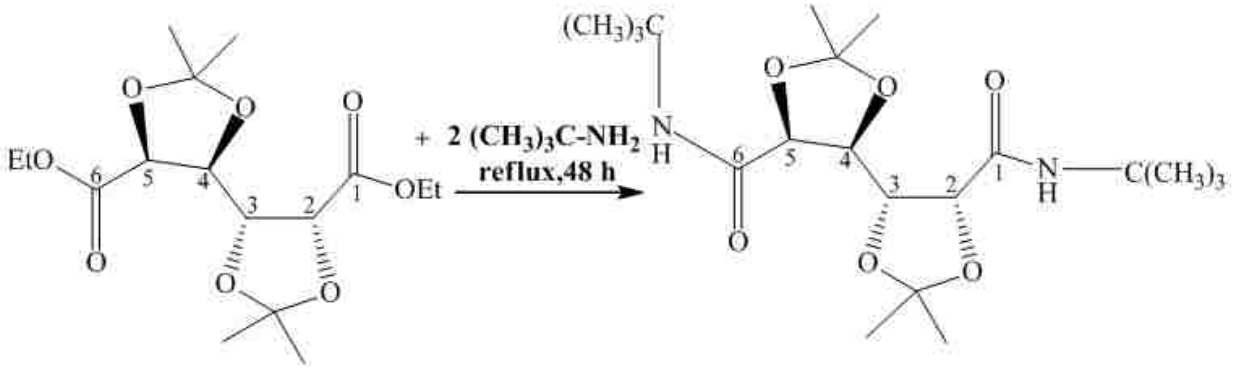

galactaric acid 2,3: 4,5-bis-*O*-isopropylidene diethylester

2,3: 4,5-bis-*O*-isopropylidene-N, N-bis-*t*-butyl-galactamide)

Scheme 2.5 Synthesis of 2,3: 4,5-bis-O-isopropylideneN, N-bis-*t*-butyl-galactamide from galactaric acid 2,3: 4,5-bis-O-isopropylidene diethyl ester

2.3.5.4 2,3: 4,5-bis-O-Isopropylidene-N, N-bis-Benzyl-Galactamide

Galactaric acid 2,3: 4,4-bis-O-isopropylidene diethylester (6 g, 17.34 mmol) and benzyl amine (0.94 g, 8.87 mmol) were added to THF (24 ml). The mixture was heated to reflux for 48h. After approximately 90 min. two layers separated: one very thick, white layer, on the bottom, and the other colorless, on top. The solvent (colorless layer) was removed by rotary vaporation. The white product was filtered, washed with methanol (2 x 5 mL) and acetone (2 x 5 mL) and dried overnight under reduced vacuum (4.534 g, 12.7 mmol, 71.96%, Scheme 2.6).

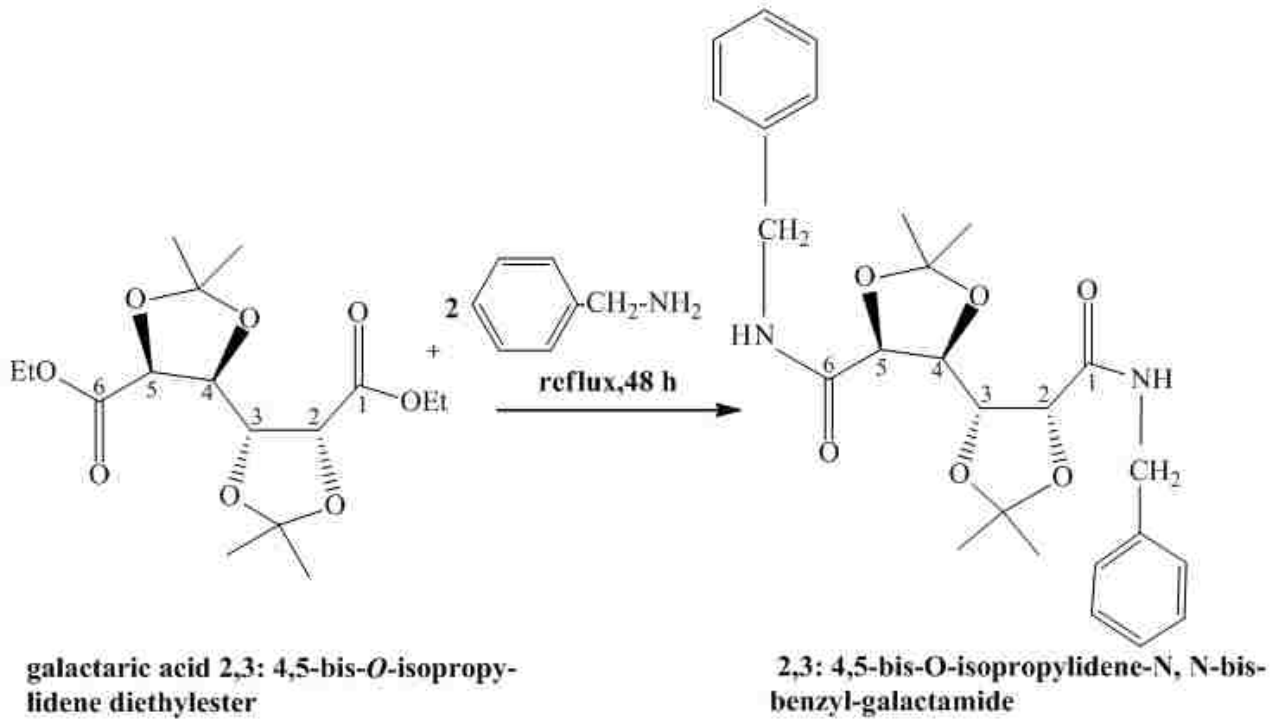

Scheme 2.6 Synthesis of poly(2,3: 4,5-bis-O-isopropylidene- N, N- benzyl-galactarate amide) from galactaric acid 2,3: 4,5-bis-O-isopropylidene diethylester

2.3.6 Poly(Alkyledene-Galactamide) (Deprotection)

2.3.6.1 Poly(1,3-Propylidene-Galactamide)

Poly(2,3: 4.5-bis-O-isopropylidene-1,3-propylidene-galactaramide), GalEt_prop, (2 g) was reacted for different reaction times (30 min. and 60 min.) at room temperature with 90% poly(2,3:4.5-bis-O-isopropylidene-1,3-propylidene-galactaramide), GalEt_prop, (2 g) was reacted for different reaction times (30 min. and 60 min.) at room temperature with 90% trifluoroacetic acid (10 ml). The solvent was removed by rotary vaporation. The residue was precipitated in ether and dried under vacuum (Table 2-7), (Scheme 2.3, step 4).

2.3.6.2 Poly(Hexamethylene Galactamide)

Poly(2,3:4.5-bis-O-isopropylidene-hexamethylene-galactaramide), GalEt_hexa, (2 g) was reacted for different reaction times (30 min. and 60 min.) at room temperature with 90% trifluo-

roacetic acid (10 ml). The solvent was removed by rotary vaporation. The residue was precipitated in ether and dried under reduced vacuum (Table 2-8), (Scheme 2.3, step 4).

Table 2-7 Deprotection of poly(2,3: 4,5-bis-O-isopropylidene galactamide) with trifluoroacetic acid at different reaction time

Nr. Crt.	GalEt_prop (g)	Trifluroacetic acid (mL)	Reaction time (min.)	Mass of unprotected polymer (g)	Molarity mmolar	Yield %
1.	2	10	30	1.245	5.02	80.84
2.	2	10	60	1.380	5.56	89.61

Table 2-8. Deprotection of poly(2,3: 4,5-bis-O-isopropylidene-hexamethylene-galactamide) with trifluoroacetic acid at different reaction time

Nr. Crt.	GalEt_hexa	Trifluroacetic acid (mL)	Reaction time (min.)	Mass of unprotected polymer (g)	Molarity mmolar	Yield %
1.	2	10	30	1.312	4.52	89.92
2.	2	10	60	1.386	4.77	94.94

2.4 N-Methyl-N-Morpholine Oxide Monohydrate (NMMO x H_2O)

To a 50% solution of NMMO x H_2O (128 g, 948.15 mmol) n-propyl-gallate, n-PG, (0.256 g, 1.2 mmol) and toluene (15.52 ml) were added. The azeotropic mixture was rotary vaporated until the ratio between NMMO and H_2O reached the values 86.66 to 13.33. The mixture was cooled and stored in special small moisture isolated bags and kept in desiccators. At room temperature the 86.66% NMMO x H_2O is a yellow solid.

2.5 1-Butyl-3-Methylimidazolium Chloride (BMIMCl)

Freshly dried 1-methylimidazole (300 ml) and 1-chlorobutane were mixed under argon in a round bottomed Schenk flask. After fresh toluene (375 ml) was added, the mixture was heated to reflux under argon for 24 h. Two layers had formed: one yellow, viscous and other transparent, colorless. The flask was allowed to cool to room temperature and placed in an ice bath overnight at -10^{o}C to yield a white solid. The mixture was decanted carefully under argon.

The white solid was dissolved in acetonitrile (225 ml). The yellow viscous liquid was added to diethyl ether and placed in the fridge to allow crystal formation. The product was dried under vacuum for 24 h.[38] The crystalline compound was identified as 1-butyl-3-methylimidazolium chloride (375 g, 64%).

CHAPTER 3 CHARACTERIZATION

3.1 Solubility

3.1.1Glucaric Acid-Based Glylons

Polymers derived from D-glucaric acid exhibited low solubility in different solvents. Table 3-1 reflects the solubility of poly(hexamethylene D-glucaramide).

Table 3-1 Solubility of Glylons-6, 6 in different solvents

polymer	water	MeOH	toluene	DMF	THF	NMMO	BMIMCl	DMSO	$CHCl_3$
Gly6,6_ MeOH	no	no	no	no	no	yes	yes	yes	no
Gly6,6_ DMSO	no	no	no	no	no	yes	yes	yes	no
Gly6,6_ NMMO	no	no	no	no	no	yes	yes	yes	no
Gly6,6lac_ MeOH	no	no	no	no	no	yes	yes	yes	no
Gly6,6lac_ DMSO	no	no	no	no	no	yes	yes	yes	no
Gly6,6_ hMw	no	no	no	no	no	yes	yes	yes	no
GluEt_ prop	slightly	no	no	no	slightly	yes	yes	yes	slightly
GluEt_ _hexa	slightly	no	no	no	slightly	yes	yes	yes	slightly

The first five polymers have the hydroxyl groups free, unprotected. An intense hydrogen bonding is suspected to occur and this might be the major factor who dictates the lack of solubility. This assumption is sustained by the behavior of the last two polymers that have two hydroxyl groups protected and two free. The decrease in hydrogen bonding intensity was the driving force to make the polymers slightly water soluble. Yet, the solubility of D-glucaric derivatives can be improved by finding a way to protect the other two OH-groups.

3.1.2 Galactaric Acid-Based Glylons

To prove the assumption made about D-glucaric acid derivatives was true, a reaction was performed to protect the hydroxyl group of galactaric diester. The spatial arrangement of galactose OH-groups makes the compound suitable for this kind of reaction. Galactaric acid 2,3: 4,5-

bis-*O*-isopropylidene diethylester has all four OH groups protected, thus the hydrogen bonding is not present. Polymers derived from protected galactaric (mucic) acid showed a very good solubility in a broad range of solvents (Table 3-2).

Table 3-2 Solubility of acetalated galactaric-based glylons acid derivatives in different solvents

polymer	water	MeOH	toluene	DMF	THF	NMMO	BMIMCl	DMSO	acetone	$CHCl_3$
galEt_prop	yes	yes	slightly	yes	yes	yes	yes	yes	yes	yes
GalEt_hexa	yes	yes	slightly	yes	yes	yes	yes	yes	yes	yes

3.2 Gel Permeation Chromatography (GPC)

Gel Permeation Chromatography (GPC) is also known as Size-Exclusion Chromatography (SEC) and is a widely technique used in the separation, purification and characterization of synthetic polymers. GPC is mostly used in determination of polymer molecular weight, by comparing the molecular weight of a sample against standards of molecular known molecular weight. The separation employs a stationary phase composed of a porous network consisting of a molecular gel. Molecules with hydrodynamic volume larger than that of the stationary phase pores cannot pass through the gel pores but can pass through the spaces between the gel beads. These molecules will elute unretarded. On the other side, molecules with smaller hydrodynamic volume can pass through both, pores and spaces between gel particles. They are retained in the stationary phase longer, function of their size and shape. Finally, they will elute later. GPC instrument involved in this work used two Phenogel (300 x 5.8 x 10μ) mm columns connected in series (10^5Å x M x M) and a guard column (5μ, 50 x 7.8 mm). The instrument has an Agilent 1100 pump (Agilent Technologies, Palo Alto, CA) and an Agilent 1100 autosampler. A Wyatt Heleos Multiangle Light Scattering (MALS) with a GaAs laser at λ= 658 nm detector was coupled in series with a Wyatt rEX Refractive Index detector with a 658 nm light source. The GPC chromatogram shows detector response (DRI) versus time or elution volume (Ve). The larger molecules elute first

therefore will be the first registered on the chromatogram. A very important role is played by the solvent chosen for elution. For the present study tetrahydrofuran (THF) was used. The samples preparation involved the polymer solubilization in THF. D-glucaric derivatives obtained after Kiely's method were first derivatized by silylation.[34] The elugrams obtained by analyzing the silylated D-glucaramides led to a limited success because the compounds didn't dissolve completely (results not shown).

The peak of gly-6,6_MeOH, deprotected glylon synthesized in methanol, (Figure 3.2**)** lies in the very small range of molecular weights. The other peak of gly-6,6_highMw, the polymer synthesized by following the Kiely's procedure to enhance the molecular weight (See 2.1.5**)**, with a maximum at 29 mL elution volume is possibly overlapped with another ones. The tail begins at 22 mL and shows a slight curvature between 24– 28 mL with a maximum around 26 mL. The molecular weight values corresponding with this elution volume range are between 12.5 KDa and 2 KDa. Polystyrene was used as standard (Figure 3.1).

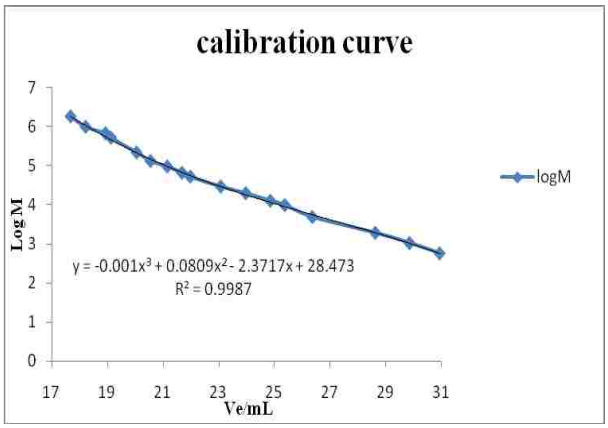

Figure 3.1 Calibration curve: polystyrene mix

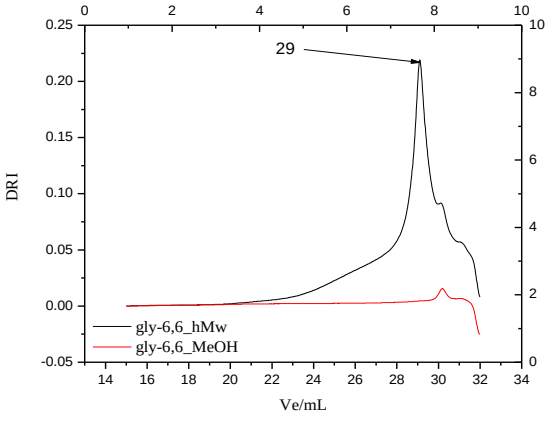

Figure 3.2 GPC elugrams of D-glucaramides: gly-6, 6_hMw and gly-6, 6_MeOH

The polymers synthesized after Prömpers *et al.* work[36] (See 2.1.7) were dissolved in THF and the solutions were filtered with 0.45 µm. The compounds dissolved to a greater extent when

compared with deprotected counterparts. The same trend was noticed: only low molecular weight species go in solution, the higher molecular weight remained inside the filter. In order to estimate the ratio of insoluble to soluble polymer a fast test was performed by dissolving a known quantity of acetalated compound (GluEt_hexa) in THF and the solution was passed through a 0.45μm filter. The difference in filter weight before and after passing the solution plus the amounts remained in the vials gave the percent of polymer insoluble and was consistent with the start supposition: only 20% of the polymer from solution passed through the filter. Because of their broad solubility in organic solvents acetalated poly(galactamides) were investigated more easily by GPC when compared with acetalated poly(D-glucaramides). As will be shown in section 3.4, the dispersity of the polymer is correlated with the evolution of the cyclic and linear forms that coexist in the system. It is suspected that a large molecular weight structures begin to aggregate inside the filter. To verify this supposition the filters used for the GPC samples filtration were injected with THF for a longer time to break up the clusters. The solutions were analyzed by MALDI-TOF MS spectroscopy.

Dried filters (0.45 μm) used for sample preparation were weighed before and after filtration. The mass difference gave the percent of polymer dissolved in THF, (Table 3-3).

Table 3-3 Percentages of solubilized acetalated galactaric acid-based glylons calculated from filter mass difference

No.	Sample	Initial Mass Of filter (g)	Final Mass Of filter (g)	Initial mass Of polymer (g)	Δm (g)	Dissolved %
1.	GalEt_prop1:1	2.9042	2.9574	0.0665	0.0532	20.00
2.	GalEt_prop1:0.98	2.8842	2.8896	0.0092	0.0054	45.65
3.	GalEt_prop1:0.95	2.9047	2.9071	0.0146	0.0024	83.56
4.	GalEt_hexa1:1	2.8812	2.8874	0.0245	0.0062	74.70
5.	GalEt_hexa1:0.98	2.8721	2.8745	0.0170	0.0024	85.88
6.	GalEt_hexa1:0.95	2.8730	2.8795	0.0205	0.0065	68.30
7.	GalEt_hexa1:0.90	2.9093	2.9120	0.0145	0.0027	81.38
8.	GalEt_hexa1:0.89	2.8942	2.9017	0.0107	0.0075	29.90

The comparison of data gathered by size exclusion chromatography method led to the conclusion that the size of the protected galactaric derivatives is much larger. The area of the peaks was reduced to unity in order to simplify the calculations. Microsoft Excel and Origin 7 software were used to analyze the data (Tables 3-4 and 3-5**)**.

Table 3-4 Percentage area and molecular weight distribution for GalEt_prop1:1

No.	Ve (max. peak) mL	% from total area	HMW KDa	MMW KDa	LMW KDa
1.	22.70	1.27	~90	-	-
2.	34.75	7.68	-	-	~1.6
3.	35.52	2.57	-	-	~1.3
4.	36.38	15.85	-	-	~1.0
5.	37.45	34.74	-	-	~0.74
6.	38.95	37.87	-	-	~0.32

Table 3-5 Percentage area and molecular weight distribution for GalEt_hexa1:1_48 h

No.	Ve (max. peak) mL	% peak area	HMW KDa	MMW KDa	LMW KDa
1.	32.28	2.22	-	~3.2	-
2.	32.88	2.90	-	-	~2.6
3.	33.62	6.48	-	-	~2.2
4.	34.48	27.04	-	-	~1.7
5.	35.62	17.82	-	-	~1.3
6.	37.72	7.92	-	-	~0.74
7.	39.8	35.60	-	-	~0.37

The elugrams show the oligomers of cyclic and linear forms and a small Gaussian deviation from the baseline corresponding to ~90kDa (maximum peak at 22.6 mL) (Figure 3.3).

3.3 Fourier Transform Infrared Spectroscopy (FTIR)

FTIR is one of the easiest and important tools to characterize chemical compounds. The range of infrared radiation used most commonly is limited between 4000 cm^{-1} and 400 cm^{-1}. The wavelengths are converted by molecules into energy of molecular vibration and quantized. A change in vibrational energy is accompanied by rotational energy changes and will appear in

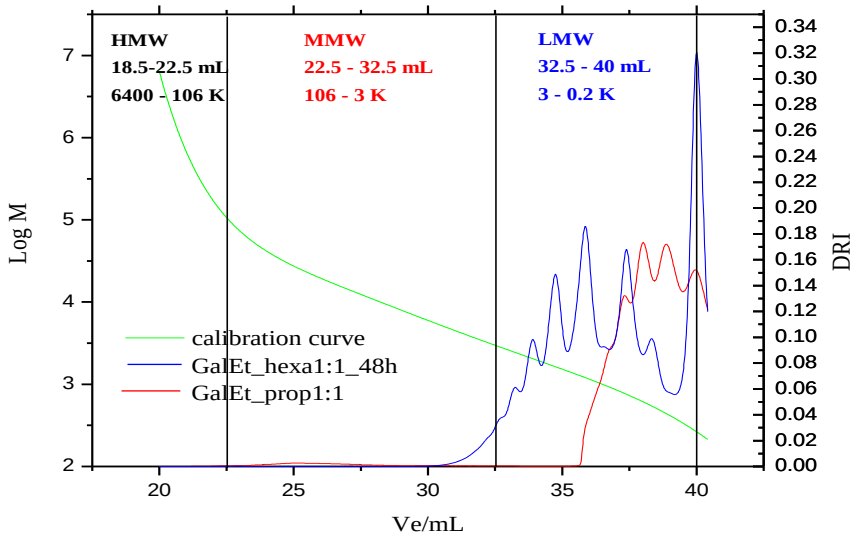

Figure 3.3 GPC traces for GalEt_prop1:1(blue) and GalEt_hexa1:1_48 h (red) and calibration curve (green).

spectra as bands rather than lines. The geometry of the atoms, the force constants of the bonds and the relative masses of the atoms dictate the frequency or the wavelength of absorption. Two types of vibrations are involved: *stretching*-a rhythmical movement along the bond axis, and *bending*- a change in bond angle between bonds of the same atom or a group of atoms with respect to the molecule remainder.[39] The spectra were recorded with a Bruker Tensor 27 equipped with a DTGS detector. The apparatus has a mid-IR source (4000 to 400 cm^{-1}) plus a KBr beamsplitter and a ZnSe crystal (orange). The maximum resolution that can be gained is 1. Another important aspect is the sample preparation. For this work the solid compounds were dried under vacuum overnight. After drying the powder was compacted using KBr pellet method. Polymers soluble in DMA were deposited on NaCl plates using thin glass pipets. The solvent was removed by evaporation, yielding a thin film of polymer. After KBr pallets and polymer films were obtained, the FTIR spectra were recorded using a blank pallet containing only KBr and a blank NaCl plate as backgrounds. The transmittance spectra were baseline corrected

and a 25 coefficient of smoothness was applied for several samples. Data were saved as Excel format files and analyzed using Origin 7 software.

3.3.1 D-Glucaric Acid-Based Glylons

All starting compounds purchased by Aldrich were investigated by FTIR in order to have a better control on the purity (monopotassium salt of D- glucaric acid (Figure 3.4),

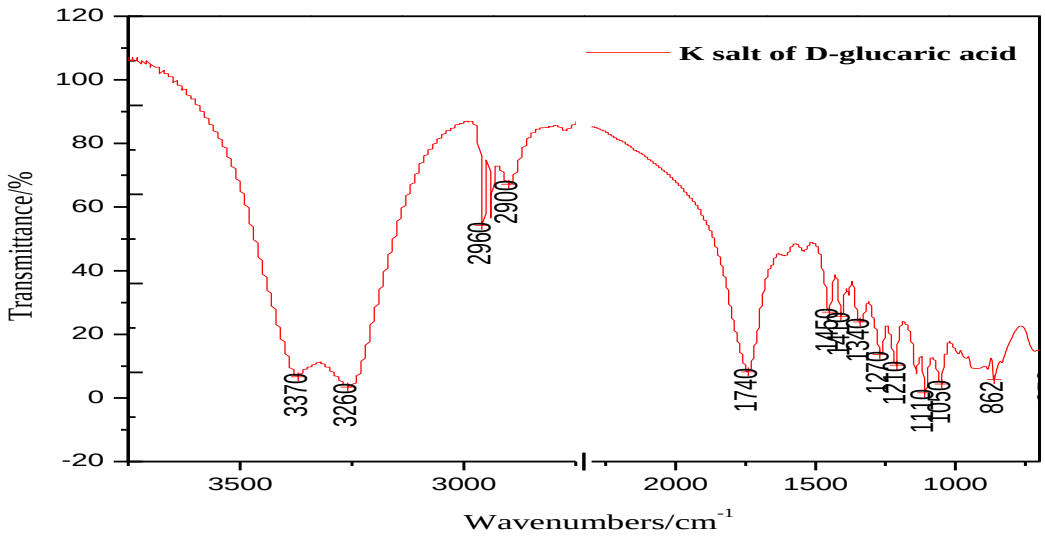

Figure 3.4 FTIR (KBr pallets) spectrum of K-salt of D-glucaric acid: carboxylic C==O stretch (possible overlapped with lactone traces), 1740 cm-1, methylene C—H stretch, 2900 cm^{-1}, 2960 cm^{-1}, broad O—H stretch, 3260- 3370 cm^{-1}, alcohol C—O stretch 1270 cm^{-1}, 1110 cm^{-1}, alcohol O—H bend, 1340 cm^{-1}, carboxylic C─O absorption bands, 1340 cm^{-1}, 1440 cm^{-1}, 1460 cm^{-1}.

D-gluconic acid-lactone form (Figure 3.5). It was suspected to have a mixture of cyclic (lactones) and linear conformations for the dimethyl D-glucaric ester based on previous studies performed by Kiely[20, 25, 40] and Ogata[10, 11] The peaks at 1734 cm^{-1} and 1776 cm^{-1} were assigned to carbonyl stretching frequency for ester and five-membered ring lactones (Figure 3.6). The failure of the efforts to synthesize the Na-salt of glucaric acid and D-glucaro-6, 3-lactone, as intermediate compounds during PHPA synthesis was reflected efficiently by the IR spectra (no peak recorded

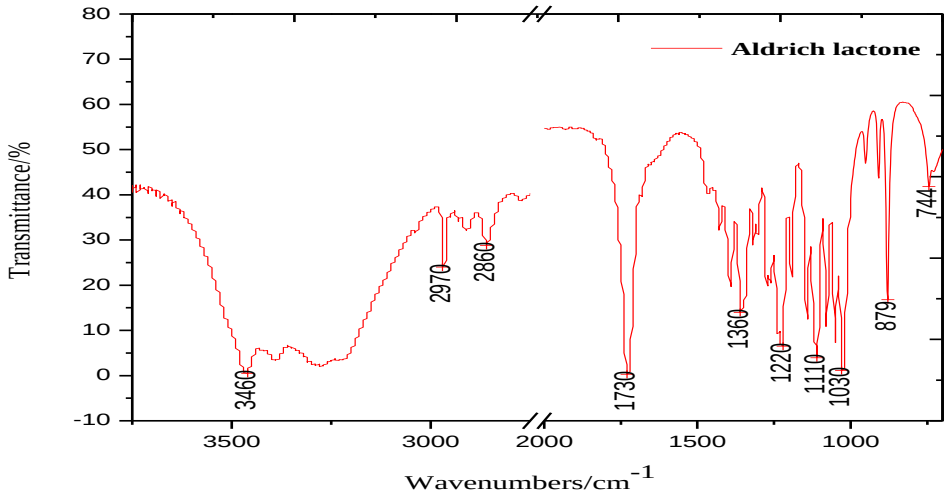

Figure 3.5 FTIR (KBr pallets) spectrum of D-glucaric acid-lactone form purchased by Aldrich: lactone C==O stretch, 1730 cm^{-1}, methylene C—H stretch, 2860 cm^{-1}, 2970 cm^{-1}, broad O—H stretch, 3225- 3460 cm^{-1}, alcohol C—O stretch 1220 cm^{-1}, 1110 cm^{-1}, alcohol O—H bend, 1360cm^{-1}, carboxylic C==O stretch possible overlapped with lactone, 1730 cm^{-1}, weak carboxylic C—O and O—H absorption bands, 1388.58 cm^{-1} and 1469.77 cm^{-1}(not labeled on the graph).

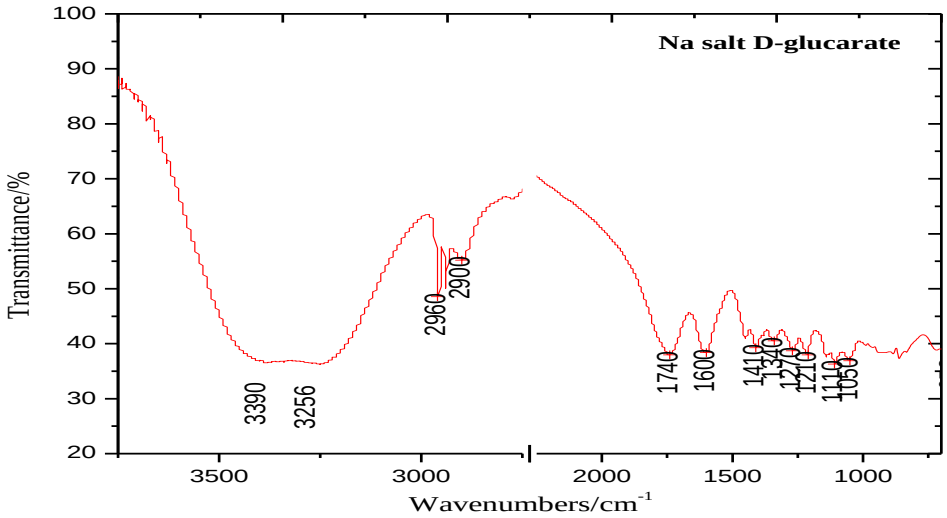

Figure 3.6 FTIR (KBr pallets) spectrum of Na salt D-glucarate: carboxylic C==O stretch (possible overlapped with lactone traces), 1740 cm^{-1}, methylene C—H stretch, 2900 cm^{-1}, 2960 cm^{-1}, broad O—H stretch, 3256- 3390 cm^{-1}, alcohol C—O stretch 1270 cm^{-1}, 1110 cm^{-1}, alcohol O—H bend, 1340 cm^{-1}, carboxylic C==O absorption bands, 1340 cm^{-1}, 1410 cm^{-1}, carboxylate asymmetrical strectching band 1600 cm^{-1}.

at 1790 cm^{-1} , Figure 3.7). The spectrum of the intermediate compound dimethyl D-glucarate is also provided and shows clearly the stretch of carbonyl for ester near 1750 cm^{-1} (Figure 3.8). Glylons-6, 6 obtained using different solvents were analyzed to see the specific bands and their chemical shifts (Figure 3.9). FTIR confirmed that the target polymers were successfully synthesized. The specific bands for amide I and II were close to those recorded for nylon 6,6 (Figure 3.10) Efforts to improve the solubility of these polymers by acetalation gave also good results (Figure 3.11, Figure 3.12 and Figure 3.13). The acetalation reaction blocked only two OH groups. The residual hydroxyl groups are reflected in FTIR spectra by a decrease in secondary alcohol band, 1062 cm^{-1} GluEt_prop and 1076 cm^{-1} GluEt_hexa when compared to gly-6, 6 compounds, 1086 cm^{-1}. The broad peak around 3350 cm^{-1} specific to OH groups can be also seen at a decreased intensity. Acetalated D-glucaric derivatives have the amide I and II band slightly shifted because of the acetal group inserted on the compound. The shift is approximately +10 cm^{-1} than gly-6, 6. However, the FTIR spectroscopy shows that polycondensation reactions gave the target polymers.

3.3.2 Galactaric Acid-Based Glylons

The starting material, mucic acid (galactaric acid), purchased by Aldrich was analyzed first by FTIR method (Figure 3.14). Diethyl galactaric ester was compared to dimethyl D-glucarate to identify the lactones. IR spectrum didn't confirm the presence of cyclic structure for galactaric compound. It is known that galactaric acid forms easily lactones.[12] The peak assigned to ester stretch can be overlapped with that of lactones (Figure 3.15). The dimethyl and diethyl D-glucaric esters are yellow, relatively viscous liquids and dimethyl and diethyl galactaric esters are crystalline compounds. These observations can be correlated with the configuration of two sugars. The single difference between glucose and galactose is the C_4 chiral center. C_4 has a

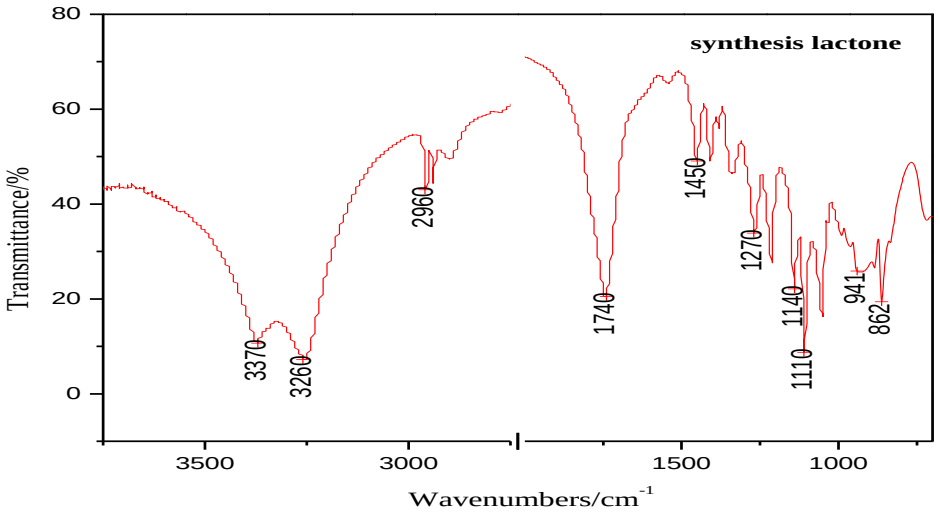

Figure 3.7 FTIR (KBr pallets) spectrum of D-glucaro-6, 3-lactone: lactone C==O stretch, 1740 cm^{-1} (possible overlapped with carboxylic C==O stretch), methylene C—H stretch,, 2960 cm^{-1}, broad O—H stretch, 32603370 cm^{-1}, alcohol C—O stretch 1270 cm^{-1}, 1110 cm^{-1}, alcohol O—H bend, 1360 cm^{-1}, weak carboxylic C—O and O—H absorption bands, 1336 cm^{-1} (not labeled) and 1460 cm^{-1}

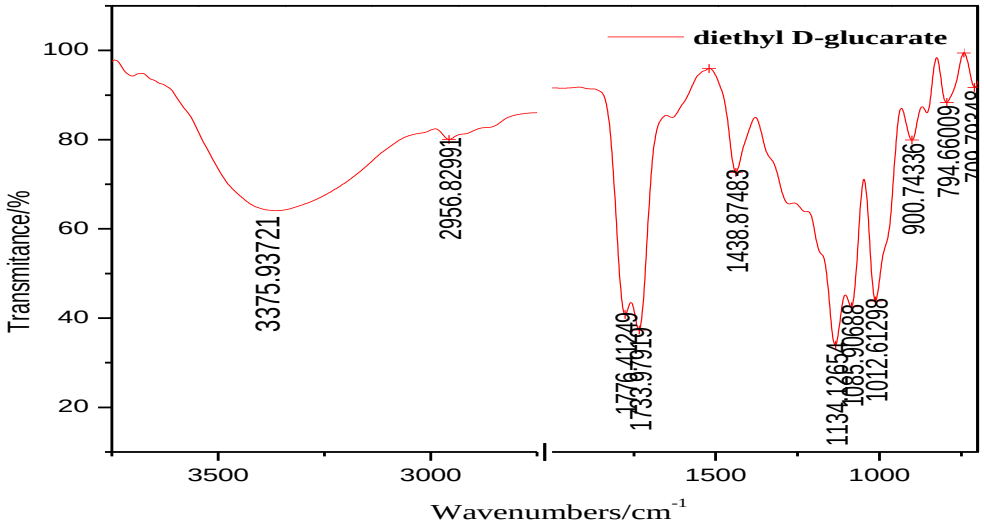

Figure 3.8 FTIR (NaCl plates) spectrum of dimethyl D-glucarate: broad O—H stretch band, 3364 cm^{-1}, lactone and ester stretch, 1734 cm^{-1}, 1776 cm^{-1}

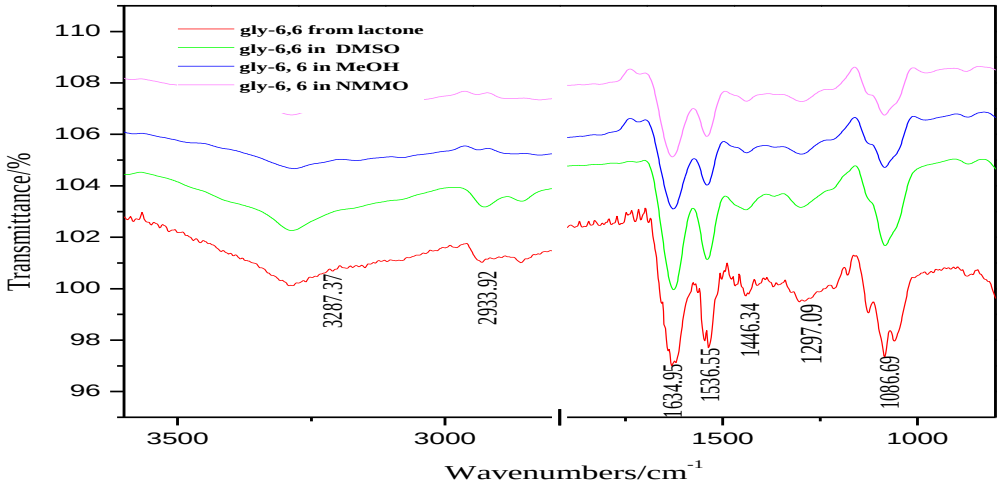

Figure 3.9 Comparative FTIR (KBr pallets) spectra of glylons-6, 6 synthesized in different solvents: O—H stretch, 3281 cm^{-1}, C—H stretch, 2933 cm^{-1}, amide I C==O stretch, 1643 cm^{-1}, amide II C==O stretch, 1536 cm^{-1}, asymmetrical and symmetrical N—H stretch 3287 cm^{-1} out-of-plane N—H wagging, 664 cm^{-1}

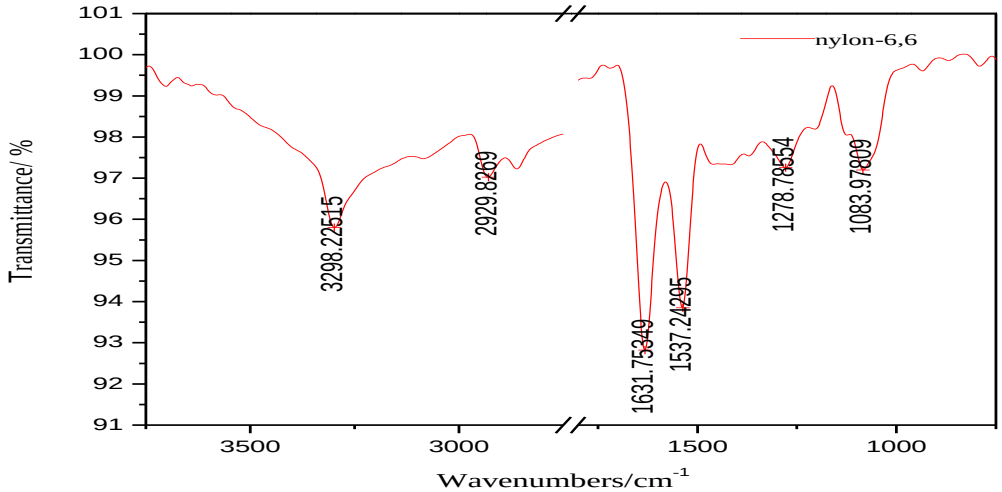

Figure 3.10 FTIR (KBr pallets) spectrum of nylon-6,6 :O—H stretch, 3298 cm^{-1}, C—H stretch,2929 cm^{-1}, amide I C==O stretch, 1631 cm^{-1}, amide II C==O stretch, 1537 cm^{-1}.

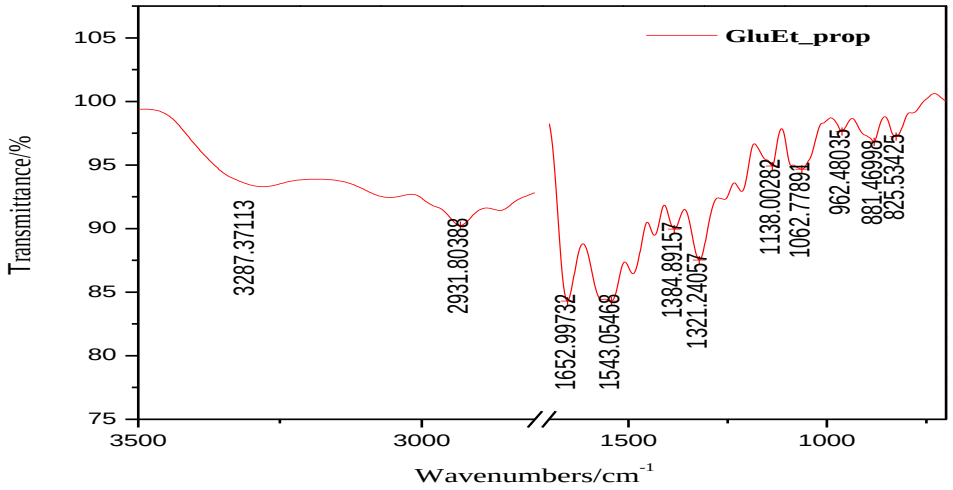

Figure 3.11 FTIR (NaCl plates) spectrum of GluEt_prop: weak broad O—H stretch band 3287 cm^{-1}, methyl and mehylene C—H stretch, 2931 cm^{-1}, amide I C==O stretch, 1662 cm^{-1}, amide II C==O stretch, 1543 cm^{-1}, acetal C—O –C stretch 1321 cm^{-1}, 1384 cm^{-1}, alcohol C—O stretch, 1062 cm^{-1}, asymmetrical and symmetrical N—H stretch 3287 cm^{-1}, out-of-plane N—H wagging, 881 cm^{-1}

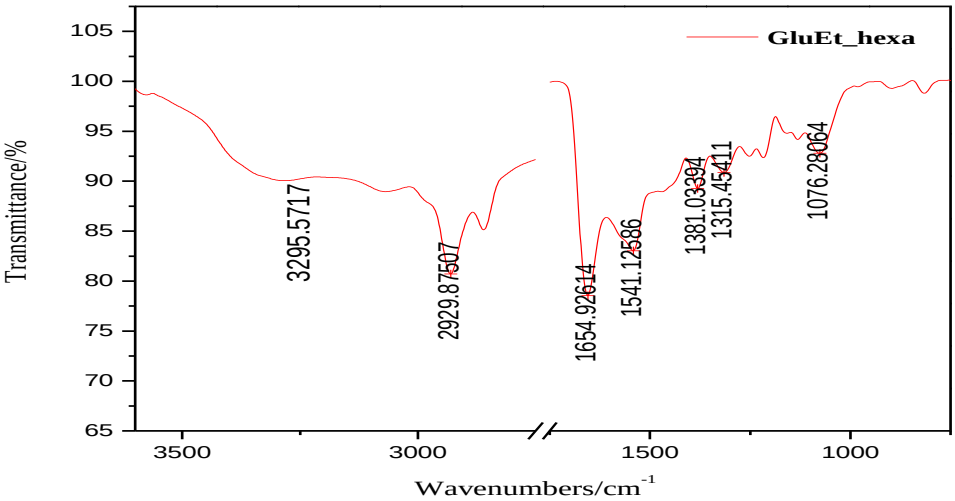

Figure 3.12 FTIR (NaCl plates) spectrum of GluEt_hexa: weak broad O—H stretch band 3295 cm^{-1}, methyl and mehylene C—H stretch, 2929 cm^{-1}, amide I C==O stretch, 1664 cm^{-1}, amide II C==O stretch, 1541 cm^{-1}, acetal C—O –C stretch 1315 cm^{-1}, 1381.03 cm^{-1}, alcohol C—O stretch 1076 cm^{-1}, asymmetrical and symmetrical N—H stretch 3295 cm^{-1}

Figure 3.13 Comparative FTIR spectra of GalEt_prop and GalEt_hexa

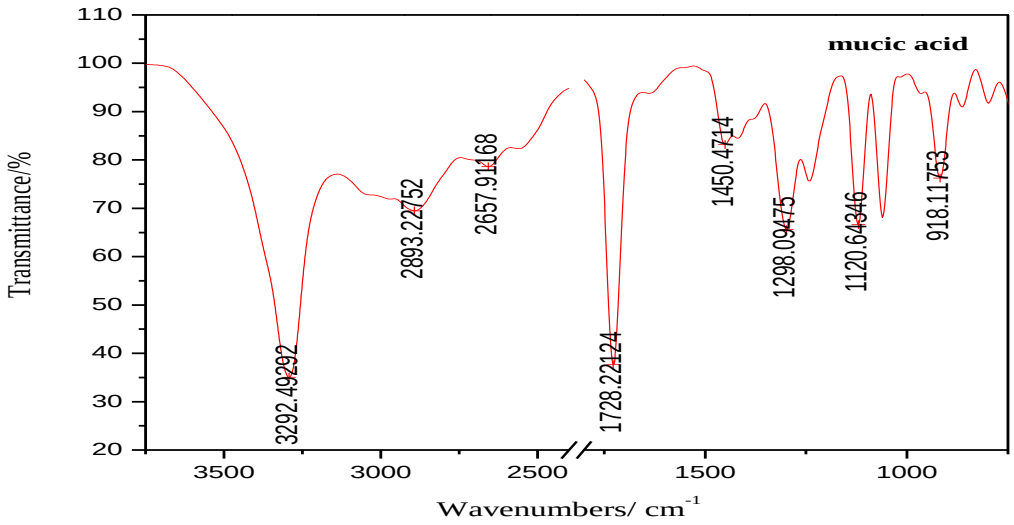

Figure 3.14 FTIR (KBr pallets) spectrum of mucic acid purchased by Aldrich: carboxyl C==O stretch, 1728 cm^{-1}, methyl C—H stretch, 2893 cm^{-1}, broad O—H stretch, 3292 cm^{-1}, alcohol C—O stretch 1120 cm^{-1}, 918 cm^{-1}, carboxylic C─O and O—H absorption bands, 1298 cm^{-1} and 1450 cm^{-1}

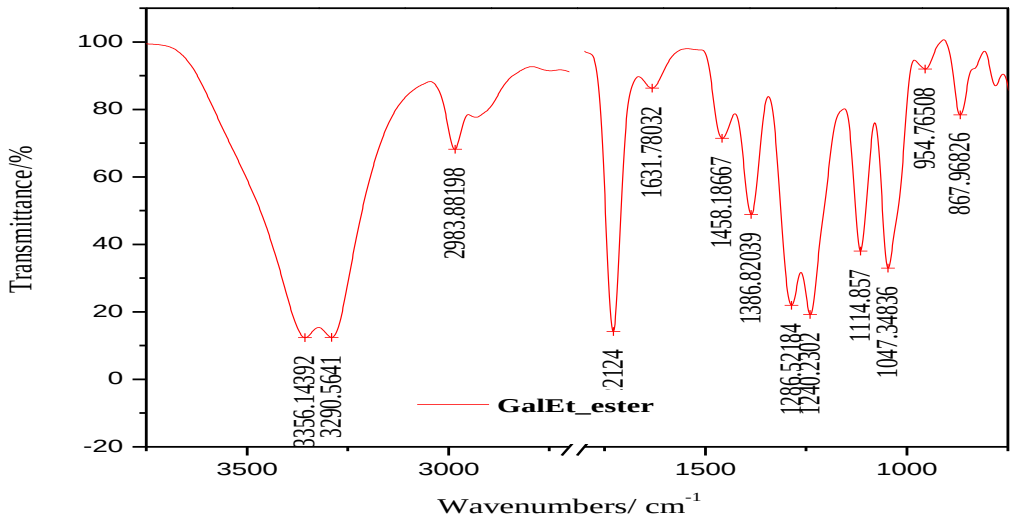

Figure 3.15 FTIR (KBr pallets) spectrum of diethyl galactarate: ester (possible lactone overlapping) C==O stretch ,1728 cm^{-1}; 1114 cm^{-1}, methyl C—H stretch, 2893 cm^{-1}, broad O—H stretch, 3290 cm^{-1}, 3356 cm^{-1}, alcohol O—H in-plane bending and C—H wag 1458 cm^{-1}, 1386 cm^{-1}, 1114 cm^{-1}.

very important impact on molecular symmetry. Galactaric acid has a symmetric configuration given by the mirror plane. These conformations favor inter and intramolecular H-bonding.

Acetalation reaction gave a valuable intermediate compound, diethyl 2,3: 4,5-bis-*O*-iso-propylidene galactarate, confirmed by FTIR (Figure 3.16). The strong bands at 1220 cm^{-1} and 1112 cm^{-1} are assigned to C—O—C stretch. The secondary alcohol C—O stretch, 1047 cm^{-1} disappeared. The broad O—H stretch, observed for diethyl galactarate, 3290 cm^{-1}, vanished (Figure 3.17). In order to increase the stability of the acetals 2, 2-dimethoxypropane, the acetalation agent, was replaced with benzaldehyde. The aromatic nucleus behaves like a withdrawn group and the resonance structure can strengthen the acetal stability. The out of plane ==C—H bend occur at 759 and 702 $cm^{-1}$and C==C ring stretch is shown at 1404 and 1462 cm^{-1}. However, these absorption bands are not as strong as expected (Figure 3.18 and 3.19). A possible explanation would be that the reaction didn't go to completion.

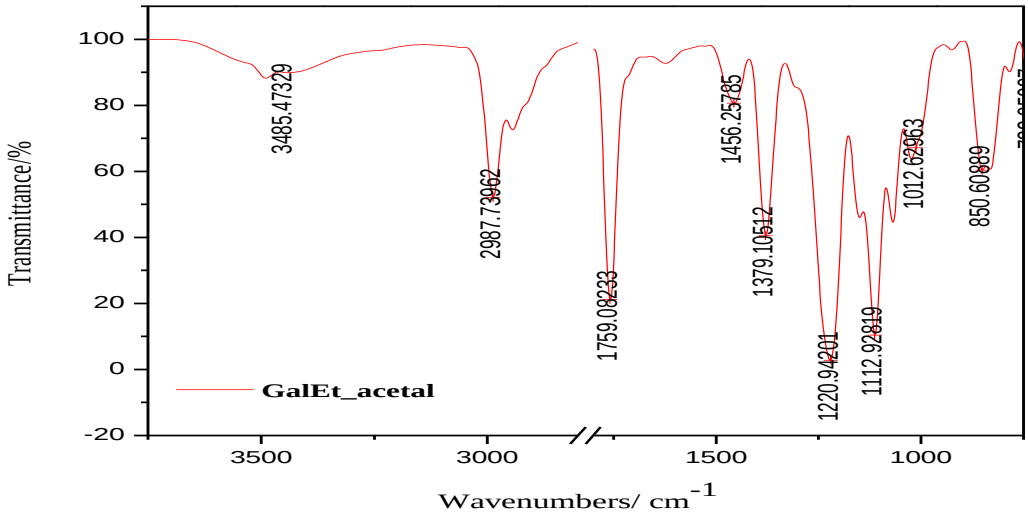

Figure 3.16 FTIR (KBr pallets) spectrum of galactaric acid 2, 3: 4, 5-bis-*O*-isopropylidene diethylester: methyl C—H stretch, 2987 cm^{-1}, ester C==O stretch, 1759 cm^{-1}, weak O—H stretch, 3485 cm^{-1}, strong acetal C—O—C stretch 1220 cm^{-1}, 1112 cm^{-1}

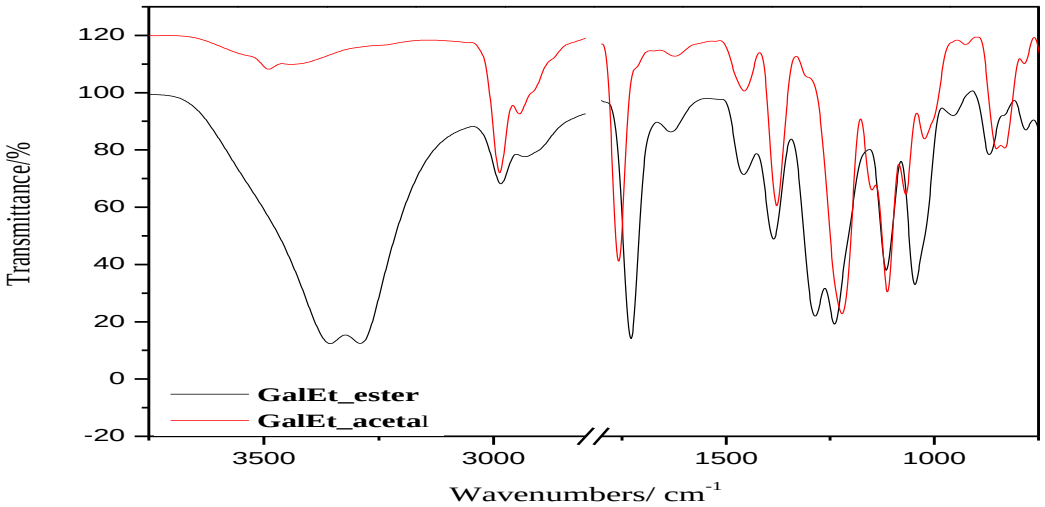

Figure 3.17 Comparative FTIR spectra for diethyl glucarate (GalEt_ester) and galactaric acid 2, 3: 4, 5-bis-*O*-isopropylidene diethylester (GalEt_acetal)

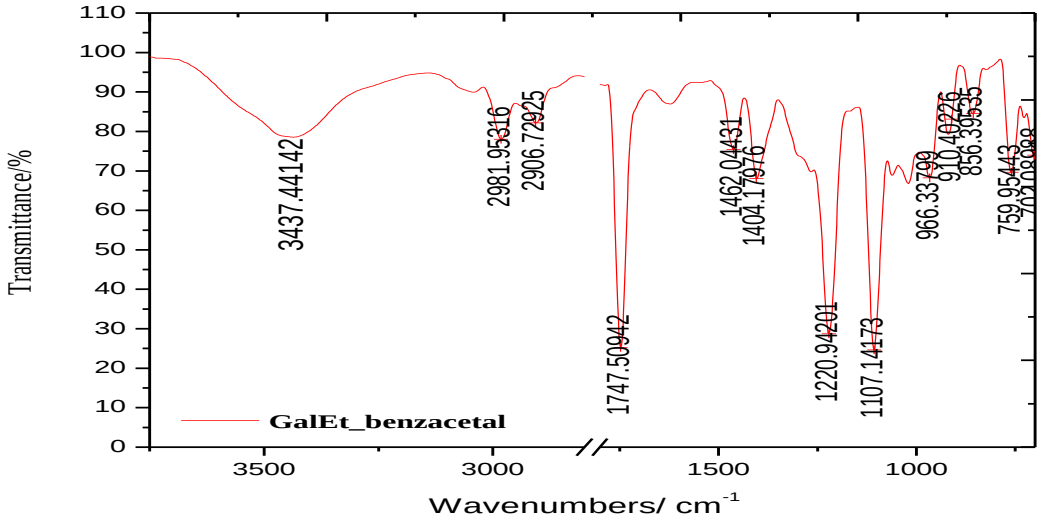

Figure 3.18 FTIR (KBr pallets) spectrum of galactaric acid 2, 3: 4, 5-bis-*O*-benzylidene diethylester (GalEt_benzacetal): methyl C—H stretch, 2981 cm^{-1}, 2906 cm-1, ester C==O stretch, 1747 cm^{-1}, broad O—H stretch overlapped with aromatic C—H stretch, 3437 cm^{-1}, strong acetal C—O—C stretch 1220 cm^{-1}, 1107 cm^{-1}, out-of-plane C—H bend, 858 cm^{-1}, 759.95 cm^{-1}, out-of plane ring C==C bend 702 cm^{-1}.

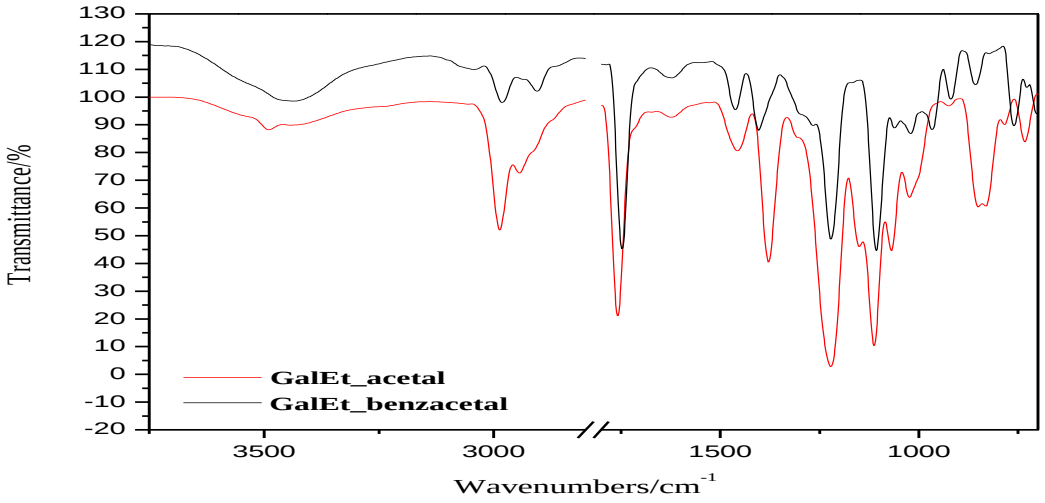

Figure 3.19 Comparative FTIR spectra of galactaric acid 2, 3: 4, 5-bis-*O*-isopropylidene diethylester (GalEt_acetal) and galactaric acid 2,3: 4,5-bis-*O*-benzylidene diethylester (GalEt_benzacetal)

The polymers derived from galactaric acid were investigated and the recorded spectra gave the confirmation of their synthesis. The bands for amide I and II can be observed at 1666 cm^{-1} and 1533 cm-1 with a shift of ±2 cm^{-1} (Figures 3.20 and 3.21). The attempts to control the stoichiometry of the GalEt_hexa led to the idea to combine different ratios of monomers. The intensity of ester band depends highly on the ratio of the monomers. A 1:1 proportion of diacid to diamine indicate a very weak band for ester (Figure 3.22). The single exception noticed is for GalEt_hexa1:0.98. The same trend can be observed for the GalEt_prop derivatives (Figure 3.23 and Figure 3.24 for comparison).

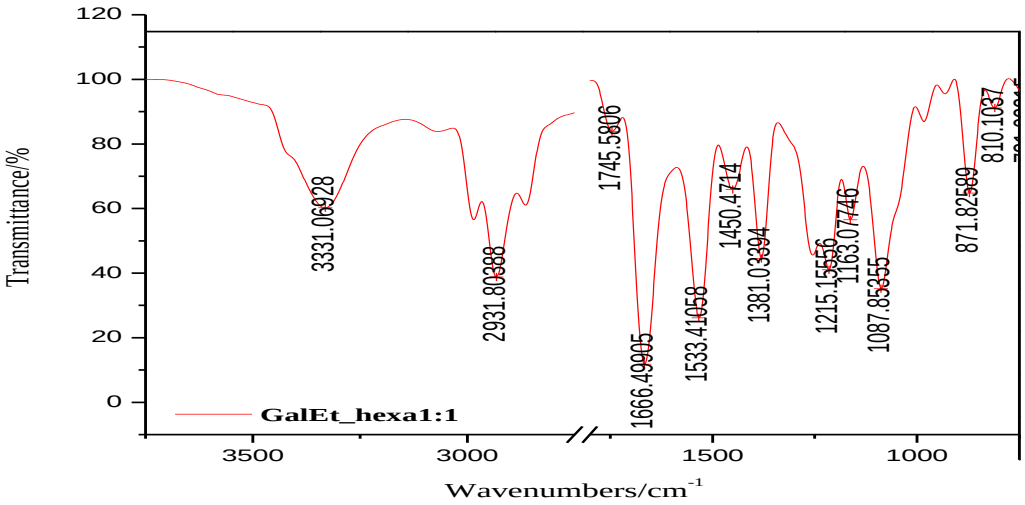

Figure 3.20 FTIR (NaCl plates) spectrum of GalEt_hexa: weak ester C==O stretch, 1745 cm^{-1}, methyl and mehylene C—H stretch, 2929 cm^{-1}, amide I C==O stretch, 1664 cm^{-1}, amide II C==O stretch, 1541 cm^{-1}, acetal C—O—C stretch 1315 cm^{-1}, 1381 cm^{-1}, alcohol C—O stretch 1078 cm^{-1}, asymmetrical and symmetrical N—H stretch 3331 cm^{-1}, out-of-plane N—H wagging,

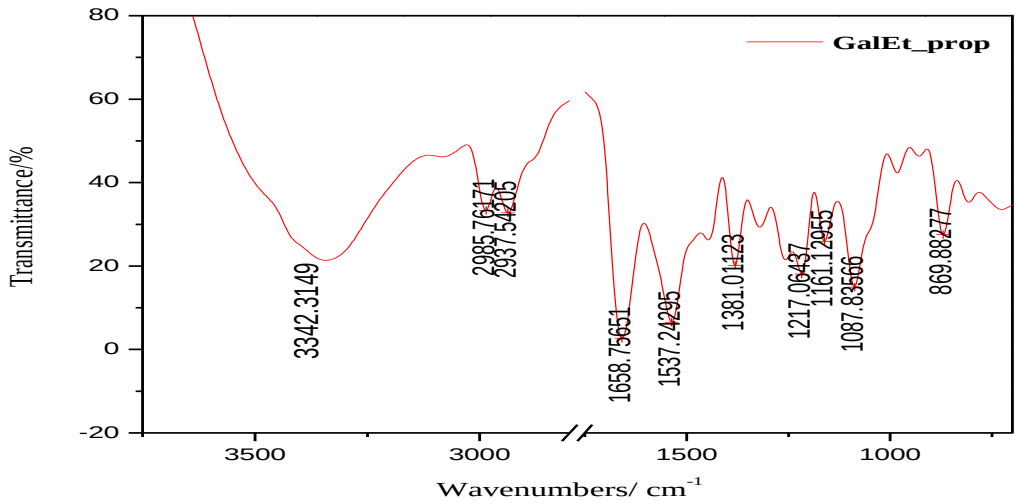

Figure 3.21 FTIR (NaCl plates) spectrum of GalEt_prop: methyl and mehylene C—H stretch, 2986 cm^{-1}, 2937 cm^{-1}, amide I C—O stretch, 1658 cm^{-1}, amide II C==O stretch, 1537 cm^{-1}, acetal C—O—C stretch 1381 cm^{-1}, 1217 cm^{-1}, asymmetrical and symmetrical N—H stretch 3342 cm^{-1} out-of-plane N—H wagging, 869 cm^{-1}

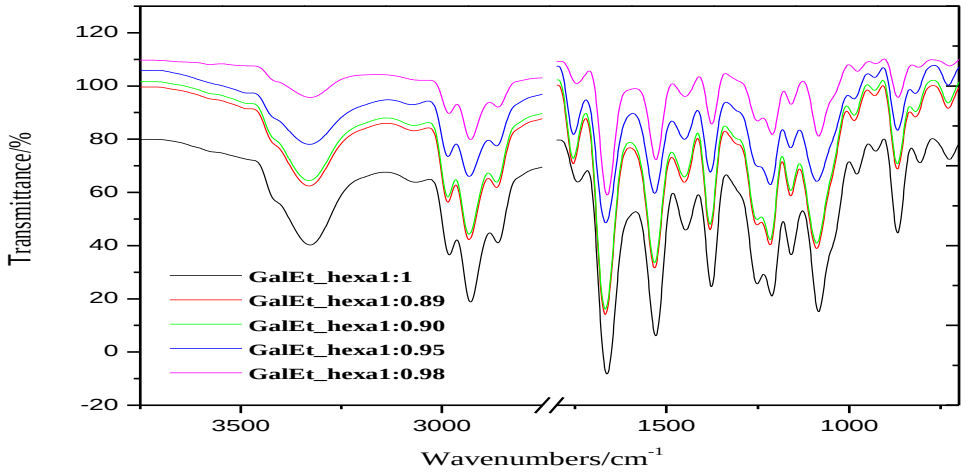

Figure 3.22 Comparative FTIR spectra of GalEt_hexa polymers synthesized by varying the ratios of monomers

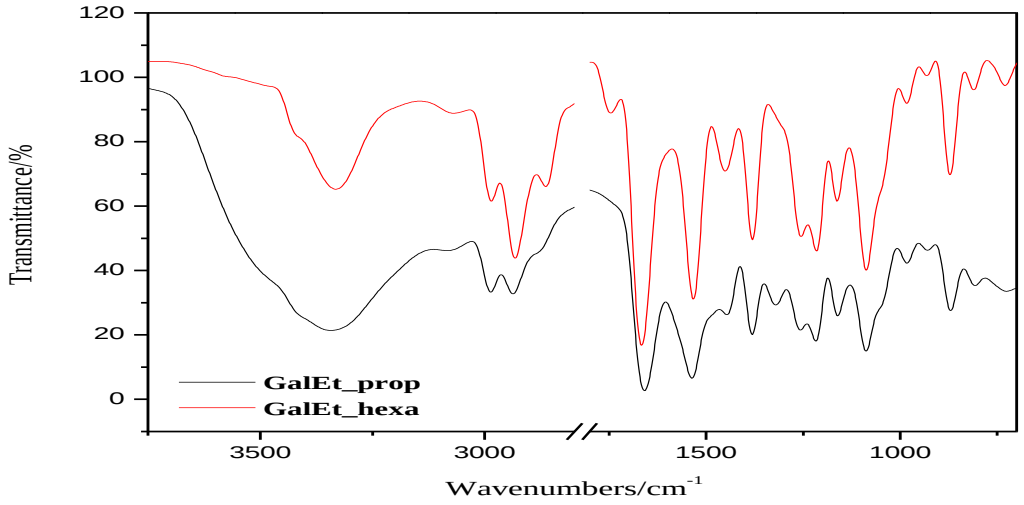

Figure 3.23 Comparative FTIR spectra of GalEt_prop and GalEt_hexa

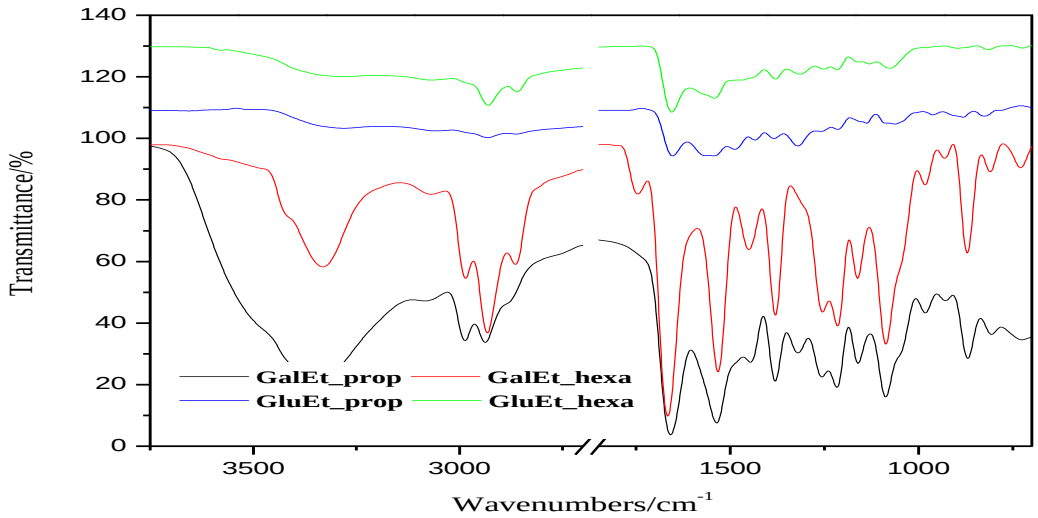

Figure 3.24 Comparative FTIR spectra of acetalated D-glucaric and galactaric acids derivatives

The polymers subjected to deprotection reaction were investigated by FTIR to visualize the appearance of secondary alcohol stretches and disappearance of the acetal bands. The deprotection was conducted for different reaction times: 30 and 60 minutes. The reaction involves hydrolysis of acetal groups by trifluroacetic acid and free OH groups' on the galactaric chain. The spectra show the broad OH stretches, 3334 cm^{-1} (GalEt_hexa30min), 3321 cm^{-1} (GalEt_hexa60min), the secondary alcohol C—O stretches, 1041 cm^{-1} (GalEt_hexa30min),1196 cm^{-1} (GalEt_hexa60min) (Figure 3.25 and Figure 3.26). The acetalated polymer has three peaks assigned to different alkyl groups of the chain. The deprotected counterpart has only two specific bands which do account for the hydrolysis of acetal groups and their removal (Figure 3.27).

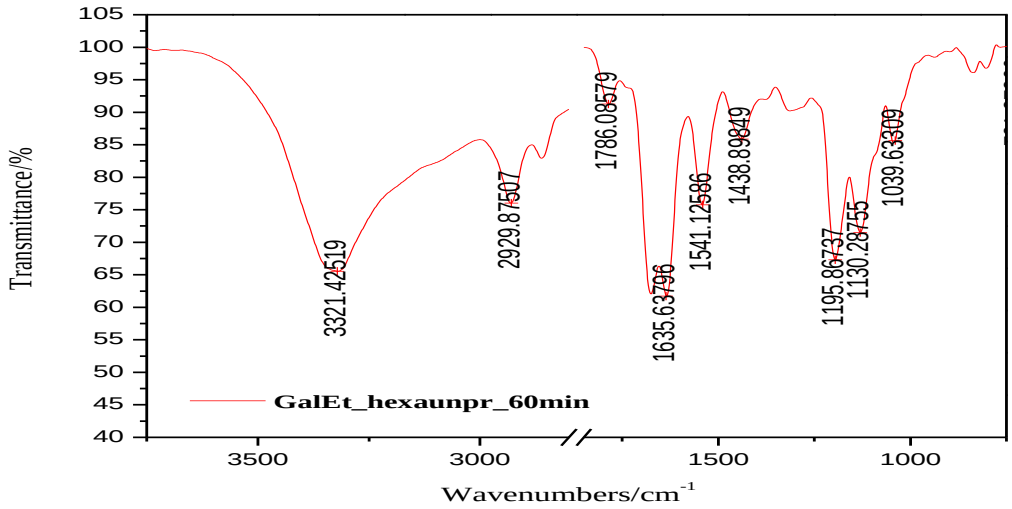

Figure 3.25 FTIR (KBr pallets) spectrum of GalEt_hexaunpr_60min**:** weak ester C==O stretch, 1786 cm^{-1}, methyl and mehylene C—H stretch, 2929 cm^{-1}, amide I C==O stretch, 1635 cm^{-1}, amide II C==O stretch, 1541 cm^{-1}, alcohol C—O stretch 1039 cm^{-1}, overlapped asymmetrical and symmetrical N—H and O—H stretch, 3321 cm^{-1} , out-of-plane N—H wagging, 721 cm^{-1}

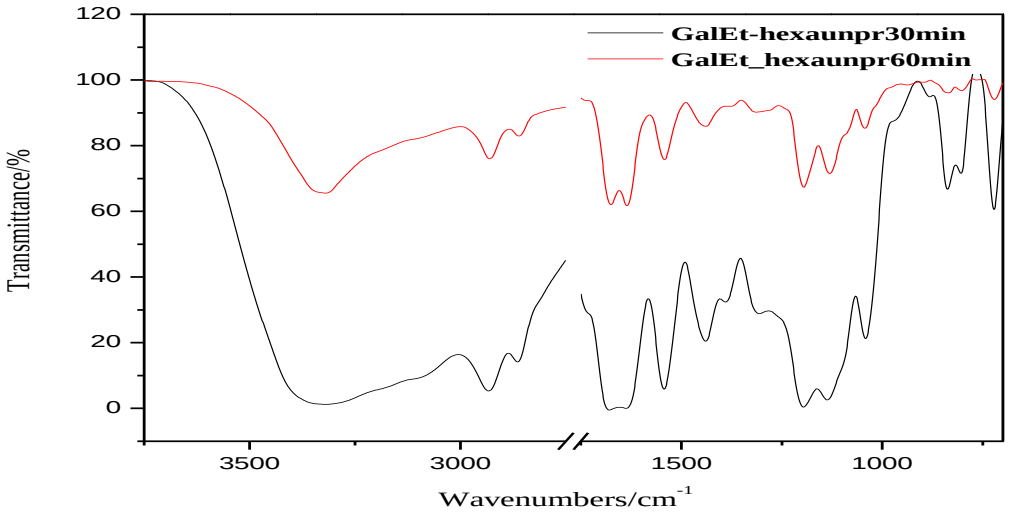

Figure 3.26 Comparative FTIR spectra of deprotected GalEt_hexa compounds synthesized at different reaction times

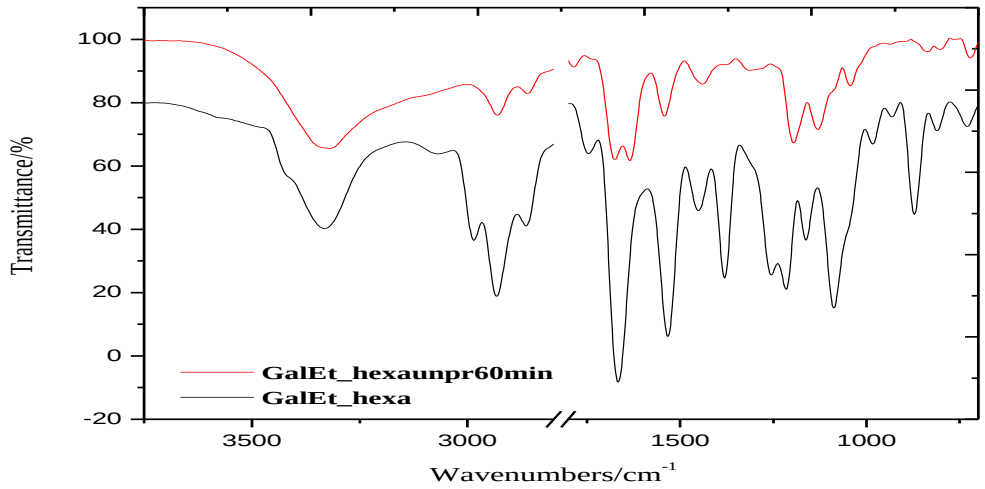

Figure 3.27 Comparative FTIR spectra of protected and deprotected GalEt_hexa

3.4 Matrix Assisted Laser Desorption/Ionization Time of Flight (MALDI-TOF)

Maldi-Tof analyzes intact biomolecules and synthetic polymers soft ionized. One important feature of the method consists of capability to investigate a broad mass range of molecules. The advantage of the technique resides emerges from its high sensitivity and fast data acquisition. The sample is mixed with excess matrix (e.g. dithranol, indolacrylic) and dried on a Maldi plate. After the deposition the plate is irradiated with laser pulses that cause the ionization of the matrix molecules. Then a matrix ion transfer a one proton to a sample molecule inducing its ionization. Ions are formed in pulses. Small ions will reach the detector faster than the large ones. The instrument records the time for ions to reach the detector.

Several studies were performed and the results produced questions about the accuracy and repeatability of the MALDI-TOF MS analysis. Therefore the study on the dependency of the various parameters revealed that for synthetic polymers the choice of the optimum matrix, the solvent and the sample purity has a great influence on the molecular mass distribution (MMD).[42] The laser energy influences as well the MMD of the polymers. Other key factor with a high impact is the instrument calibration.[43] For this work, the measurements were performed with a ProFLEX™ III BRUKER DALTONICS instrument equipped with a nitrogen laser (377 nm).

3.4.1 Glucaric Acid-Based Glylons

D-glucaric derivatives were difficult to characterize by MALDI-TOF because of their low solubility explained in section 3.3. The H-bonding and asymmetrical configuration of D-glucose are responsible for these properties pointed out earlier by Kiely[26] and Ogata.[11] Furthermore during the polymerization reaction of acetalated derivatives cyclic and linear species are suspected to form. The cyclization reactions terminate the polymerization. In order to improve the polymer solubility different mixtures of polar and unpolar solvents were used (Tables 3-6, 3-7 and 3-8).

Table 3-6 Different ratios of DMSO/$CHCl_3$ used to form a 5% solution of glylons-6, 6

No.	Glylon-6, 6 (g)	Dimethylsulfoxide DMSO, (g)	Chloroform $CHCl_3$, (g)
1	0.1	5	15
2	0.1	10	10
3	0.1	15	5

Table 3-7 Different ratios of DMSO/DCM used to form a 5% solution of glylons-6, 6

No.	Glylon-6, 6 (g)	Dimethylsulfoxide DMSO, (g)	Dichloromethylene CH_2Cl_2, (g)
1	0.05	2.5	0.7.5
2	0.05	5.0	5.0
3	0.05	7.5	2.5

Table 3-8 Different ratios of hexane/ethylacetate used to form a 5% solution of glylons-6, 6

No.	Glylon-6, 6 (g)	Hexane (g)	Ethylacetate (g)
1	0.05	2.5	7.5
2	0.05	5.0	5.0
3	0.05	7.5	2.5

Various matrices were tried as standards to record the spectra. The results were not very promising. In addition to these mixtures BMIMCl was tried as well in the attempt to find the best solvent to solubilize the polymer and in the same time to be suitable for mass spectroscopy. The spectra recorded are shown in the Figures 3.28, 3.29, 3.30, 3.31 and 3.32. The soluble part of polymer observed on these spectra can be assigned to the very low molecular species, oligomers, formed during the condensation process.

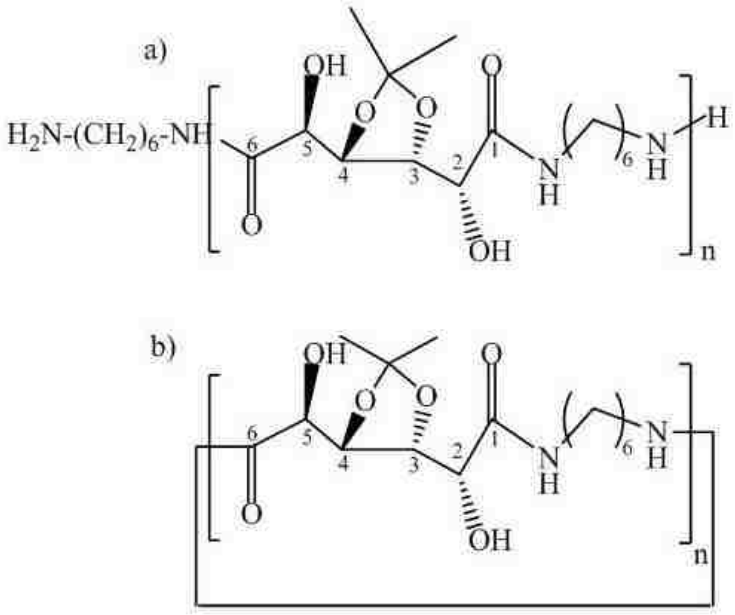

Figure 3.28 Linear, a), and cyclic, b), structures identified by MALDI-TOF MS for D-glucaric acid derivatives. The unit mass is 330 g· mol^{-1}.

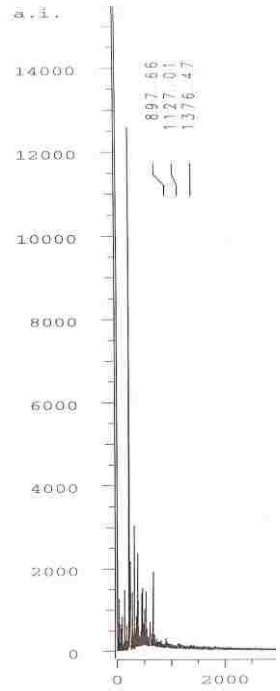

Figure 3.29 MALDI-TOF spectrum of a 5% solution of glylon-6, 6 in a mixture of hexane/ethylacetate (2.5:7.5). The unit mass is 218 g· mol^{-1}

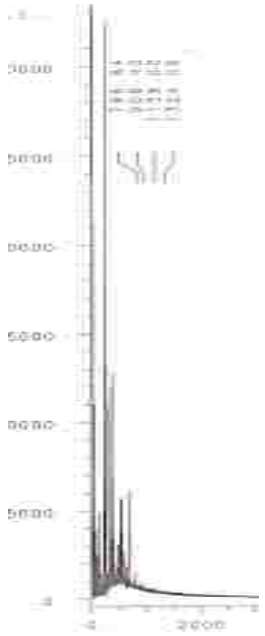

Figure 3.30 MALDI-TOF spectra of a 5% solution of glylon-6, 6 in a mixture of DMSO/$CHCl_3$ (5.0:5.0). The unit mass is 218 g· mol^{-1}

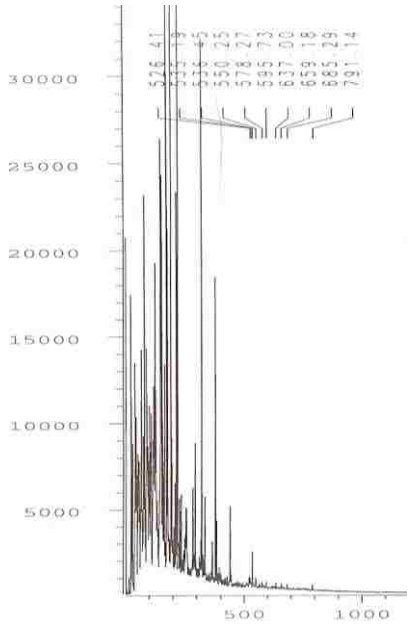

Figure 3.31 MALDI-TOF spectra of a 5% solution of glylon-6, 6 in a mixture of DMSO/DCM (7.5:2.5). The chosen combination of solvents failed to give fragments separated by unit mass.

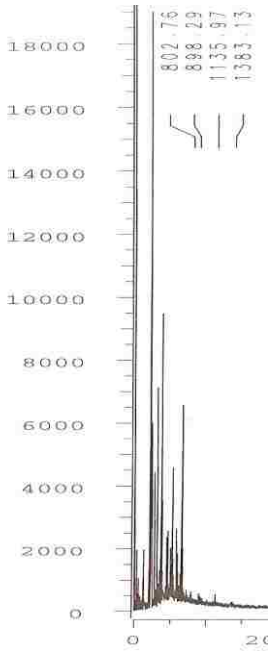

Figure 3.32 MALDI-TOF spectra of a 5% solution of glylon-6, 6 in BMIMCl.

Another approach was to protect the OH groups by acetalation reaction. Indeed an improvement in solubility was noticed and allowed the recording of better resolved MALDI-TOF MS spectra. Yet the polymer didn't go totally in solution. By visual evaluation, less than 20% was found dissolved. Due to their conformation acetalated D-glucose derivatives still have two OH free groups. The H-bonding is present but at low intensity. The best solvent tried for the solubilization of acetalated D-glucaric derivatives was chloroform. It is true that the resolution depends on how volatile the solvent is and on the ability of polymer to form complexes with the metal from chromophore. The results may be corrupted by the other species formed during heating of chromophore and ion formation. The polymer molecules can be fragmented during ionization and ion acceleration, and the fragments will appear in the spectra as multiple peaks. Even with these limitations, the analysis of the spectra confirmed the hypothesis regarding the coexistence of cyclic and linear structure as shown in Table 3-9, for GluEt_hexa (Figure 3.33

and Figure 3.34). The spectrum for GluEt_prop failed to reveal the expected species because the amount of polymer dissolved was too low to be detected by MALDI-TOF spectrometer (Figure 3.35). The modifications performed on the D-glucaric derivatives by acetalation reaction gave hope for an improvement in solubilities and higher molecular weight species (Figure 3.35).

Table 3-9 Relative peak species of GluEt_hexa (20mg/ml) shown by MALDI-TOF MS

No.	n	Linear $[M+A^*]^+$+82	Cyclic $[M]^+$+80
1.	n=2	857	738
2.	n = 3	1188	1069
3.	n = 4	1518	1399
4.	n = 5	1848	1729
5	n = 6	2179	2060
6.	n = 7	2509	2390
7.	n = 8	2840	2721

A*- hexamethylene diamine

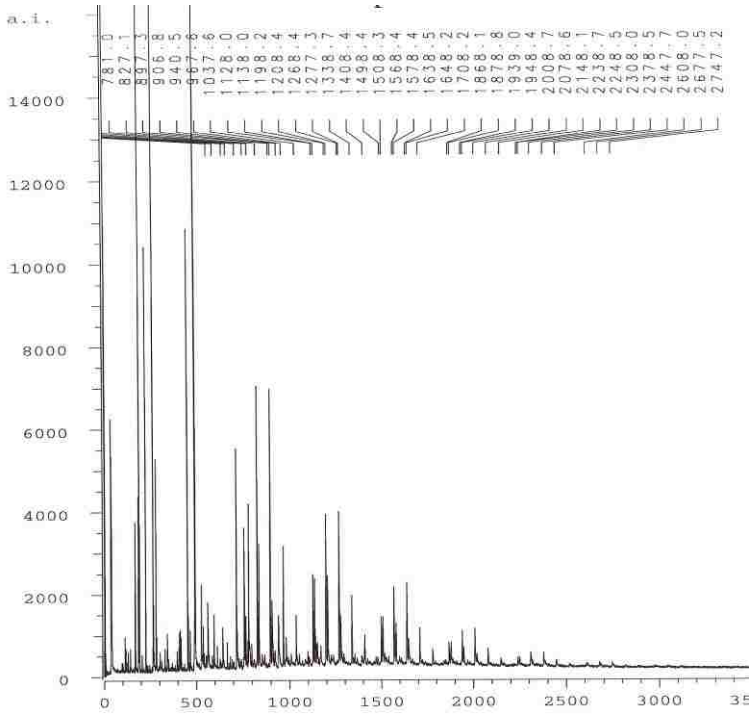

Figure 3.33 MALDI-TOF spectra of a 20 mg/ml solution of GluEt_hexa in $CHCl_3$. The spectrum shows several species obtained during fragmentation. The cyclic and linear forms are dominant. The unit mass is 320 g·mol^{-1}.

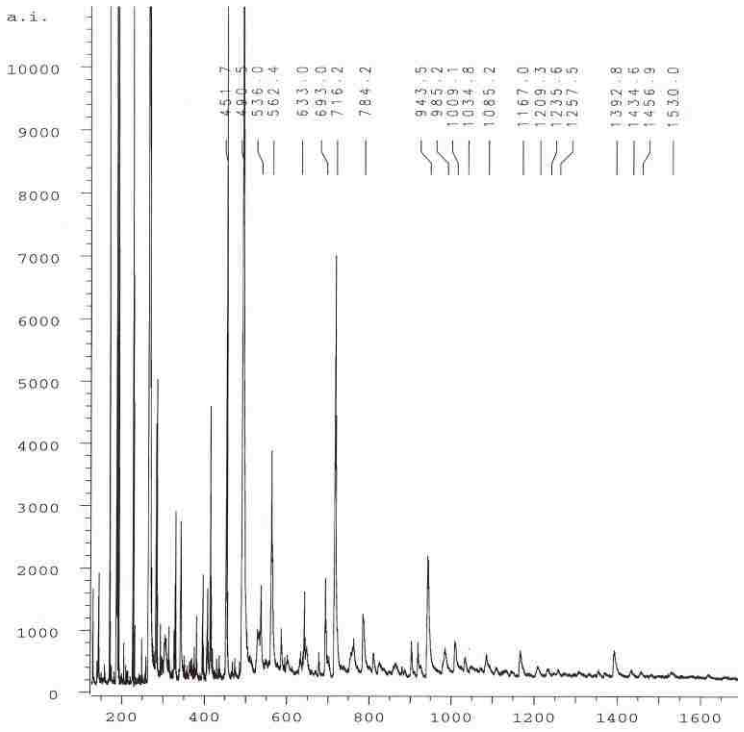

Figure 3.34 MALDI-TOF spectra of a 20% solution of GluEt_hexa in acetone.

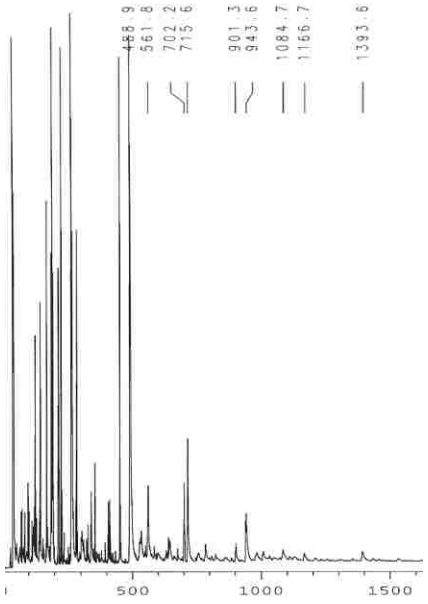

Figure 3.35 MALDI-TOF spectrum of a 20% solution of GluEt_prop in $CHCl_3$. The spectrum shows the pair of cyclic and linear structures formed during polymerization reaction. The unit mass is 216 g mol^{-1}.

MALDI-TOF analysis leads to idea that a procedure can be devised to block the other two OH. One good approach can be the methylation reaction. The molecule will became more organic suitable to dissolve in organic solvents.

The spectra of unprotected D-glucaric derivatives are not well resolved. It is apparent that the fragmentation process during ion acceleration gave a variety of fragments recorded in MALDI spectra. However the structures showed in Figure 3.28 were identified relatively easy. The distance between peaks for each linear or cyclic form equals the unit mass (330g/mol). Another issue was the identification of the terminal groups.

3.4.2 Galactaric Acid-Based Glylons

The broad range of solubility exhibited by acetalated galactaric acid-based glylons allows the use of MALDI-TOF MS spectroscopy as a main tool to characterize these compounds. The method has the capability to provide not only information about molecular mass moment and polydispersity but also on end group. The highest molecular weight species found in the spectra correspond to 15 units for GalEt_hexa. Yet the investigation encountered several difficulties. The results indicated that molecular mass distribution depends on instrumental and sample preparation. With these considerations the present investigation on galactaric derivatives started by finding the best matrix that can give reproducible results. The samples were analyzed in dithranol with 1, 1, 1-trifluoroacetone (TFK) (Figures 3.36, 3.37, 3.38, 3.39, 3.40 and 3.41) and indolacrylic acid (IAA) (Figures 3.42, 3.43, 3.44, 3.45, 3.46 and 3.47), positive mode, used as matrices and the results were compared. The data for GalEt_hexa1:0.95 and GalEt_prop1:0.95 are presented **(**Tables 3-10, 3-11, 3-12 and 3-13). The same trend is valid when calculations are performed on the other polymers.

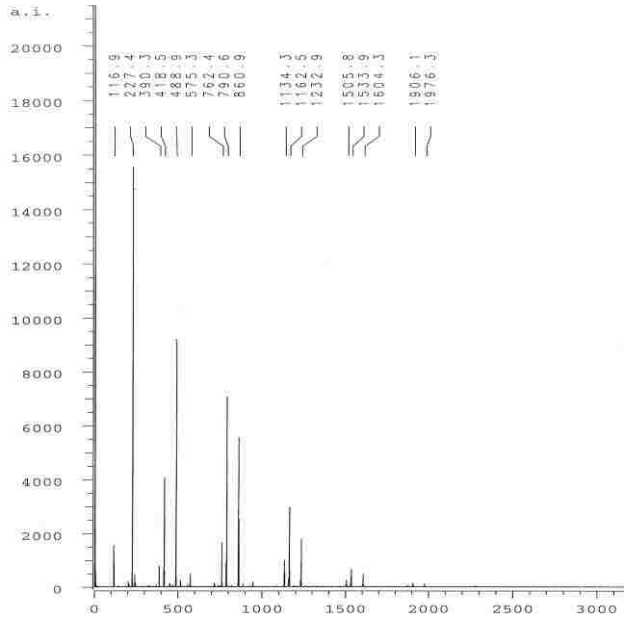

Figure 3.36 MALDI-TOF spectrum (dithranol as matrix) of a 20mg/ml solution of GalEt_hexa1:0.98.

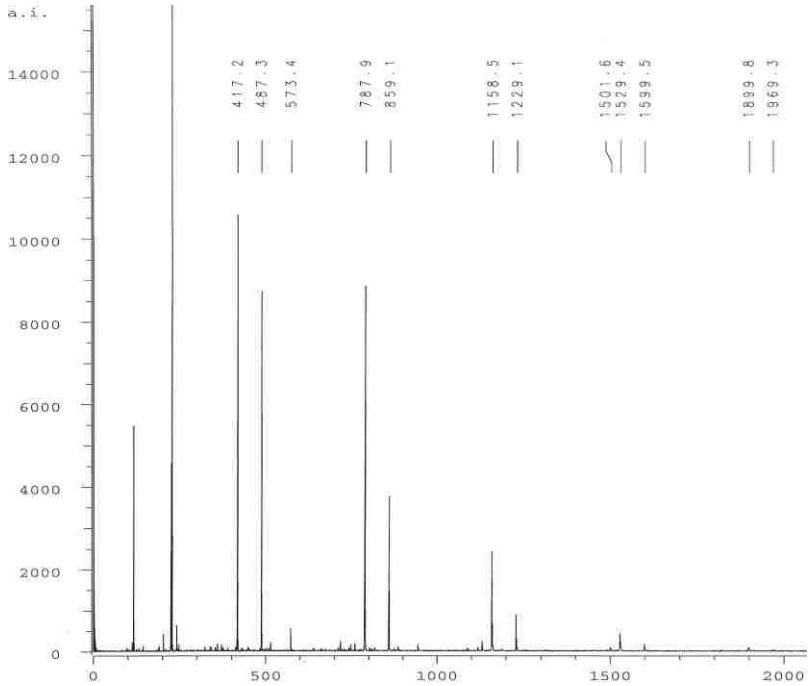

Figure 3.37 MALDI-TOF spectrum (dithranol as matrix, positive) of a 20mg/mL solution of GalEt_hexa1:0.95. Spectrum is well resolved.

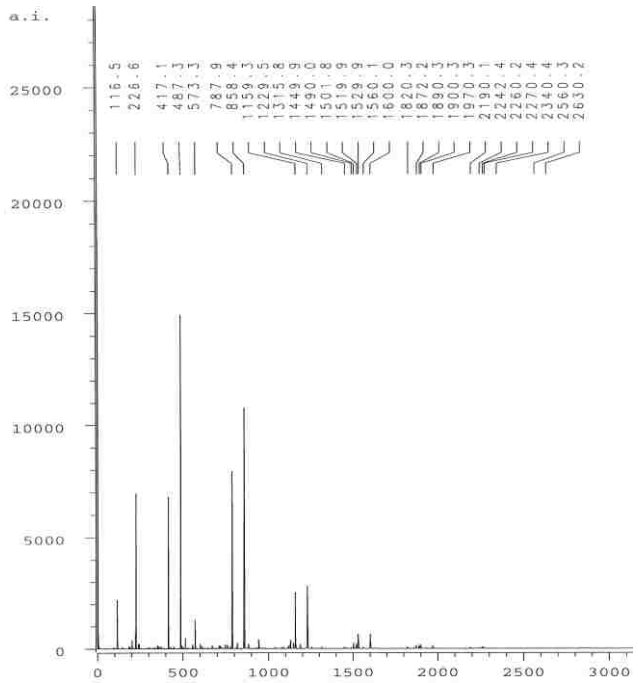

Figure 3.38 MALDI-TOF spectrum (dithranol as matrix) of a 20mg/ml solution of GalEt_hexa1:0.90 in chloroform. Spectrum run in dithranol as matrix is better resolved when compared with the one using IAA/TFK

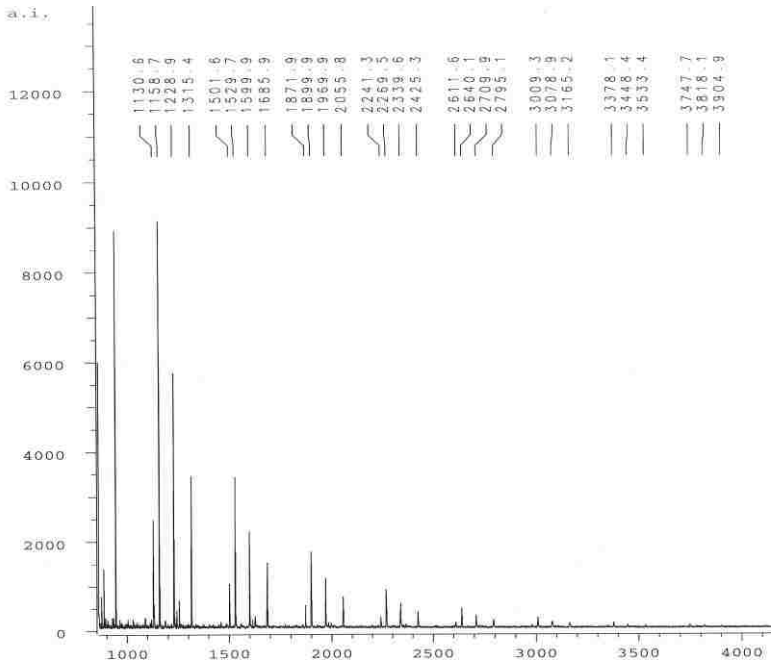

Figure 3.39 MALDI-TOF spectrum (dithranol as matrix) of a 20mg/ml solution of GalEt_hexa90h in chloroform.

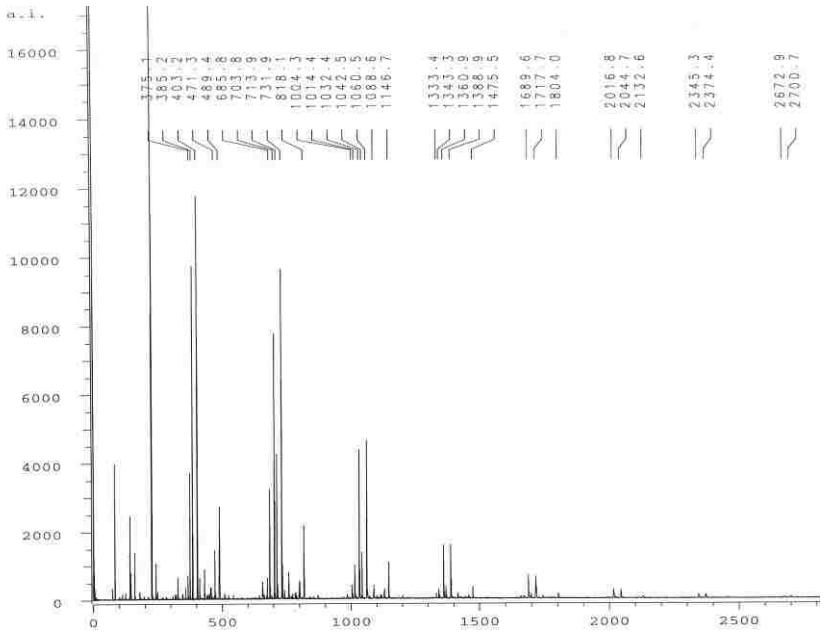

Figure 3.40 MALDI-TOF spectrum (dithranol as matrix) of GalEt_prop1:0.95 in $CHCl_3$.

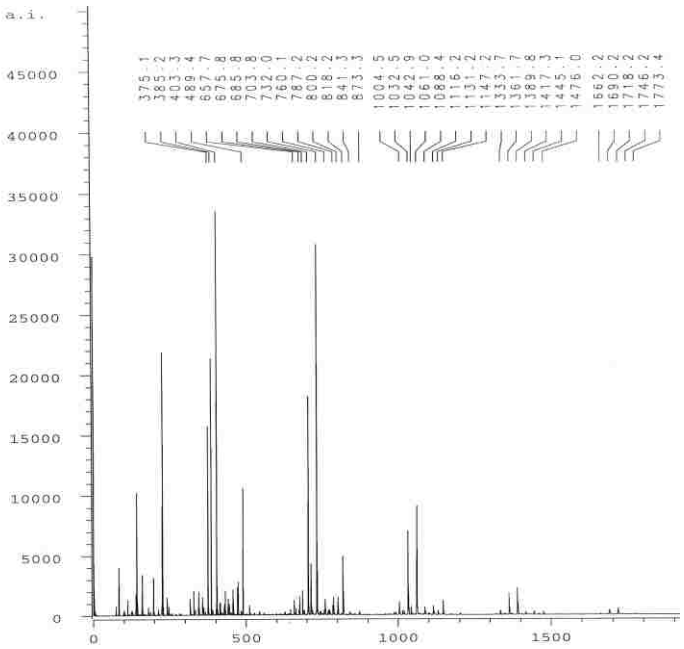

Figure 3.41 MALDI-TOF spectrum (dithranol as matrix) of a 20mg/ml solution of GalEt_prop1:0.98 in chloroform.

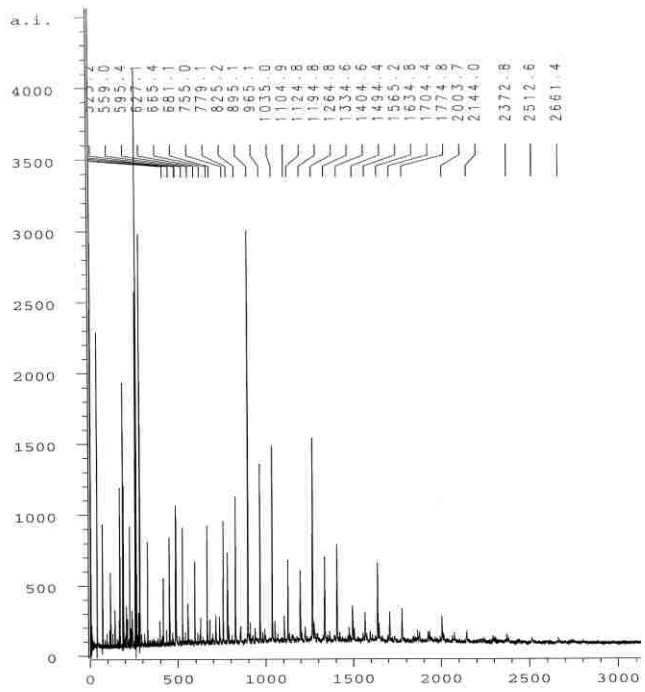

Figure 3.42 MALDI-TOF spectrum (IAA as matrix with TFK) of a 20% solution of GalEt_hexa 1:0.90 in $CHCl_3$.

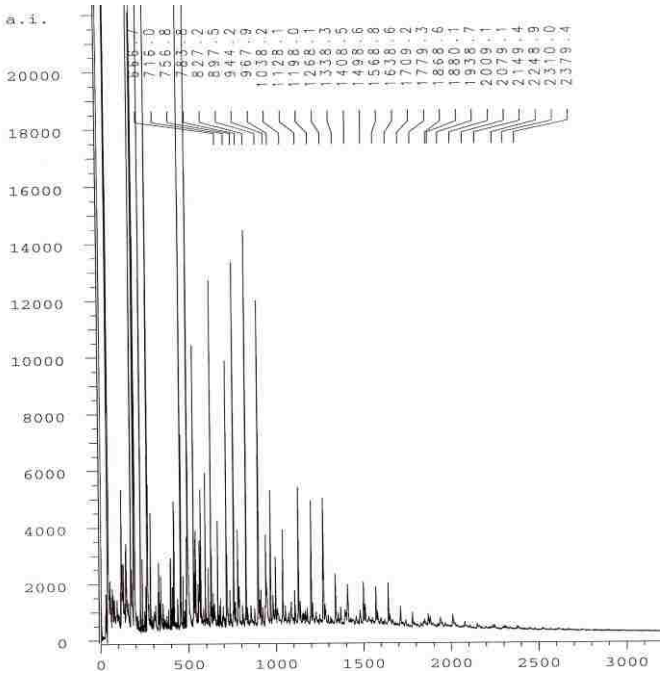

Figure 3.43 MALDI-TOF spectrum (IAA as matrix with TFK) of a 20% solution of GalEt_hexa 1:0.89 in $CHCl_3$

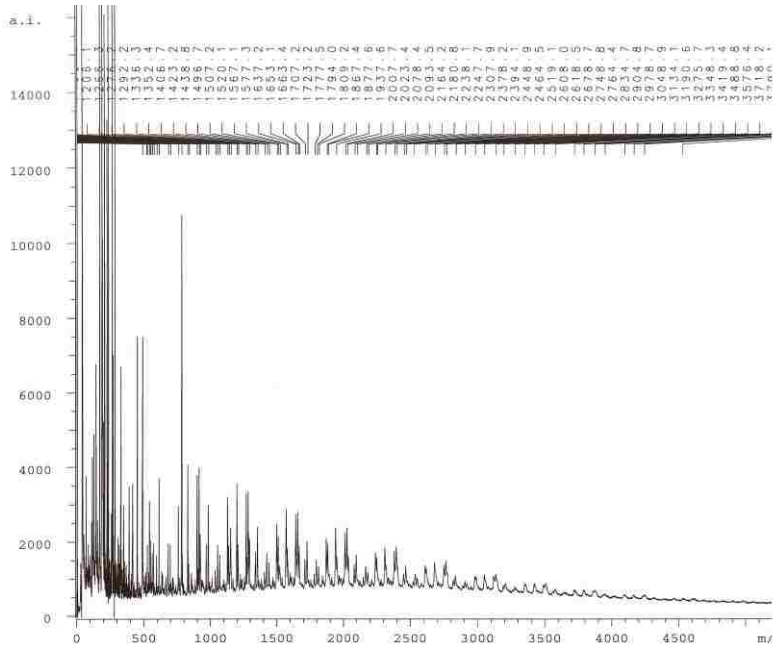

Figure 3.44 MALDI-TOF spectrum (IAA as matrix with TFK) of GalEt_hexa1:1 obtained after 90 h reaction time

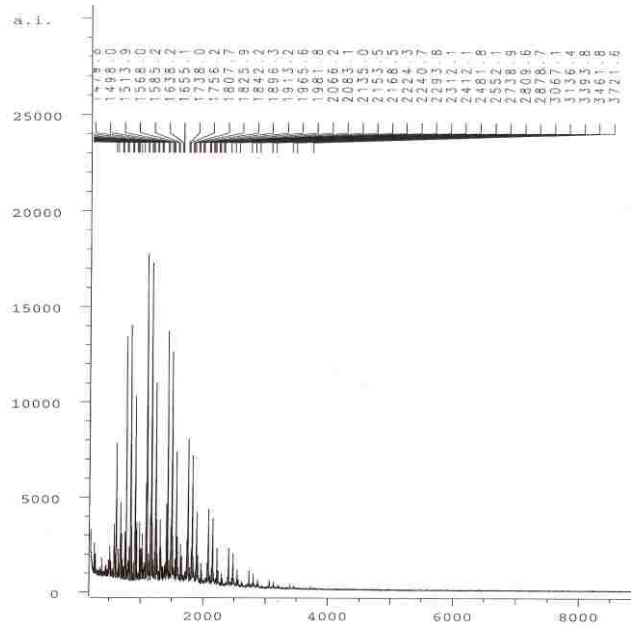

Figure 3.45 MALDI-TOF spectrum (IAA/TFK) of GalEt_prop1:1 in THF

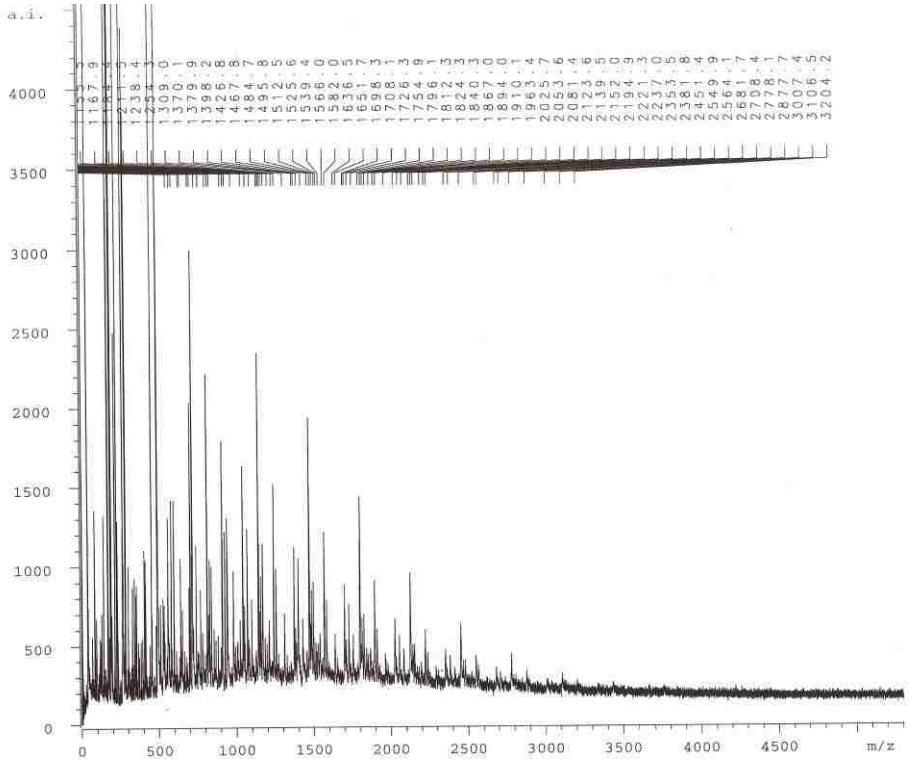

Figure 3.46 MALDI-TOF spectrum (IAA as matrix with TFK) of GalEt_prop1:0.95 in THF

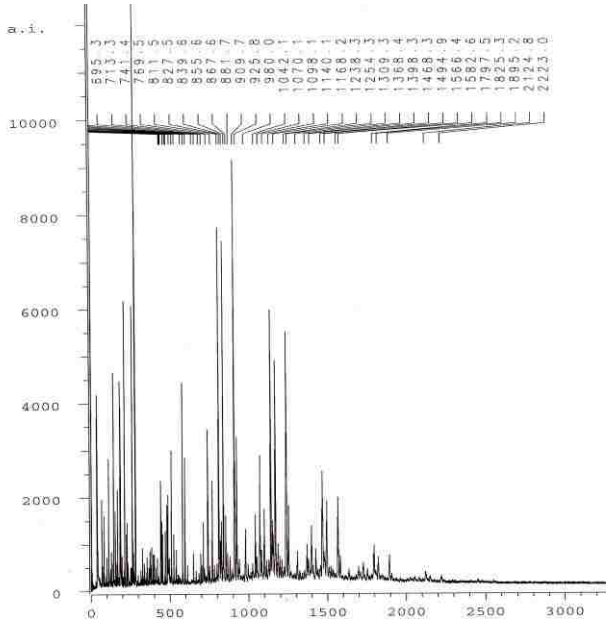

Figure 3.47 MALDI-TOF spectrum (IAA as matrix with TFK) of GalEt_prop1:0.98 in THF

Table 3-10 Linear and cyclic fragments identified in MALDI-TOF spectrum for GalEt_prop1:0.95 when positive mode, IAA with TFK was used as matrix

No.	n	Calculated (u)	Observed linear [M]+252u	Observed Cyclic [M] +154u
1.	N=2	646	909	811
2.	N=3	984	1238	1139
3.	N=4	1312	1566	1467
4.	N=5	1640	1894	1796
5.	N=6	1968	2221	2123
6.	N=7	2296	2549	2451
7.	N=8	2624	2877	2778
8.	N=9	2952	3204	3106

Table 3-11 Linear and cyclic fragments identified in MALDI-TOF spectrum for GalEt_hexa1:0.95 when positive mode, IAA with TFK was used as matrix

No.	n	Calculated (u)	Observed Linear [M]+ 156u	Observed Cyclic [M]+ 86u
1.	N=2	740	895	825
2.	N=3	1110	1266	1195
3.	N=4	1480	1636	1566
4.	N=5	1850	2007	1937
5.	N=6	2220	2377	2307
6.	N=7	2590	2746	2676
7.	N=8	2960	3116	3046

Table 3-12 Linear and cyclic fragments identified in MALDI-TOF spectrum for GalEt_prop1:0.95 when positive mode, dithranol was used as matrix

No.	n	Calculated (u)	Observed Linear [M]+ 162u	Observed Cyclic [M]+ 76u
1.	N=2	646	818	713
2.	N=3	984	1146	1060
3.	N=4	1312	1475	1388
4.	N=5	1640	1804	1717
5.	N=6	1968	2132	2044
6.	N=7	2296	2374	2345
7.	N=8	2624	2700	2672

Table 3-13 Linear and cyclic fragments identified in MALDI-TOF spectrum for GalEt_hexa1:0.95 when dithranol was used as matrix

No.	n	Calculated (u)	Observed Linear [M]+ 119u	Observed Cyclic [M]+ 49u
1.	N=2	740	859	787
2.	N=3	1110	1229	1158
3.	N=4	1480	1599	1529
4.	N=5	1850	1969	1899

The analysis of the two polymers showed that mass moments are significantly influenced by the matrix used. The moments of polymers analyzed in dithranol were found to be lower when compared with those obtained in IAA. Probably the IAA requires higher laser energy to ablate the polymers into the gas phase than dithranol.[42] Another effect observed is the multitude of peaks obtained that corresponds to various fragments. This can be explained by a lower thermal stability of the polymers confirmed by TGA analysis. The end group analysis revealed the diamine termination for linear structures. This finding is enforced by the basic pH of the polymer solutions. However the variance of 49u and 76u noticed in dithranol for cyclic form can be assigned to potassium ion plus a variance of 10u and 35u. It was suspected that the polymerization of galactaric acid derivatives will follow a similar trend as D-glucaric acid counterparts. More, cyclic species formation is favored and the condensation fails to proceed to high values of molecular weight. The occurrence of these forms might depend on the ratio of the monomers used or the diamine structure. Several ratios of monomers were tried in order to control the stereochemistry of the glylons. The molecular weights recorded by MALDI-TOF spectroscopy tend to decrease when the ratio of GalEt_acetal monomer to hexamethylene diamine is greater than 1 (Figures 3.48, 3.49, 3.50, and 3.51).

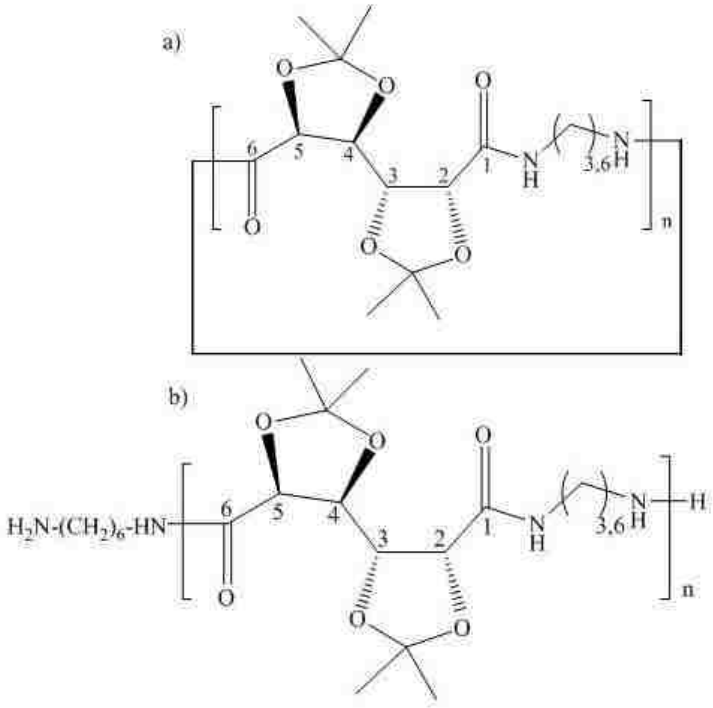

Figure 3.48 Cyclic (a) and linear (b) structures found in MALDI-TOF spectra for galactaric acid derivatives. The unit mass: 328 g· mol^{-1} (when 1, 3-propylene diamine is used) and 370 g· mol^{-1} (when hexamethylene diamine is used).

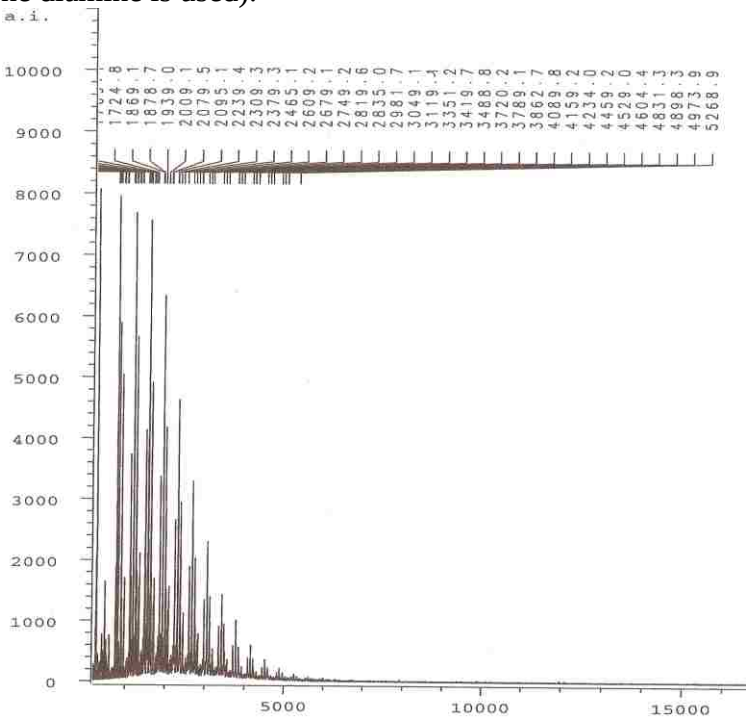

Figure 3.49 MALDI-TOF spectrum (ion positive mode) of a 20% solution of GalEt_hexa 1:1 in $CHCl_3$. The multitude of species obtained during fragmentation process can be noticed. For each region of spectrum the pair of cyclic and linear form is predominant.

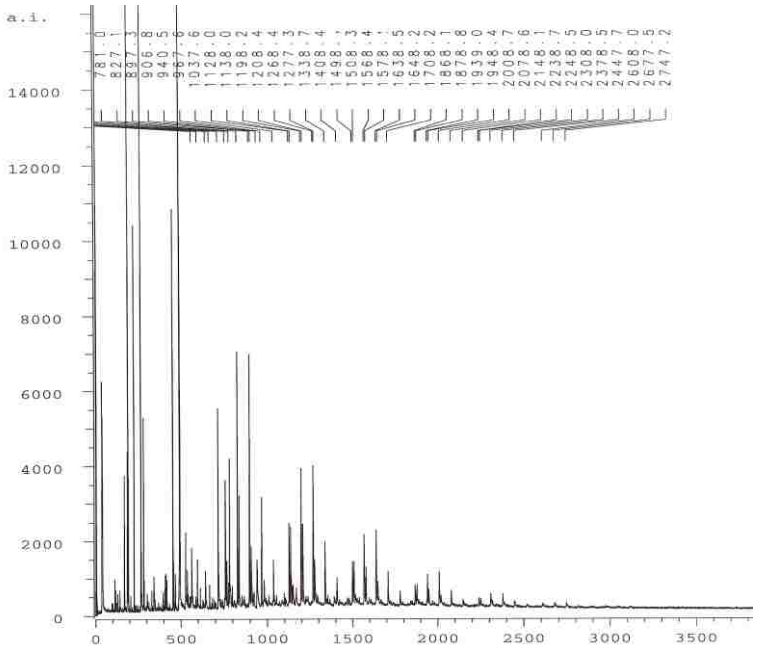

Figure 3.50 MALDI-TOF spectrum (IAA as matrix with TFK) of GalEt_hexa1:0.98. A decrease in MMD numbers can be observed and the multitude of species.

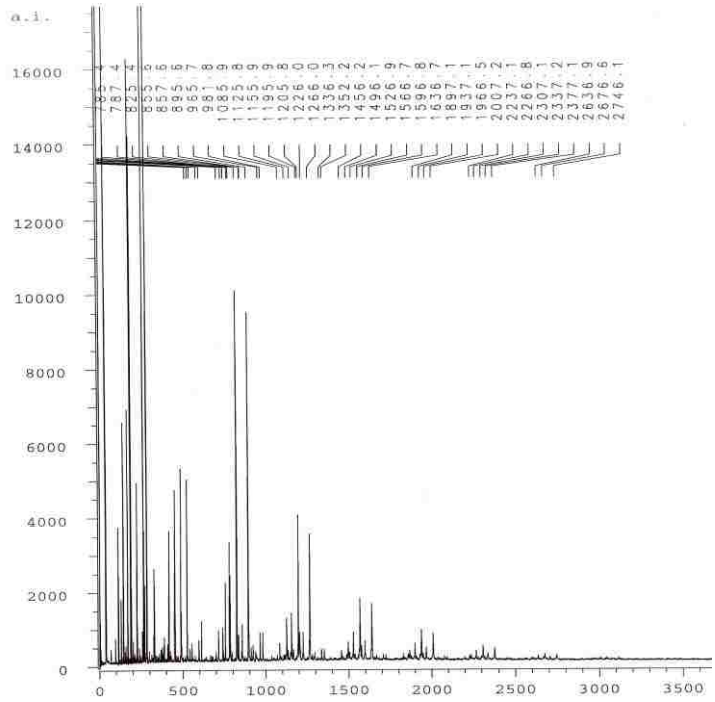

Figure 3.51 MALDI-TOF spectrum (IAA as matrix with TFK) of a 20% solution of GalEt_hexa 1:0.95 in $CHCl_3$.

Yet, the formation of cyclic structure cannot be assigned to the monomer ratios. The configuration of diamine governs the cyclization process. Probably diamines with linear, long and flexible chains can form cycles energetically favored. This could explain the higher peak for them when compared with linear counterparts. An efficient way to prove the supposition is to use branched diamines. The sterical hindrance imposed by the groups attached to the diamine backbone will not allow the cyclization. The need to understand and to control the stoichiometry of the polymerization reaction by varying the monomer ratios gave better results for 1:0.95 diacid to diamine for both type of polymers: GalEt_hexa and GalEt_prop.

MALDI-TOF method was used to prove the existence of larger size molecular weight species. As stated in section 3.2, the results provided by GPC sample preparation (filters weigh after use and drying) confirmed the presence of 13 even 15 unit species for GalEt_hexa. It is suspected that polymer chains self-assemble and form aggregates. Furthermore, the aggregates might be present in the system right from the beginning and during dissolution the solvent doesn't have enough energy to break them. In order to have an idea about the size of the polymer that didn't pass through filter a very simple test was performed: in one filter (GalEt_hexa1:1 sample) THF was injected slowly and for a long time (35-40 min.). The solution was collected and subjected to the MALDI-TOF analysis. The concentration was very low 3 mg/mL compared with the optimum of 20 mg/mL used in these kinds of investigations. The goal was to record the disappearance of low molecular weight peaks and to see the appearance of higher mass moments (Table 3-14). Figure 3.52 shows the spectrum of GalEt_hexa1:1 form GPC filter. The dimer peak vanished and for 3, 4 mers the intensities are lower when compared with the first spectrum (Figure 3.49). The majority of low molecular weight polymer solubilized and was recorded first time. This can explain a slight increase in the higher molecular weight moment in the recovered

polymer spectrum. Plus, the filter was weighed before been injected with THF and after drying.

The difference in mass was assigned to the polymer that didn't dissolve. The end group analysis

Table 3-14 Linear and cyclic fragments identified in MALDI-TOF spectrum for GalEt_hexa1:1 recovered from GPC filter. Dithranol with TFK was used as matrix.

No.	n	Calculated (u)	Observed Linear [M]+ 174u	Observed Cyclic [M]+ 18u
1.	N=2	740	not recorded	not recorded
2.	N=3	1110	1284	1128
3.	N=4	1480	1650	1498
4.	N=5	1850	2024	1868
5.	N=6	2220	2394	2238
6.	N=7	2590	2764	2609
7.	N=8	2960	3136	2979
8.	N=9	3330	3505	3348
9.	N=10	3700	3874	3719
10.	N=11	4070	4087	Too low intensity

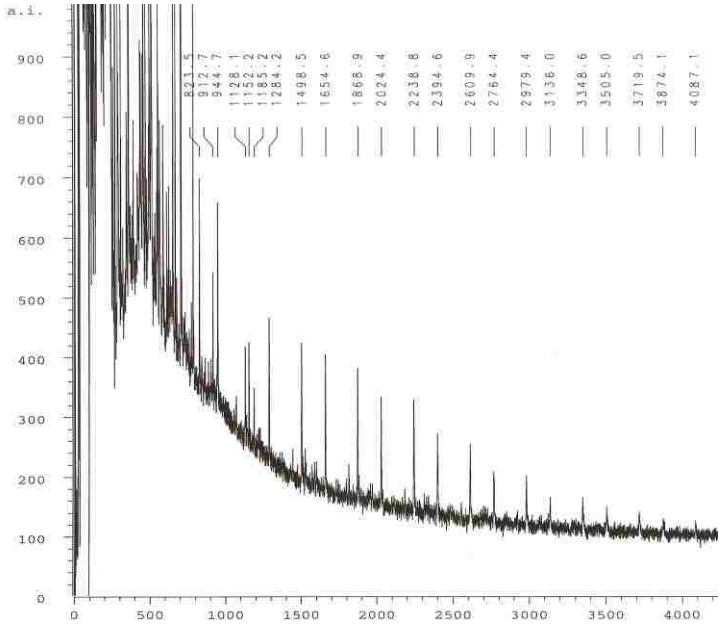

Figure 3.52 MALDI-TOF spectrum (dithranol as matrix with TFK, c= 3mg/ml) of a chloroform solution of GalEt_hexa1:1 recovered from filters used during GPC sample preparation

assigns the 174 units recorded for linear structure to diamine (confirmed by the basic pH also) plus potassium ion and possibly an oxygen ion. One end is diamine and the other could be potassium carboxylate (COO^-K^+). The use of 1,4-dioxane as an alternate solvent didn't give the expected values for the molecular mass distribution but confirmed the aggregation process (Figure 3.53). It is possible that longer reaction time to favor the formation of self assembly structures and this could be the reason for lower MMD numbers obtained when compared with the 48 h sample. The deprotection of OH groups at different reaction times showed a slight decrease in molecular weight comparing with protected counterparts, suggesting that the treatment with trifluoroacetic acid (TFA), can cause the degradation of the polymer (Figure 3.54 and Figure 3.55).

Conclusively, the acetalated galactaric and D-glucaric acid derivatives show a tendency to form cyclic and linear structures. The cyclization process is responsible for the lower MMD numbers observed in the spectrograms and, also, impede the evolution of linear structure to high

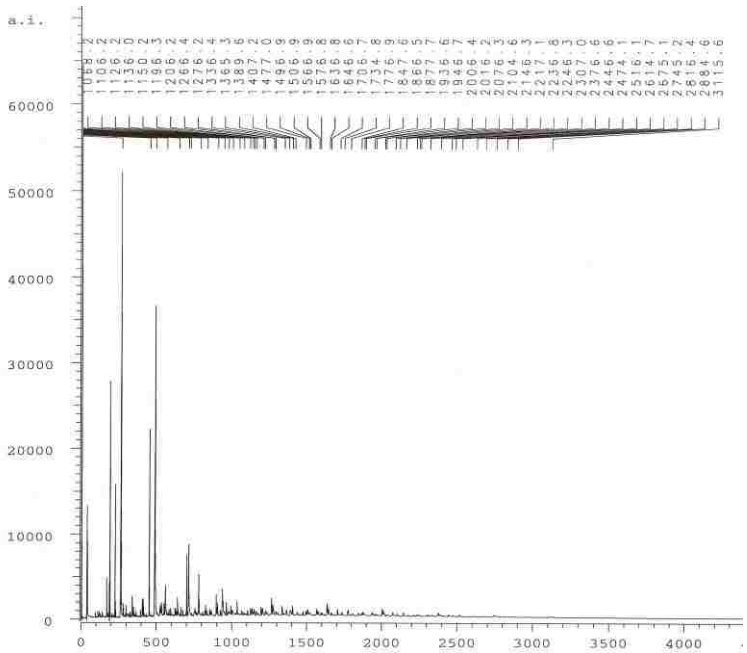

Figure 3.53 MALDI-TOF spectrum (IAA/TFK) of GalEt_hexa synthesized in 1,4-dioxane

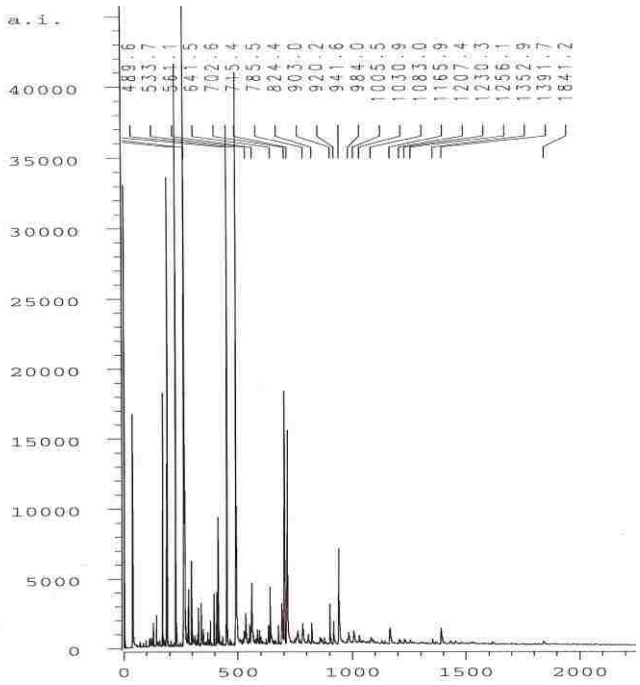

Figure 3.54 MALDI-TOF spectrum (IAA as matrix with TFK) of GalEt_hexaunpr30min

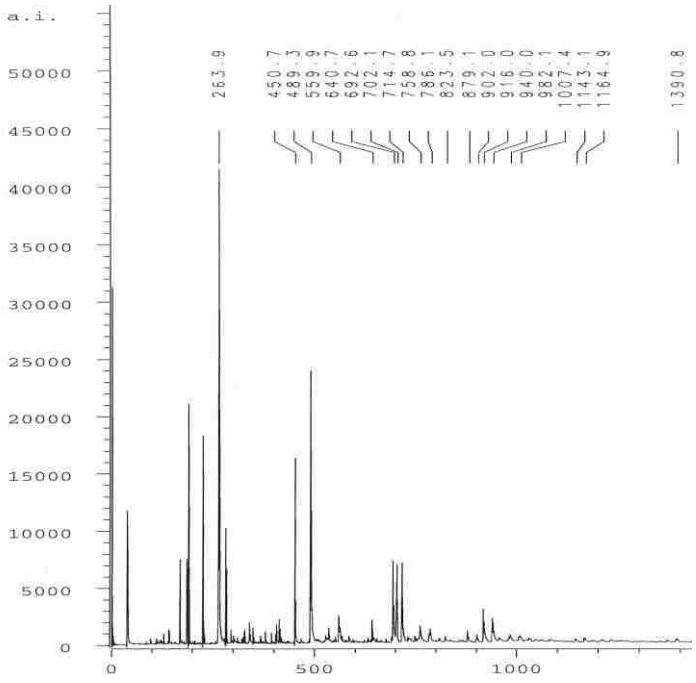

Figure 3.55 MALDI-TOF spectrum (IAA as matrix with TFK) of GalEt_hexaunpr60min

molecular weight values. The energy necessary to grow a longer linear chain is consumed to form the competitive cyclic structures. Yet, it is not very well understood what factor favors the parallel evolution of these two species. Further investigations on the diamine structure used in condensation reaction should clear this part.

3.5 Thermal Analysis and Calorimetry

Differential Thermal Analysis (TGA) and Differential Scanning Calorimetry (DSC) are two of the most widely methods of investigation. They provide information on thermal changes in a sample by heating or cooling it alongside an inert atmosphere.[44] The distinction between the DTA and DSC consists in the nature of the signal gathered from instrument. The signal for a differential thermal analyzer is proportional with the temperature difference between sample and reference when compared to a differential scanning calorimeter where the signal is proportional to the difference in thermal flow between the sample and reference.[44]

3.5.1 Differential Scanning Calorimetry (DSC)

Differential Scanning Calorimetry was carried out using a 2920 MDSC V2 6A instrument from TA Instruments at a scan rate of 5°Cmin^{-1}, under nitrogen, for both heating and cooling. The samples weight was in the range of 3-6 mg. The reference consisted of empty aluminum pans identical to those used to hold the sample. The purpose of DSC method was to investigate the transitions involved when the polymers are subjected to heating or cooling. Most of the samples showed glass-to-rubber, Tg, (endothermic), crystallization, Tc, (exothermic) and melting, Tm, (endothermic) phenomena. Glylons exhibited decomposition after melting. Therefore the attention was focused on transitions taking place at lower temperatures, such as Tg and Tc. The DSC traces were analysed using a TA universal analysis software.

3.5.1.1 D-Glucaric Acid-Based Glylons

Differential Scanning Calorimetry (DSC) was a very useful tool used to characterize

protected and unprotected glylons. The synthesis of lactone (2.1.1) didn't lead to success and the confirmation came from DSC analysis. When the lactone (2.1.1) was compared with that purchased from Aldrich the melting points were different (Figure 3.56). Aldrich lactone showed a transition (endothermic) at 195ºC while the other (labeled Cornelia lactone) exhibited it at 163ºC. These transitions are assigned to melting. The temperature variance is too high. Probably the analyzed compound contains a mixture of both monolactones: 1, 4 and 3, 6. The equilibrium between these species is very dynamic as shown by NMR investigations (see 3.7).Yet the FTIR spectra for the Aldrich lactone enforce a believe that the purity is not exactly that labeled on the bottle (98%). Glylons-6, 6 exhibited melting transitions in the range of 180- 197°C. The glass-to-rubber transitions are situated between 65- 75°C. The values point to low crystalline polymers. Another important behavior noticed is that glylons-6, 6 decompose right (Figure 3.57 and Figure 3.58) after melting.

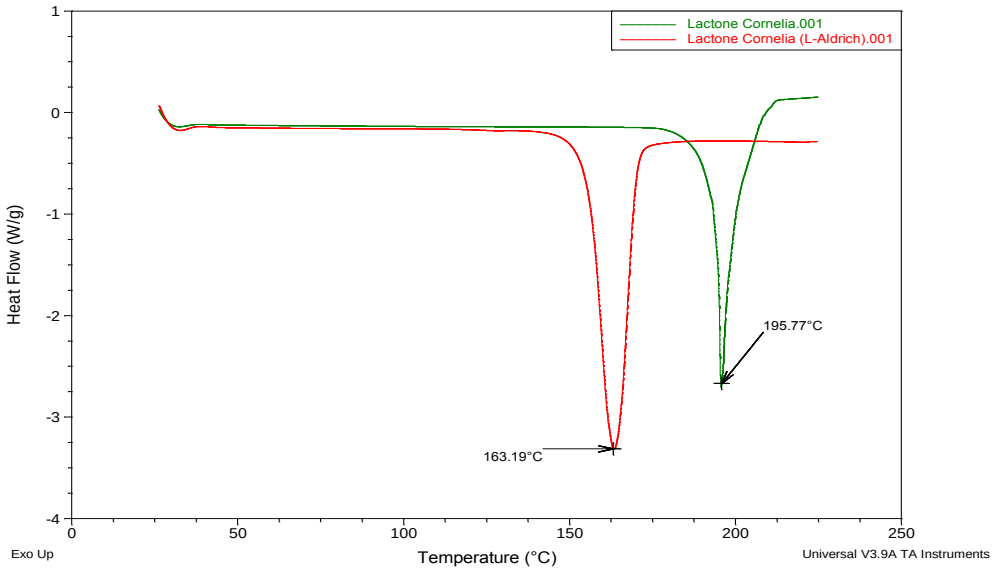

Figure 3.56 DSC thermograms of D-glucaric lactones obtained from synthesis (green) and purchased from Aldrich (red). Heating rate was 10°Cmin^{-1}.

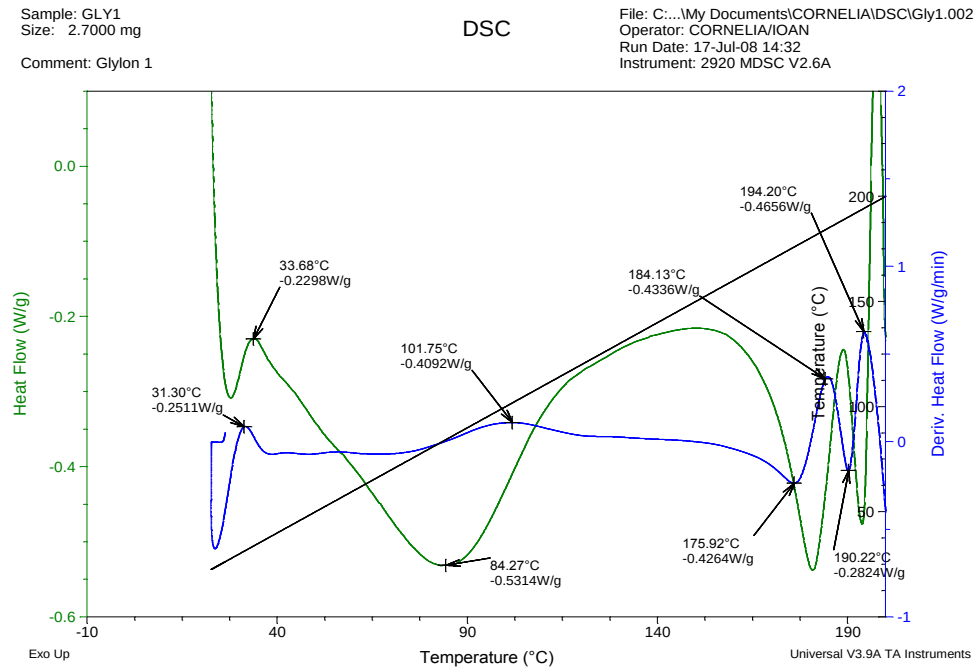

Figure 3.57 DSC thermogram of poly(hexamethylene-D-glucaramide), gly-6, 6_MeOH. Heating rate was 10°Cmin^{-1}

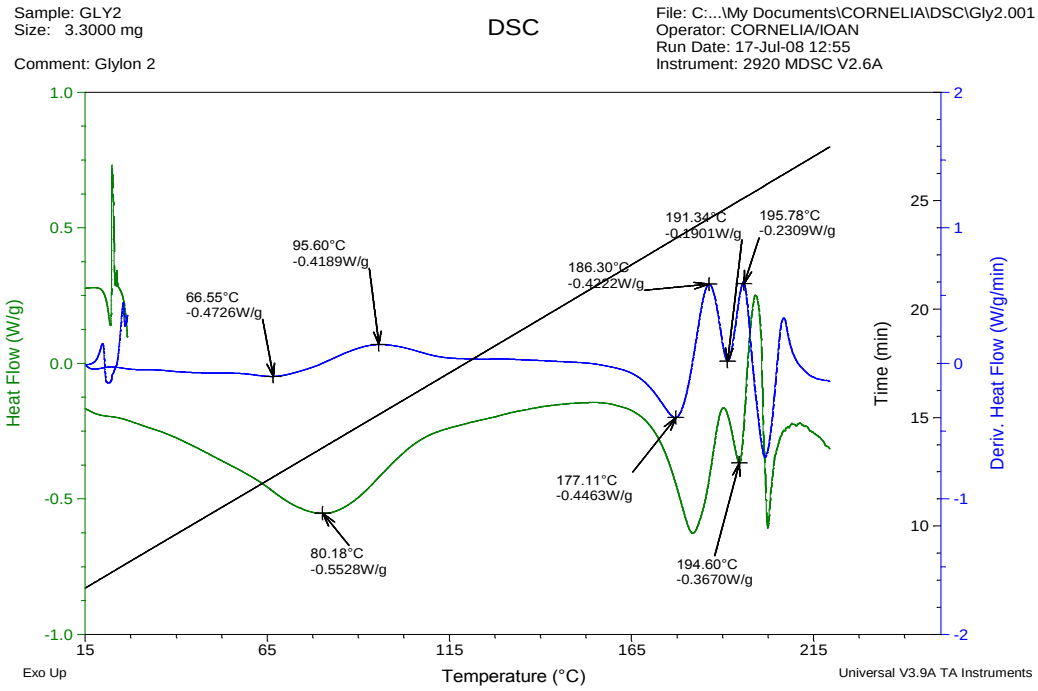

Figure 3.58 DSC curve of poly(hexamethylene D-glucaramide), gly-6, 6_DMSO. Heating rate was 10ºCmin^{-1}

The final goal of spinning fibers must take in consideration this issue. The spectra of glylons-6,6 were compared with the DSC traces of nylon-6,6 (Figure 3.59). The protection of pendant hydroxyl groups resulted in compounds with better thermal properties. The DSC and DDSC curves show the melting transitions starting at 102°C (Figure 3.60). The multitude of melting transitions is assigned to the oligomers present in the mixture. Furthermore the melting for unreacted monomer can be identified.

3.5.1.2 Galactaric Acid-Based Glylons

Protected and unprotected galactaric derivatives exhibit slightly different thermal properties when compared with D-glucaric counterparts. The melting transition of the diester monomer was identified first (Figure 3.61). The melting transitions for the protected galactaric derivatives started at 119°C (GalEt_prop1:1, Figure 3.62 and 112ºC (GalEt_hexa1:1, Figure 3.63). Decomposition process didn't occur before 200°C. As previously discussed, the multiple melting peaks are attributed to the oligomers. The higher values for melting transitions observed could be assigned also to macrocycles that, probably, require more energy to melt due tothe cycle's stability. Galactaric-based polymers with pendant hydroxyl groups showed a tendency to decompose after melting. This behavior is very similar with D-glucaric derivatives On the other hand the multiple meltings noticed on the spectrum are consistent with MALDI-TOF data which reflected that even after treating the protected glylons with an aqueous solution of trifluoroacetic acid the cyclic species are still present (Figure 3.64).

3.5.2 Thermogravimetric Analysis (TGA)

Thermal Gravimetric Analysis (TGA) was performed on a Lab: METTLER, STAR^{e} SW 8.10 instrument at a scan rate of 10°C min^{-1} under nitrogen. Thermogravimetric analysis provides data about the decompositions steps involved and also the percentages of sample lost at that specific step. All the samples were vacuum dried prior analysis.

The thermogram of D-glucaric lactone confirmed that the one obtained had a higher purity than that purchased by Aldrich (Figure 3.65).

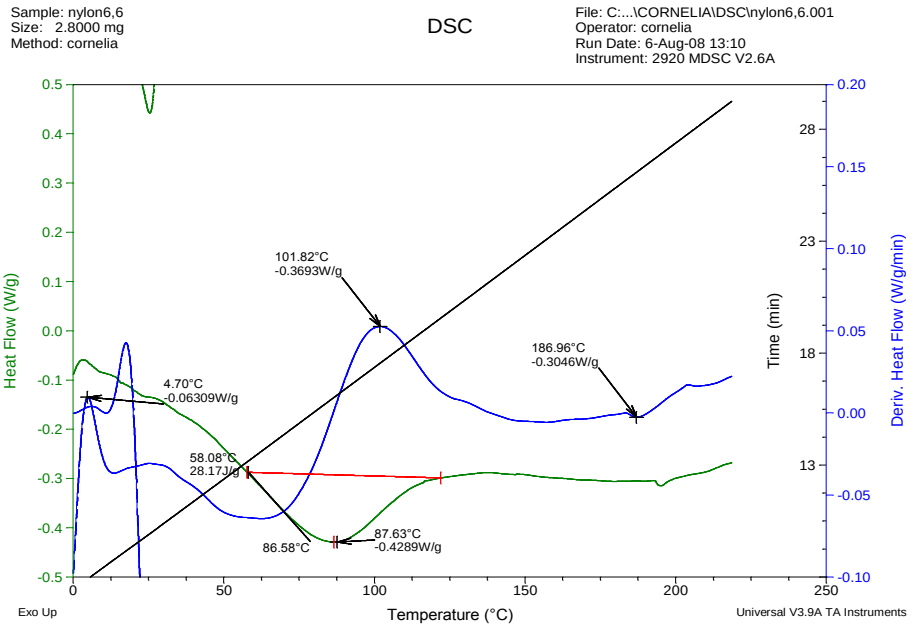

Figure 3.59 DSC and DDSC curves for classic nylon 6, 6. Heating rate was 10°Cmin^{-1}.

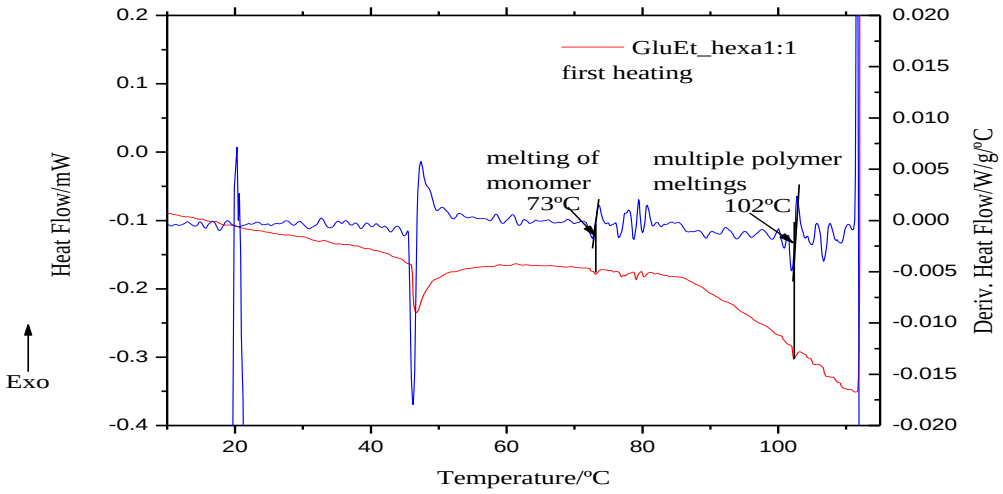

Figure 3.60 DSC and DDSC curves for GluEt_hexa1:1. Heating rate was 5°Cmin^{-1}.

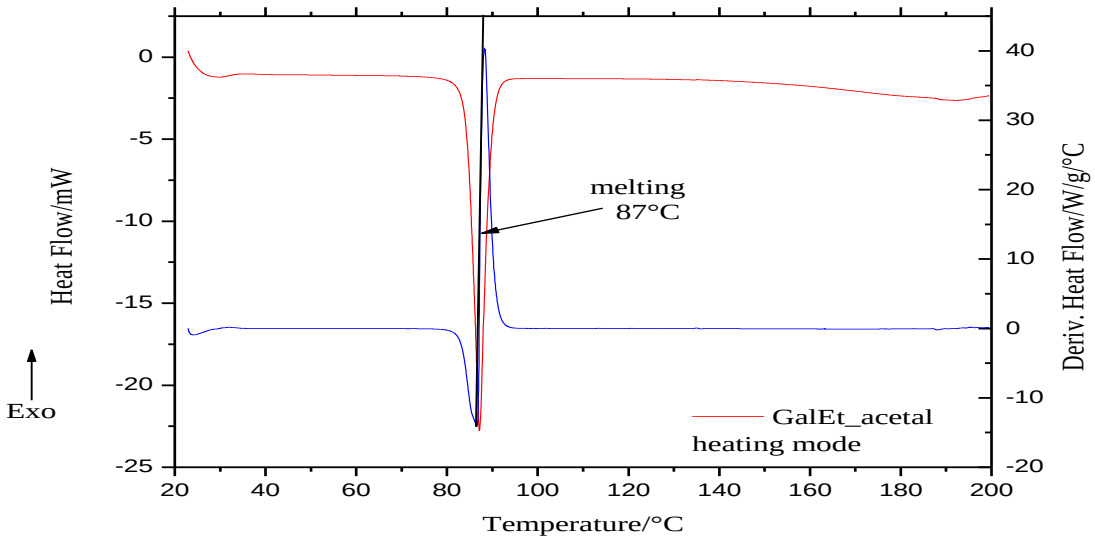

Figure 3.61 DSC and DDSC traces of GalEt_acetal on heating mode. Heating rate was 5°Cmin^{-1}.

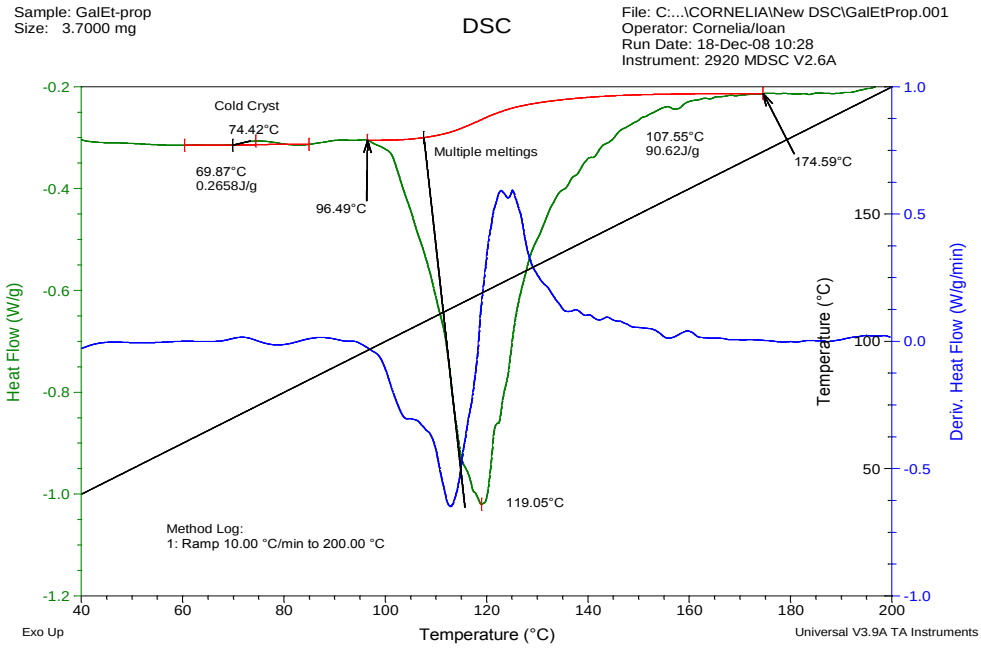

Figure 3.62 DSC and DDSC traces for GalEt_prop1:1 on heating mode. Heating rate was 5°Cmin^{-1}.

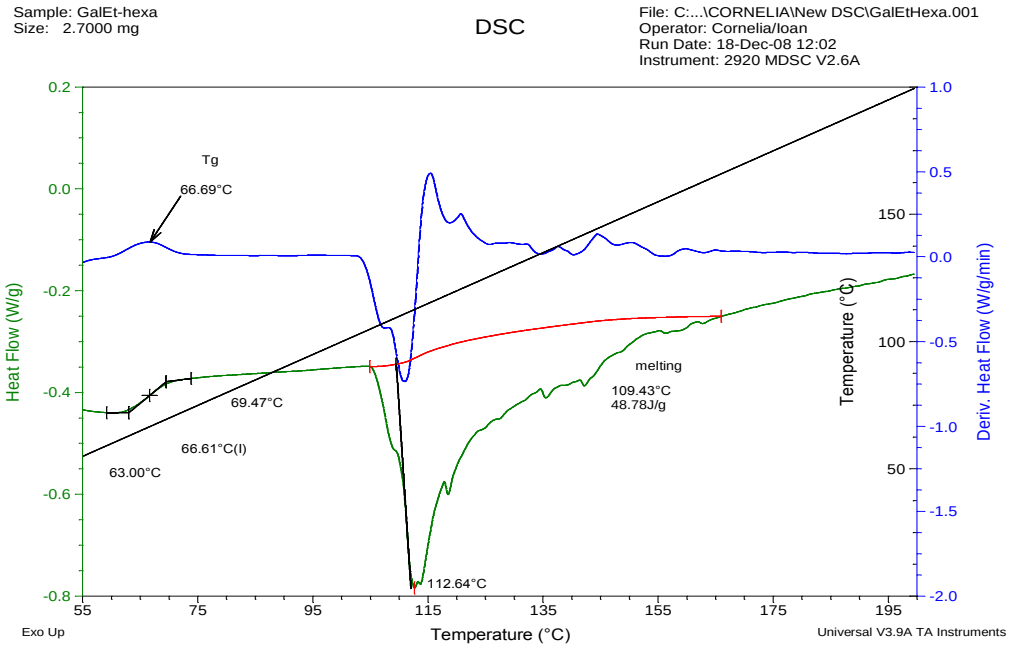

Figure 3.63 DSC and DDSC traces of GalEt_hexa1:1 on heating mode. Heating rate was 5°Cmin^{-1}.

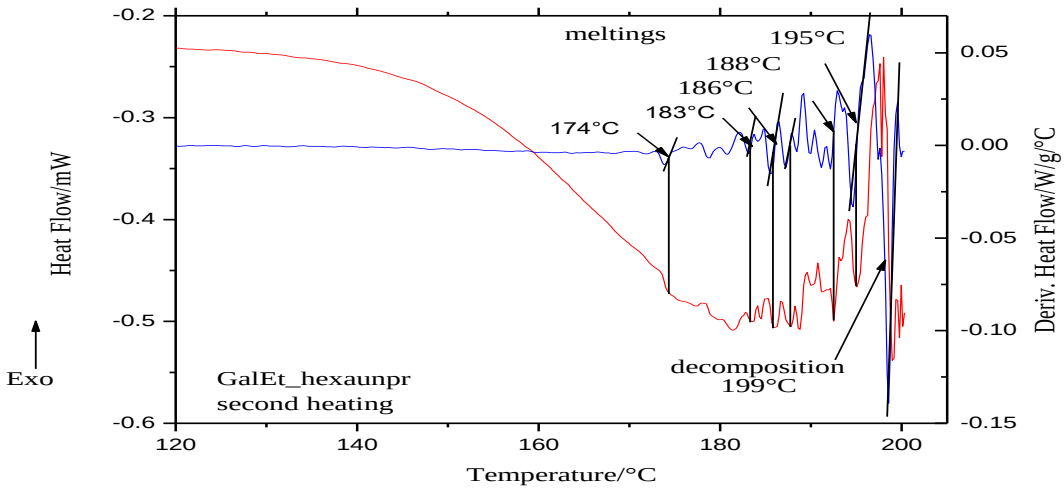

Figure 3.64 DSC and DDSC traces of GalEt_hexaunpr on heating mode. The graph displays the second heating at a rate of 5°Cmin^{-1}.

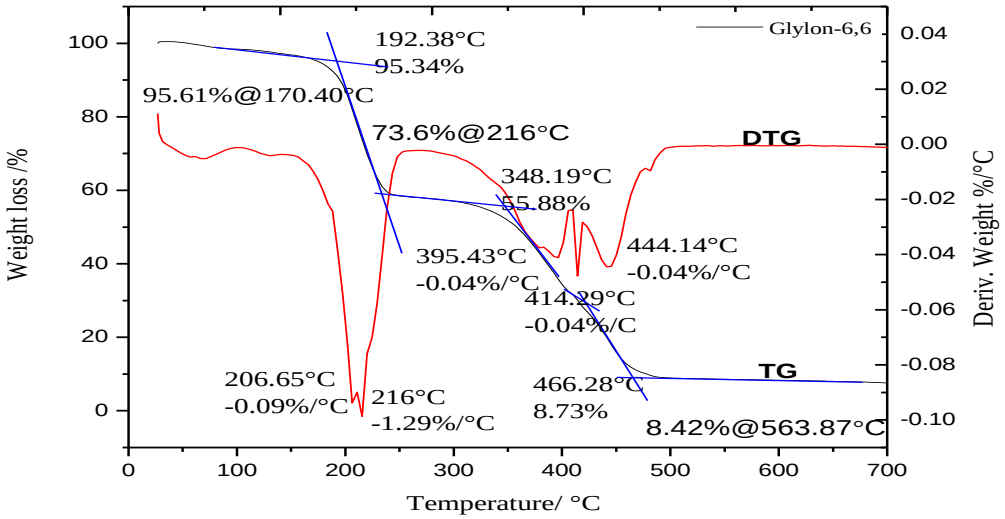

Figure 3.65 TG and DTG thermograms of poly(hexamethylene-D-glucaramide), Glylon 6, 6. Heating rate was 10°Cmin^{-1}.

The starting reagents were also analyzed (Figures 3.66 and 3.67) premonomer (Figures 3.68, 3.69 and 3.70).

Glylons-6,6 decomposes in three major steps (Figure 3.71). The loss of 5% mass up to 150- 170°C is due to the absorbed water. The broad peak registered around the maximum of 216°C corresponds to the free hydroxyl group cleavage from sugar backbone. The strong intra-molecular H-bonding explains the higher temperature necessary to induce the cleavage of OH groups. The other two maxima, one at 395°C and the other at 444°C with a spike at 414°C can be assigned to amidic group degradation followed by the backbone part decomposition. The pro-tected counterparts followed relatively the same path (Figure 3.72 and 3.73). Yet supple-mental peaks can be identified. The cleavage of pendant free hydroxyl groups was registered at lower temperature (maxima130- 140°C) due to the weaker H-bonding. Protected glucaric-based glylons have only half of hydroxyl groups on the backbone. The decomposition of the acetal and amidic groups are probably overlapped in the region of 230- 270°C.

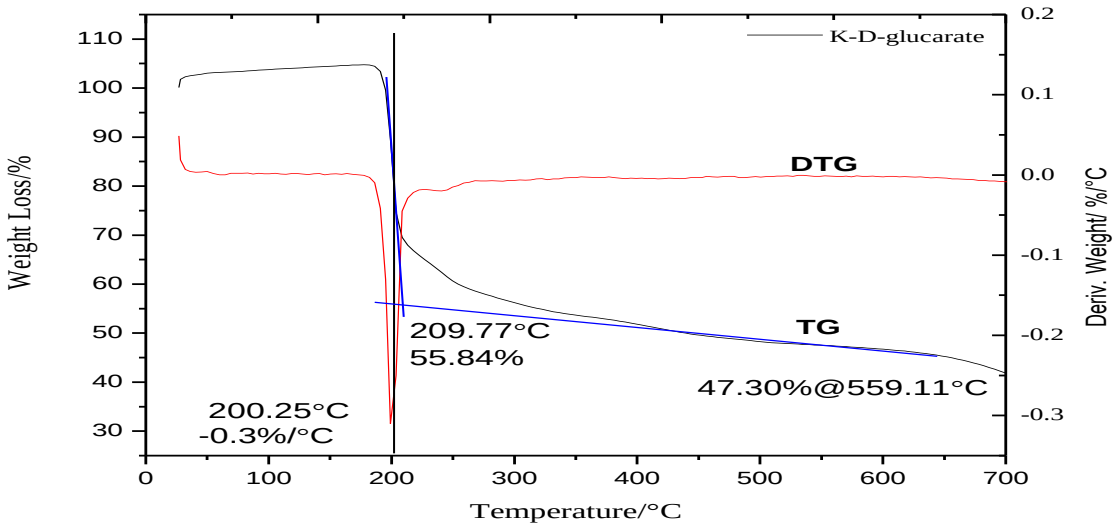

Figure 3.66 TG and DTG thermograms of potassium D-glucarate salt. Heating rate was 10°Cmin^{-1}.

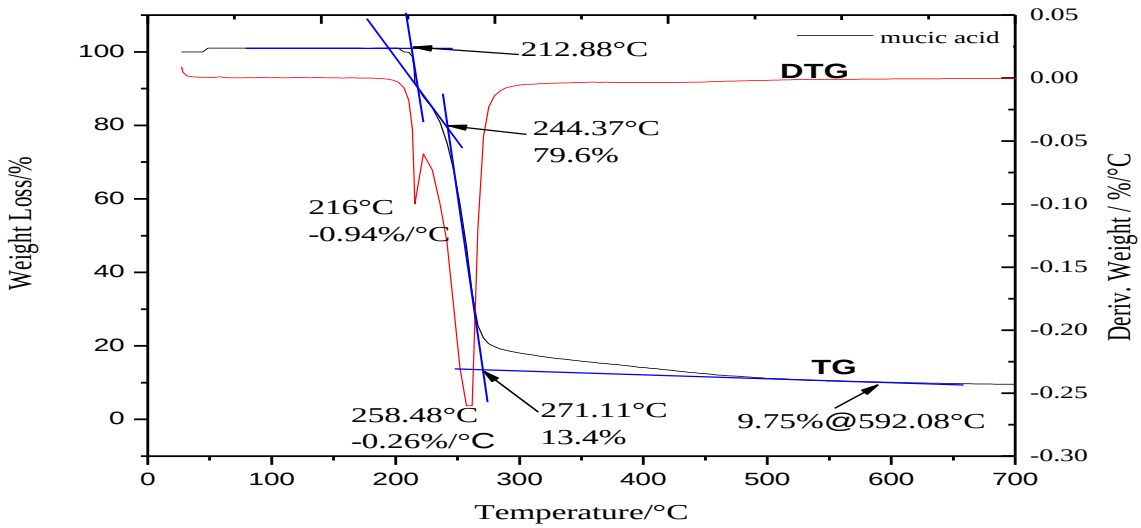

Figure 3.67 TG and DTG thermograms of D-galactaric acid (mucic acid). Heating rate was 10°Cmin^{-1}.

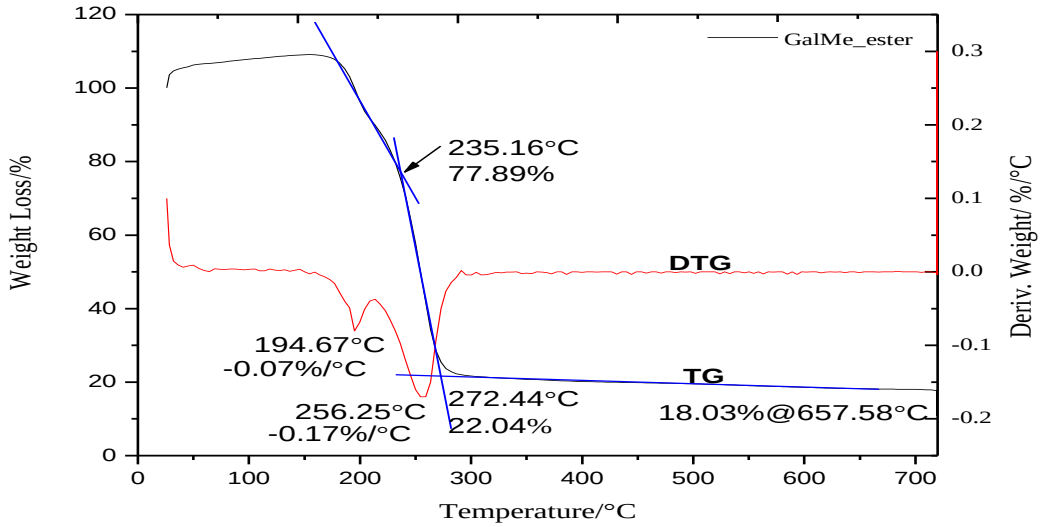

Figure 3.68 TG and DTG thermograms of dimethyl galactarate. Heating rate was 10°Cmin^{-1}.

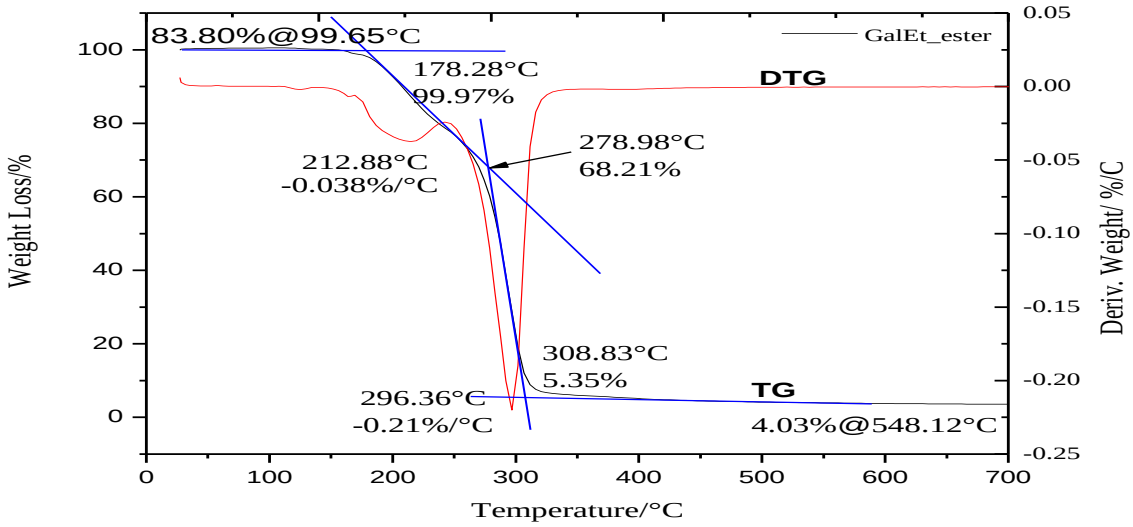

Figure 3.69 TG and DTG thermograms of diethyl galactarate. Heating rate was 10°Cmin^{-1}.

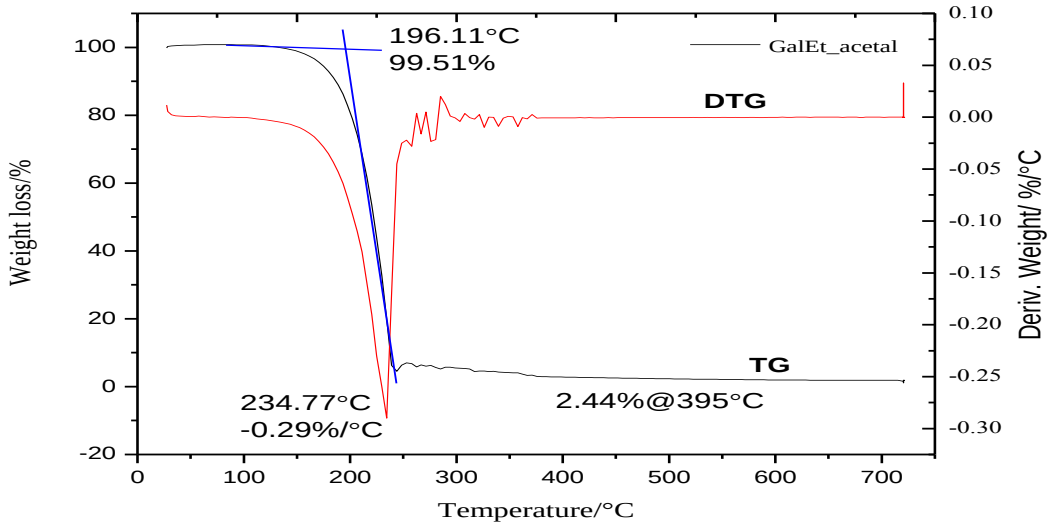

Figure 3.70 TG and DTG thermograms of diethyl 2,3: 4,5-bis-*O*-isopropyledene galactarate. Heating rate was 10°Cmin^{-1}.

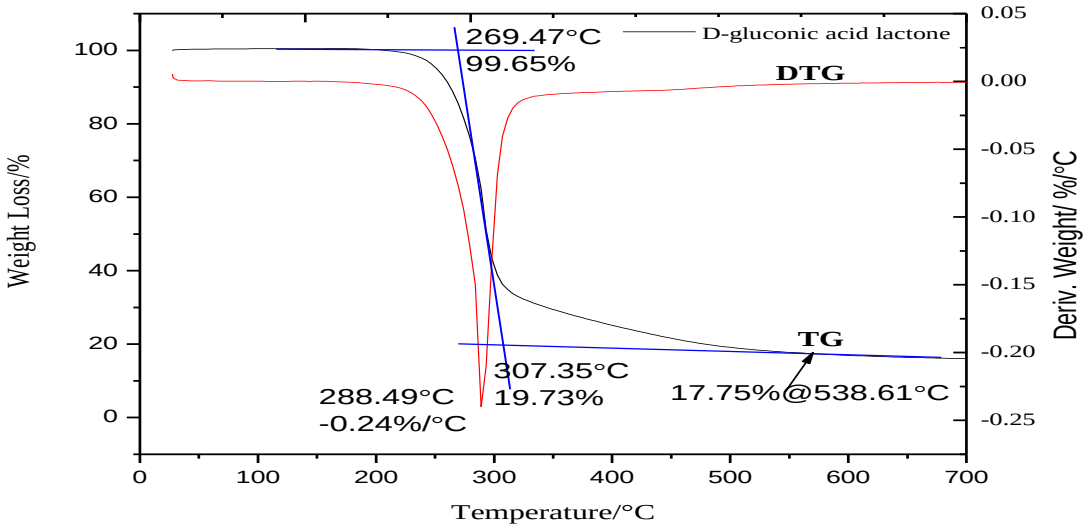

Figure 3.71 TG and DTG thermograms of D-gluconic acid lactone. Heating rate was 10°Cmin^{-1}.

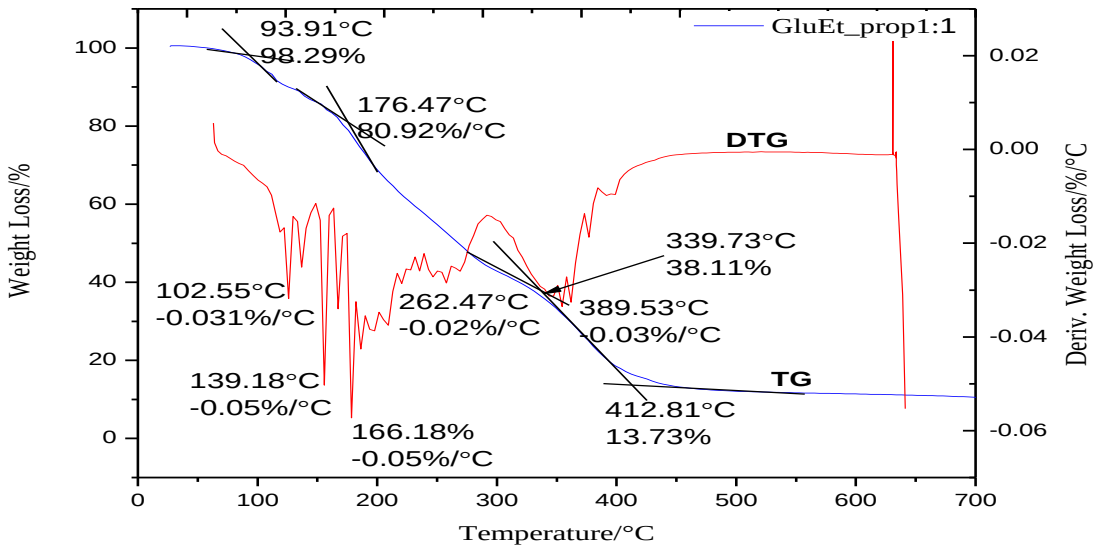

Figure 3.72 TG and DTG thermograms of poly(2,3: 4,5-bis-O-isopropylidene-1,3-propyledene-D-glucaramide). Heating rate was 10°Cmin^{-1}.

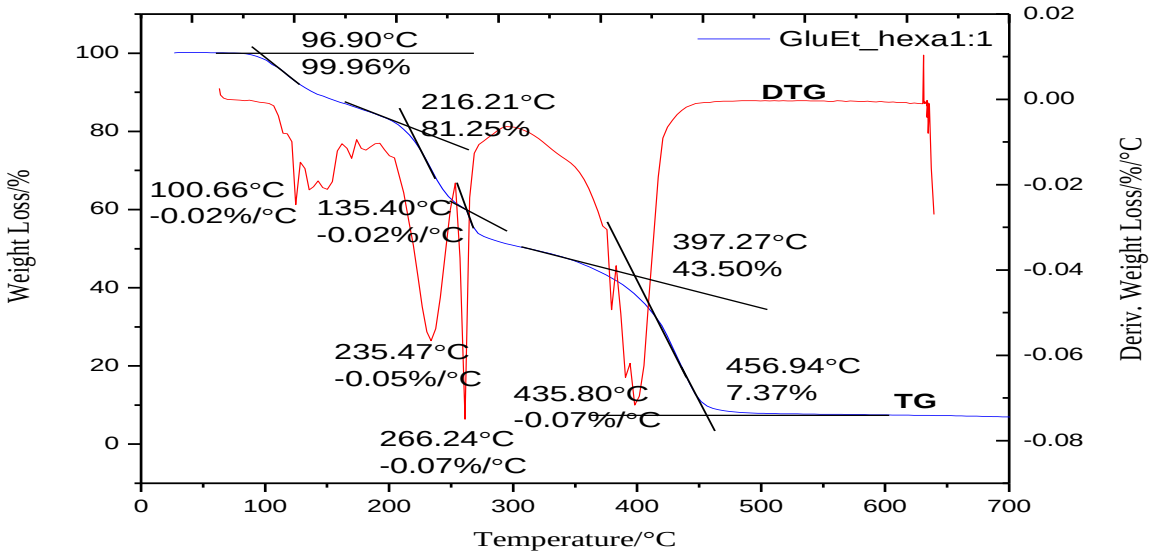

Figure 3.73 TG and DTG thermograms of poly(2,3: 4,5-bis-O-isopropylidene-1,6-hexamethylene-D-glucaramide). Heating rate was 10°Cmin^{-1}

In order to have a better understanding on the reactions and their yields TG analysis was performed on the starting reagents as well. TG data coupled with DSC traces can offer details about the traces of the initial reagents in the final mixture. The protected galactaric derivatives exhibited different behavior. On the thermograms the peak assigned to OH elimination is no longer present. The small peaks at maximum 115°C recorded for GalEt_hexa1:1 **(**Figure 3.74) and GalEt_hexa1:95 (Figure 3.75) can be assigned to the absorbed water. GalEt_prop (**Figure** 3.76) and GalEt_hexa polymers showed better thermal stability when compared with D-glucaric derivatives.

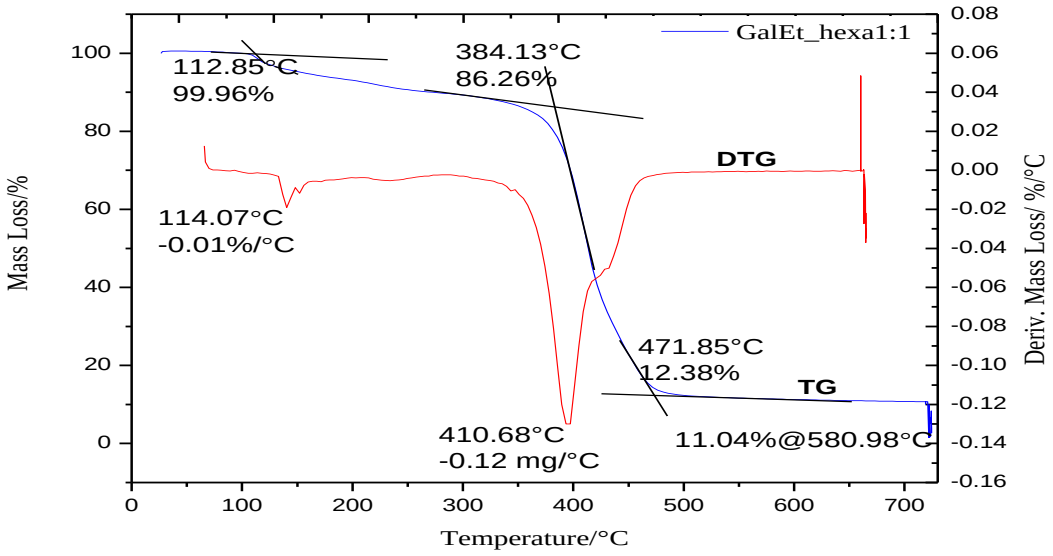

Figure 3.74 TG and DTG thermograms of GalEt_hexa1:1. Heating rate was 10°C/min.

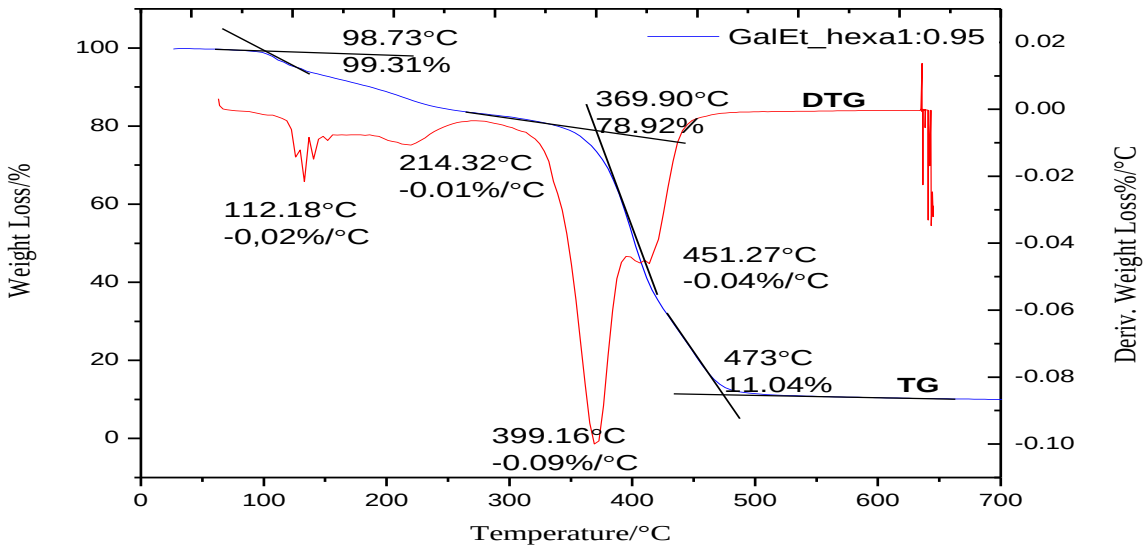

Figure 3.75 TG and DTG thermograms of GalEt_hexa1:0.95. Heating rate was 10°Cmin^{-1}.

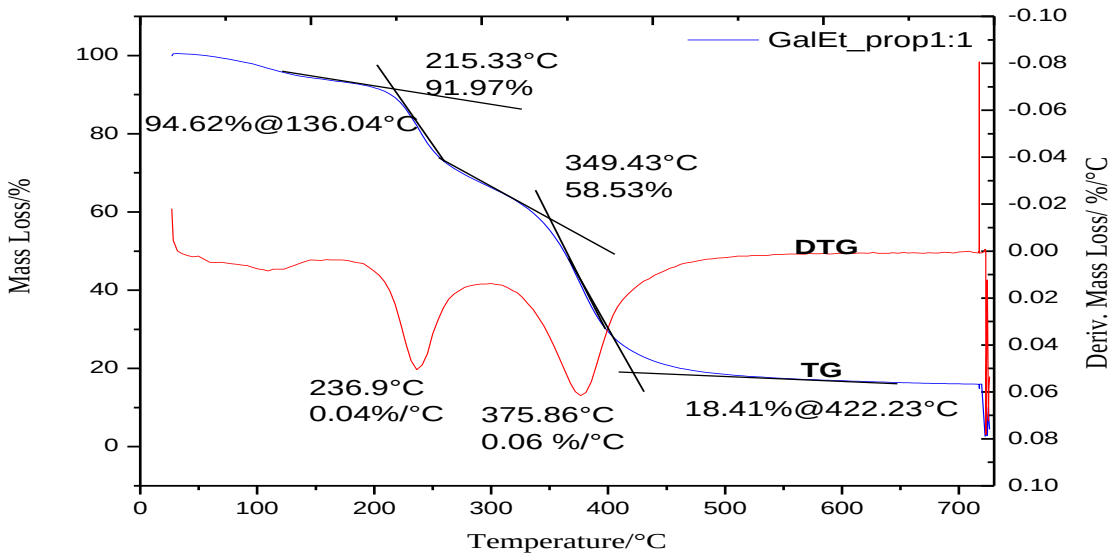

Figure 3.76 TG and DTG thermograms of GalEt_prop1:1. Heating rate was 10°Cmin^{-}

3.6 Nuclear Magnetic Resonance (NMR)

Nuclear Magnetic Resonance spectroscopy, NMR, is a very valuable tool used specially in organic synthesis to analyze the compounds. The synthesis of the expected products was confirmed by this technique. The spectra were recorded with an INOVA 500 Mhz machine. The samples were dissolved in deuterated chloroform, $CDCl_3$ or methanol-d_4.

Previous studies on hydroxylated nylons synthesis reported the presence of a mixture of linear diesters and γ-lactones. Ogata and Hoagland stated that the lactones form during aminolysis of diethyl or dimethyl esters with diamines.[12,13] Later Kiely determined the coexistence of the structure during transesterification of D-glucaric acid in acidic methanol solution.[22] One of the goals for the present work was to identify the occurrence and the evolution of these species previously reported. After filtration of inorganic salts (KCl) the mixture was subjected to rotavaporation to remove the methanol. The samples of dimethyl D-glucarate were collected at 15, 25, 35 and 50 min. from the start. To these samples methanol-d_4 was added. Additional spectra were recorded after several days of sample collection (Figures 3.77 and 3.78). ^{1}H NMR spectrum recorded the presence of linear and cyclic species (Table 3-15).

The results confirm the Kiely's observations regarding the dynamics of the four species mixture. The proton signals were found between 4.05 and 5.60 ppm. Spectra recorded also traces of residual methyl ester groups that didn't undergo transesterification and residual methyl acetate carried in the syrup mixture. The proton signals for these methyl groups lay between 3.2 and 3.77 ppm. At room temperature dimethyl D-glucaric acid consists in three distinctive species: one linear and two monolactones. Once the mixture is warmed up to 100-110°C under vacuum the 1H NMR spectra recorded new chemical shifts positions attributed to the new component formed, the bicyclic D-glucaro-1,4;1,6-dilactone. All recorded spectra were compared with the data for authentic compounds presented in Kiely's work.[45]

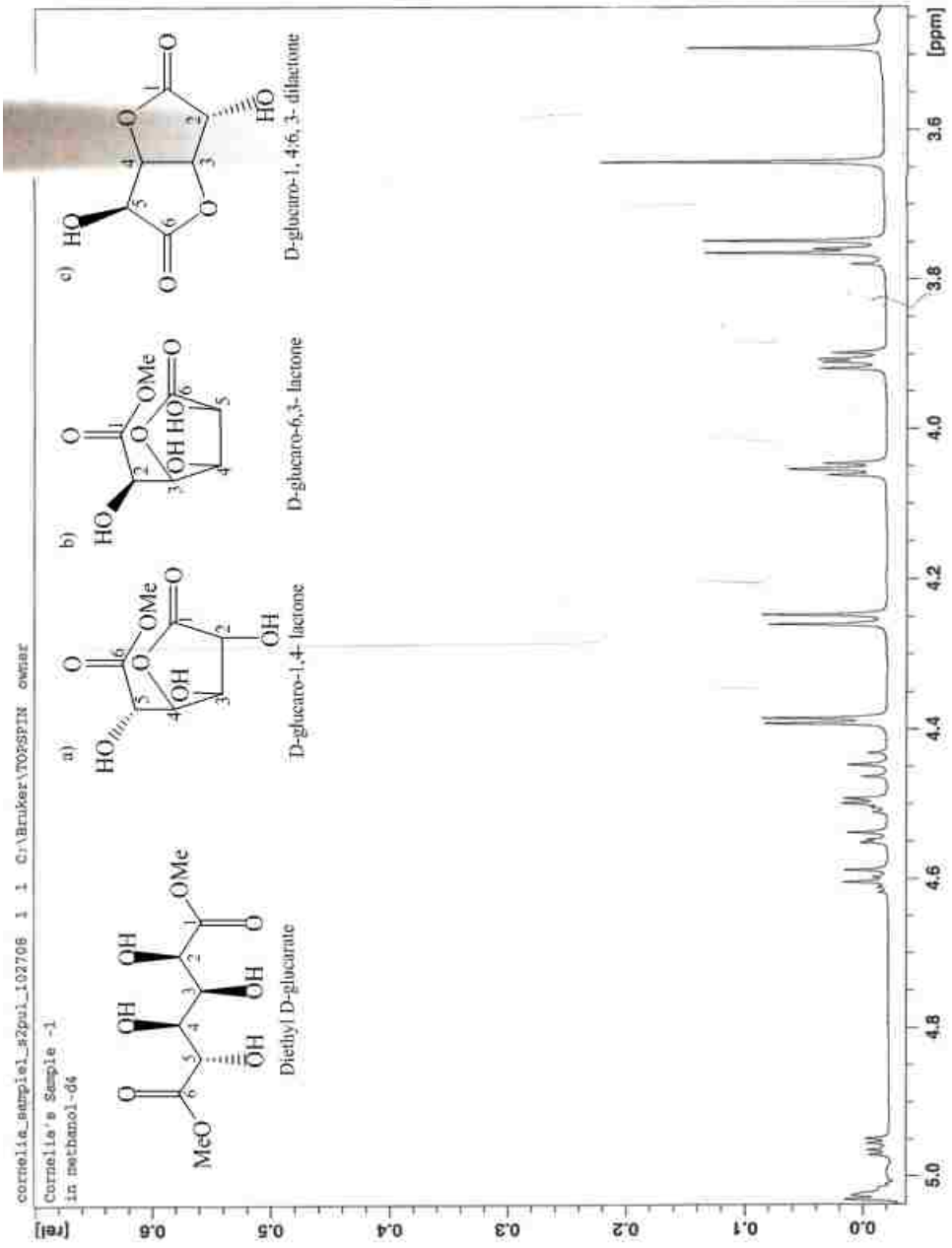

Figure 3.77 ^{1}H NMR spectrum of a mixture of linear and diethyl D-glucarate plus mono- and dilactones (50mg/mL, methanol-d4, tetramethylsilane, 25ºC, 500MHz). The spectrum was recorded in methanol-d_4 and the sample was collected after 15 min. to the reaction start.

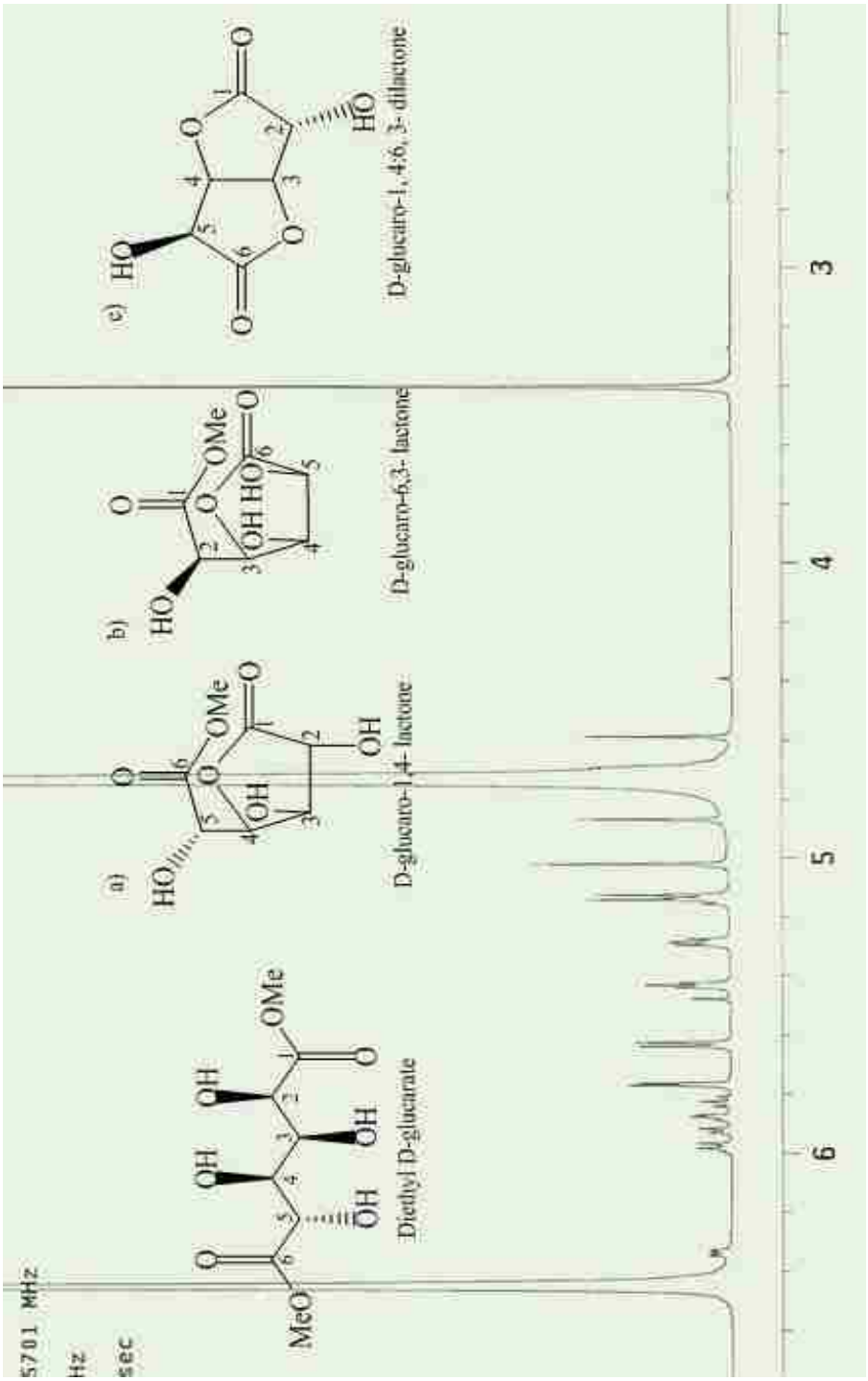

Figure 3.78 ^{1}H NMR spectrum of a mixture of linear dimethyl D-glucarate plus mono- and di-lactones. The spectrum was recorded in methanol-d_4. The sample was collected after 45 min. to the reaction start.

Table 3-15 Relative ^{1}H NMR chemical shifts of dimethyl D-glucarate in methanol-d_4

Compound	Species	δ (ppm)
Methyl D-glucarate 1,4-lactone	H-2 (doublet)	4.60
	H-3 (triplet)	4.45
	H-4 (triplet)	5.25
	H-5 (doublet)	4.50
Methyl D-glucarate 6, 3-lactone	H-2 (doublet)	4.60
	H-3 (triplet)	4.50
	H-5 (doublet)	4.50
D-glucaro-1,4;6,3-dilactone	H-2 (singlet)	4.60
	H-3 (triplet)	5.22
	H-4 (triplet)	5.60
	H-5 (doublet)	5.16
Dimethyl-D-glucaric acid	H-2 (doublet)	4.25
	H-3 (triplet)	4.05
	H-4 (triplet)	4.95
	H-5 (doublet)	4.39

NMR observations on the carbon skeleton (^{13}C) (Figure 3.79 and 3.80) and the population of the ^{1}H nuclei (Figure 3.81 and 3.82) offered the confirmation of acetalated galactaric acid derivatives structures (Tables 3-16, 3-17, 3-18 and 3-19). The samples were dissolved in deuterated chloroform, $CDCl_3$. Residual acetalated diester can be also identified around 3.6- 4 ppm. The presence of another species besides linear polymer was suspected because the multitude of CH_2 and CH carbons recorded (Figure 3.83). The 2D spectrum COSY NMR gave the ^{1}H-^{1}H connectivities for GalEt_hexa1:1 (Figure 3.84). From the intersection of crosspeaks with the diagonal ^{1}H spectra, supplemental couplings are identified. These results coupled with MALDI-TOF confirmed the presence of cyclic species beside the linear ones.

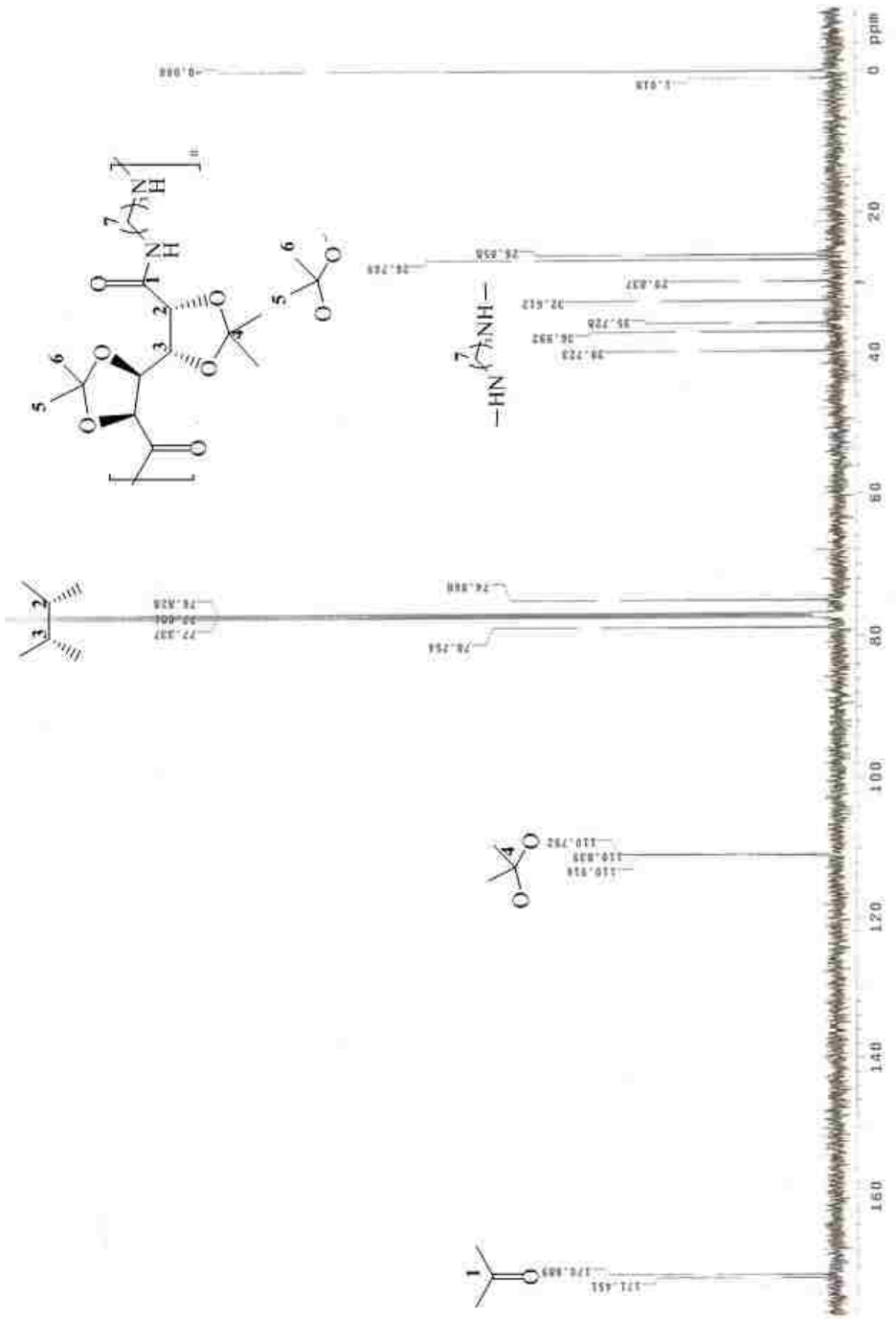

Figure 3.79 ^{13}C NMR spectrum of GalEt_prop1:1 in $CDCl_3$.

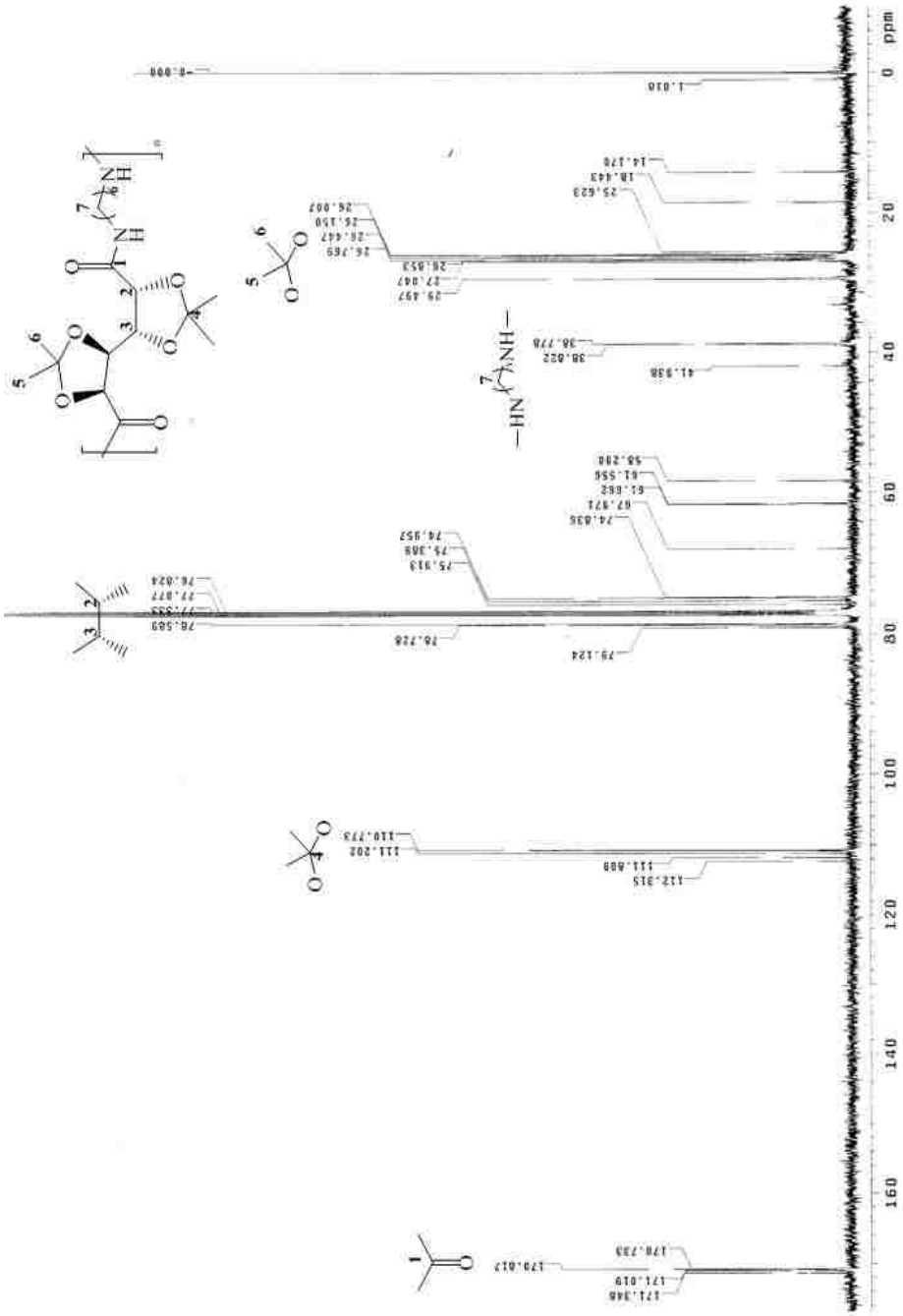

Figure 3.80 ^{13}C spectrum of GalEt_hexa1:1 in $CDCl_3$

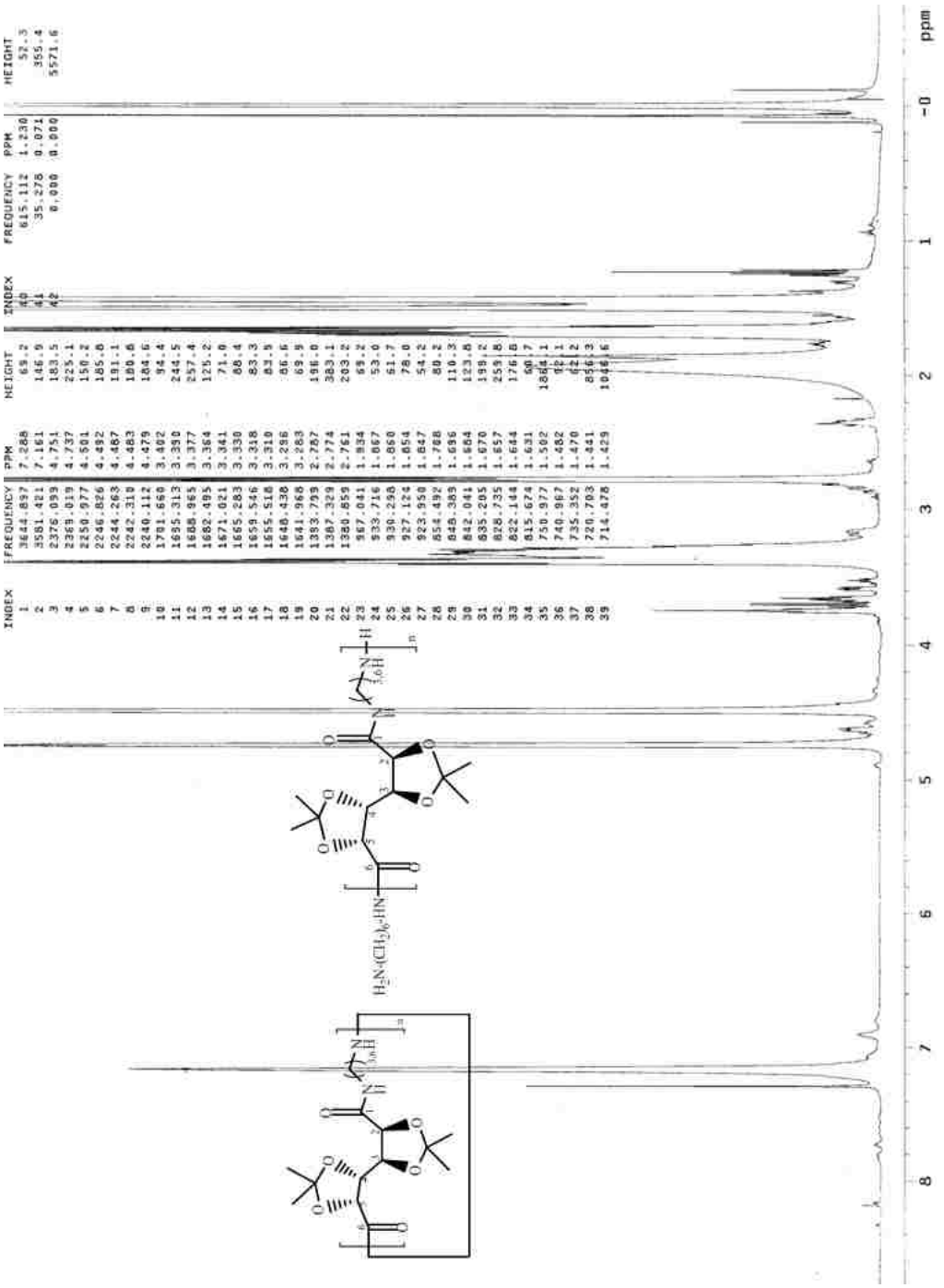

Figure 3.81 ^{1}H NMR spectrum of GalEt_prop in $CDCl_3$.

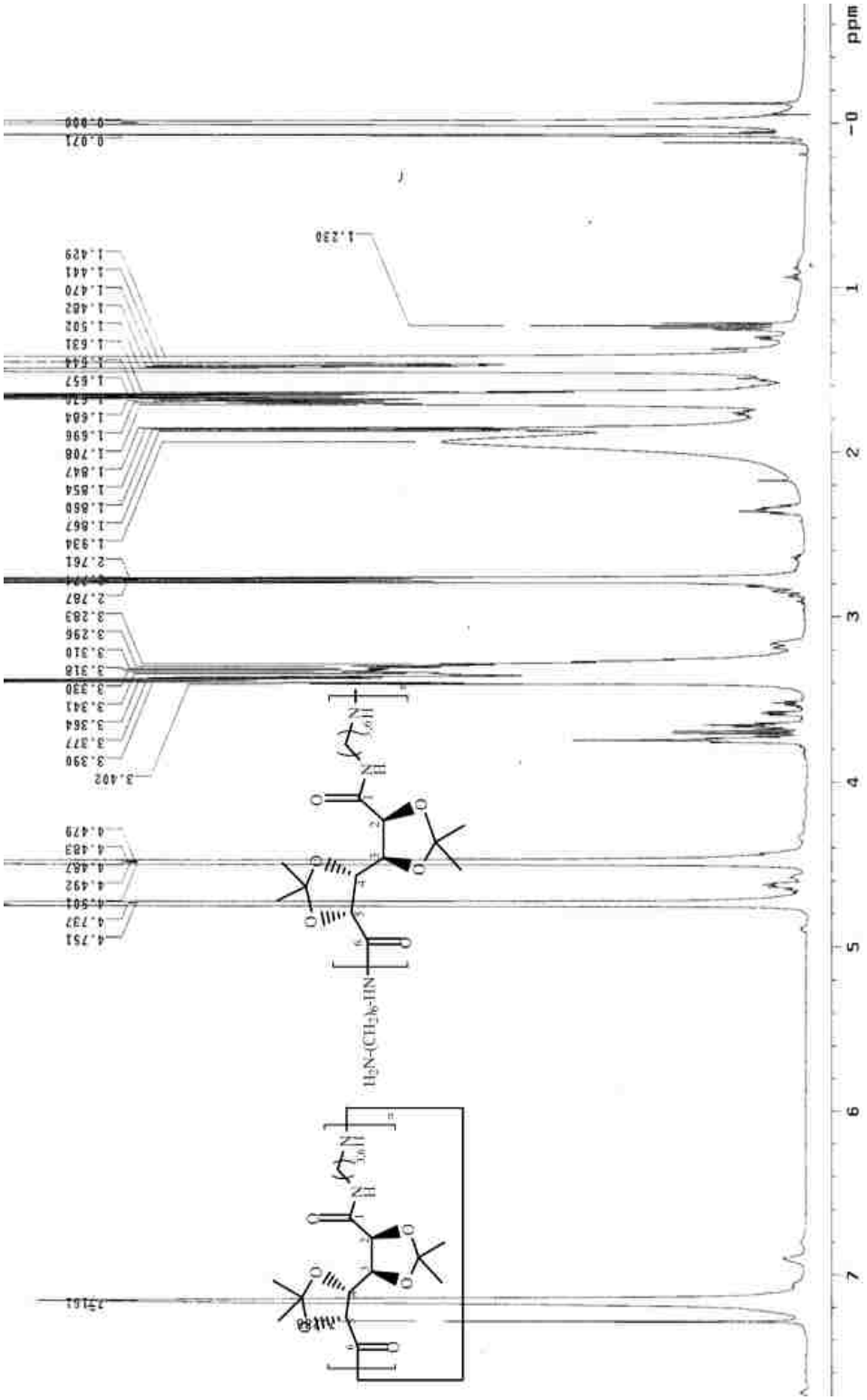

Figure 3.82 ^{1}H spectrum of GalEt_hexa1:1 in $CDCl_3$.

Table 3-16 Relative ^{13}C NMR chemical shifts of GalEt_hexa1:1

Carbon-atom	Shift ppm
C-1	171
C-2,3	77
C-4	111.2
C-5,6	26.7
C-7	38.8

Table 3-17 Relative ^{1}H NMR chemical shifts of GalEt_hexa1:1

Proton	Species	δ ppm
-H (-CH_2, diamine)	pentet	1.2- 1.7
-H (-CH_2, diamine)	quartet	1.8- 2
-H (-CH, sugar backbone)	doublet	3.7
-H (-NH, diamine)	triplet	2.6
-H (-CH_3, acetal group)	singlet	4.8
-H (-NH, amidic)	triplet	7.2

Table 3-18 Relative ^{13}C NMR chemical shifts of GalEt_prop1:1

Carbon-atom	Shift ppm
C-1	171
C-2,3	77.1
C-4	110.8
C-5,6	26.7
C-7	29

Table 3-19 Relative ^{1}H NMR chemical shifts of GalEt_prop1:1

Proton	Species	δ ppm
-H (-CH_2, diamine)	pentet	1.3- 1.7
-H (-CH_2, diamine)	quartet	1.7- 2
-H (-CH, sugar backbone)	doublet	3.7
-H (-NH, diamine)	triplet	2.5- 3.3

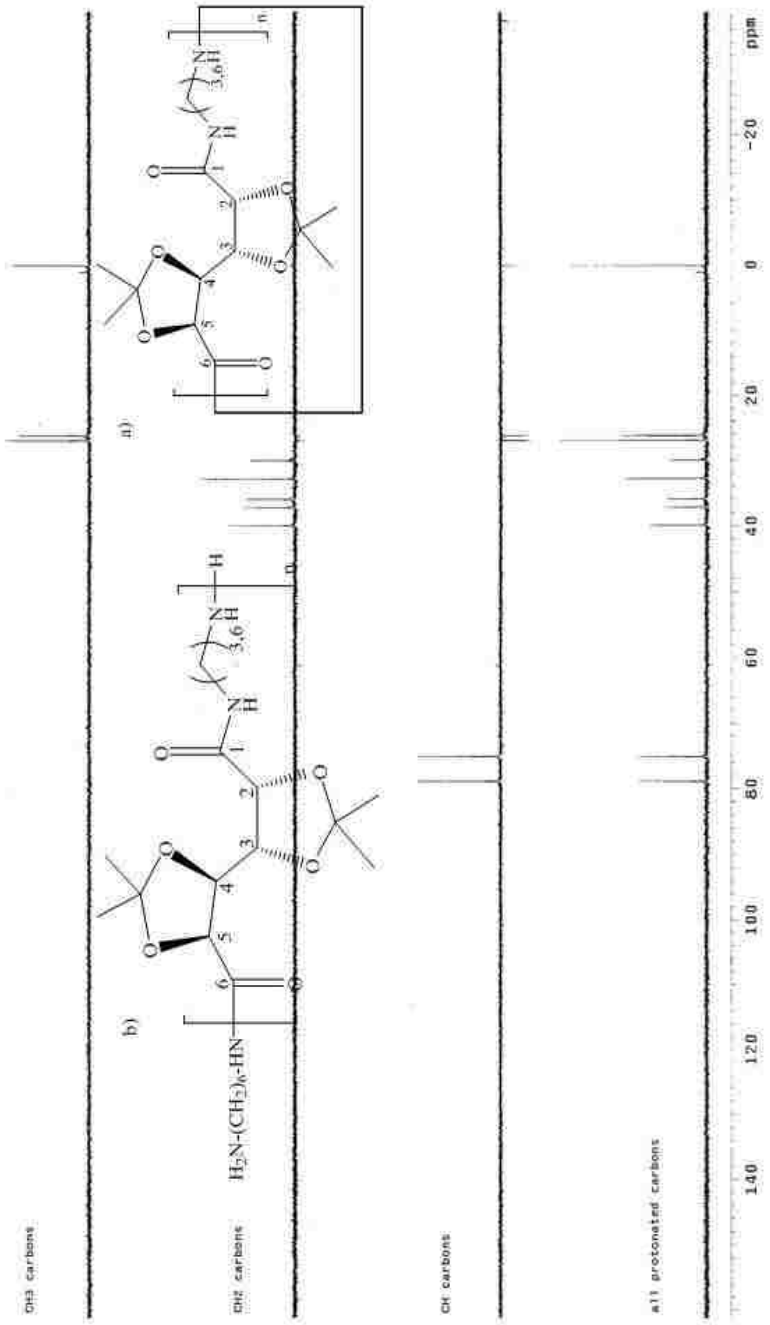

Figure 3.83 Carbon species present in the GalEt_hexa1:1. The spectrum was recorded in chloroform-d_1.

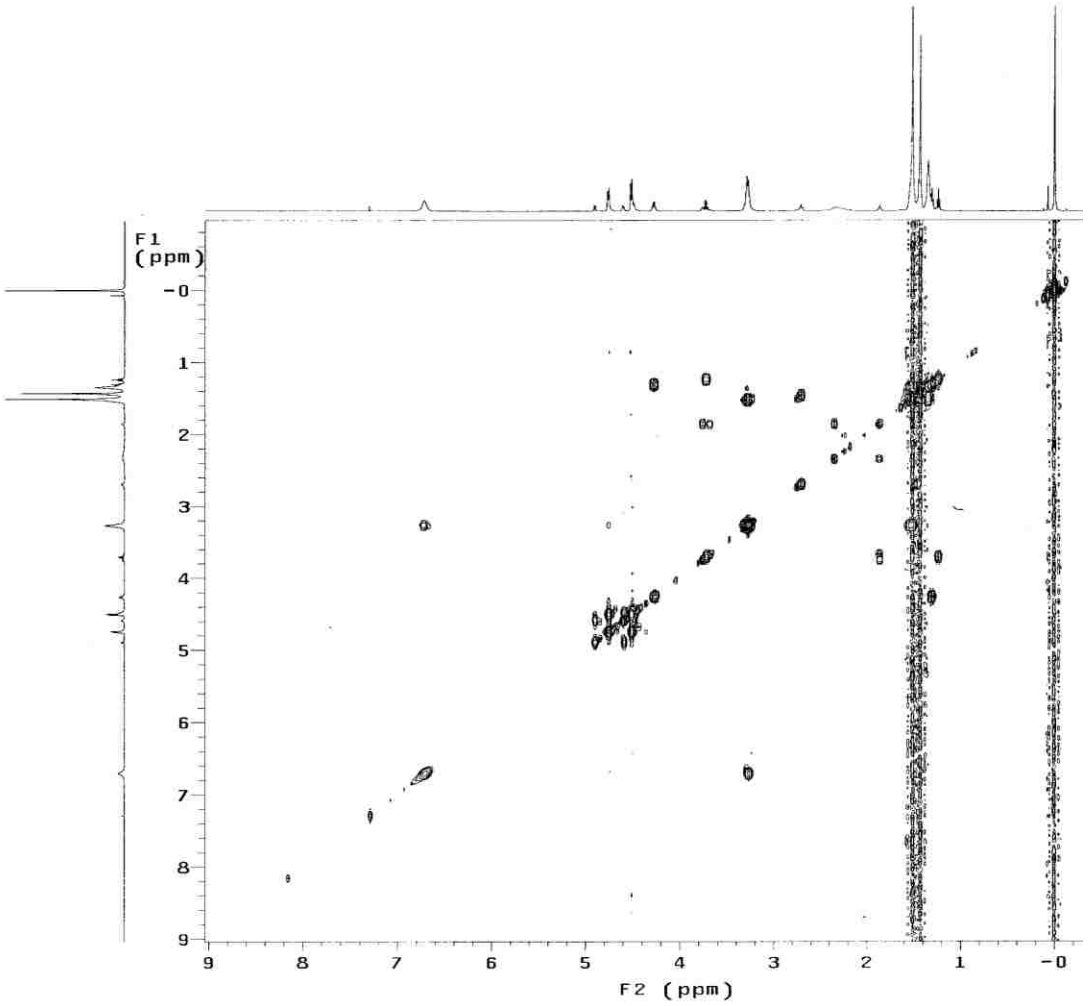

Figure 3.84 COSY spectrum of GalEt_hexa1:1 in $CDCl_3$ at 500 MHz.

CHAPTER 4. SPIRAL/TREE RINGS

4.1 General Considerations

Naturally occurring organized resembling patterns attracted a special attention in the past decades because of their potential applications. The focus of this work is on such organizations called *spherulites*. The term "spherulites" is used to suggest a spherical shape observed to form in a wide range of materials: metallurgical alloys pure Se-based[46,47] mineral aggregates and volcanic rocks,[48]simple organic liquids,[49] polymers,[50,51] liquid crystals,[52,53] and biological molecules.[54] The forms they appear are diverse[46,52-57] and the mechanism behind their microstructure is still poorly understood. Over the past decades experimental studies performed on these systems reported two main categories of spherulites.[57,58] The first category regards the radial growth from the nucleation point with an intermittent branching in order to maintain a space filling. In contrast, the second kind of morphology starts to grow as threadlike fibers with subsequent formation of new grains at the vicinity of growth front.[59]

Keith,[60] Schuur[61] and Schramm[62] reported for the first time the formation of concentric-ringed (banded) crystalline structures in polymer thin films. According to Keith and Padden[63] the occurrence of such concentric morphologies is highly determined by the static heterogeneities (impurities, molecular defects and a polydisperse polymeric material). Their presence can cause the rejection of impurities from the growth front leading to channel formation.[59] Recent studies on banded structures suggests that the formation of these spherulites follows a much simpler path: the depletition zone created as a consequence of a lower diffusion rate of the polymer when compared with the rate necessary for mass to be used in crystallization process, favors the continuous flow of the polymer melt onto it. Furthermore, if the polymer has a higher polydispersity a molecular fractionation can result: the high molecular weight chains will diffuse first onto the depletition zone causing the rejection of the shorter chains. The system tries this way to conserve

conserve its energy by minimizing the interfacial free energy.[64]

One of the most studied polymer that forms spherulites is poly(L-lactic acid).[65-67] As well, polymers found to form spherulitic morphologies are chitin, chitosan[68] and cellulose[69] Recently, Negulescu and coworkers observed the milimeter-scale concentric-ringed structures in poly(hexamethylene-D-glucaramide), Glylon-6, 6, solutions in N-methyl-N-morpholine oxide monohydrate, NMMO x H_2O.[2]

4.2 Experimental

Glylon-6, 6 synthesized according with the procedure described in the Chapter 2 were dissolved in the N-methylmorpholine-N-oxide. The solvent was prepared following the procedure described in the Chapter 2, Section 2.3. At room temperature both reagents are solid: polymers (glylon-6, 6, GalEt_hexaunpr) exist as a white powder, and N-methylmorpholine-N-oxide is an yellow solid. Samples were heated to a temperature close to 80ºC followed by cooling at room temperature. During cooling they exhibited the patterns called *spiral*/*tree rings* and *picotees.* A series of solutions were prepared: 2, 5, 10, 15, 20, 30, 40, 50, 60, 70, and 80% by weight (Table 4-1).

Table 4-1 Mass of the components and concentration of the glylon-6, 6 solutions

No.	Concentration %	NMMO g	Polymer g	n-PG g
1	2	2	0.04	0.004
2	5	2	0.01	0.004
3	10	2	0.2	0.004
4	15	2	0.3	0.004
5	20	2	0.4	0.004
6	30	2	0.6	0.004
7	40	2	0.8	0.004
8	50	2	1.0	0.004
9	60	2	1.2	0.004
10	70	2	1.4	0.004
11	80	2	1.6	0.004

NMMO monohydrate was added to each crop of glylon-6, 6 (labeled as gly_1, gly_2, glylac_methanol, gly_hMw, gly_met1, gly_met2, glylact_DMSO, Gly_DMSO and GalEt_hexaunpr) in scintillation vials (20 ml) with a bottom diameter of 20mm. To the mixture above 0.2% of n-PG (propyl gallate) was added in order to prevent the oxidation of NMMO. A multitude of steps were followed to obtain these solutions. First the vials were labeled and weighed empty with the cap on. A magnetic stir bar was placed inside of each vial and the masses were recorded again. The weighing process was repeated after adding NMMO, the polymer, and n-PG. The solvent was handled in an argon atmosphere to prevent the contact with the moisture from the air. The vials were placed in a water bath and heated under stirring close to 80ºC. The time needed for reagents to mix and to form clear solutions was directly dependent on the concentration percentage: longer time for higher concentration. For some solutions the amount of n-PG added couldn't prevent the oxidation of NMMO: the mixture changed the color from light yellow to light or intense red-brown. Once the solutions were formed they were cooled down to the room temperature. The lower concentrations exhibited the nucleation and growth relatively fast. The higher concentrations required a lower temperature to nucleate; they were placed in the fridge for a time and checked often to see when the nucleation starts. After the solidification ended the vials were filled with argon and the caps sealed with Teflon band to prevent NMMO contact with the moisture from atmosphere. The patterns spiral or tree rings were recorded with a CANON EOS DIGITAL REBEL XT and KODAK EASY SHARE M753 camera (Figures 4.1 and 4.2). The next pictures show stages of nucleation and growth for several solutions of glylon-6,6 in NMMO x H_2O, (Figures 4.3, 4.4, and 4.5).

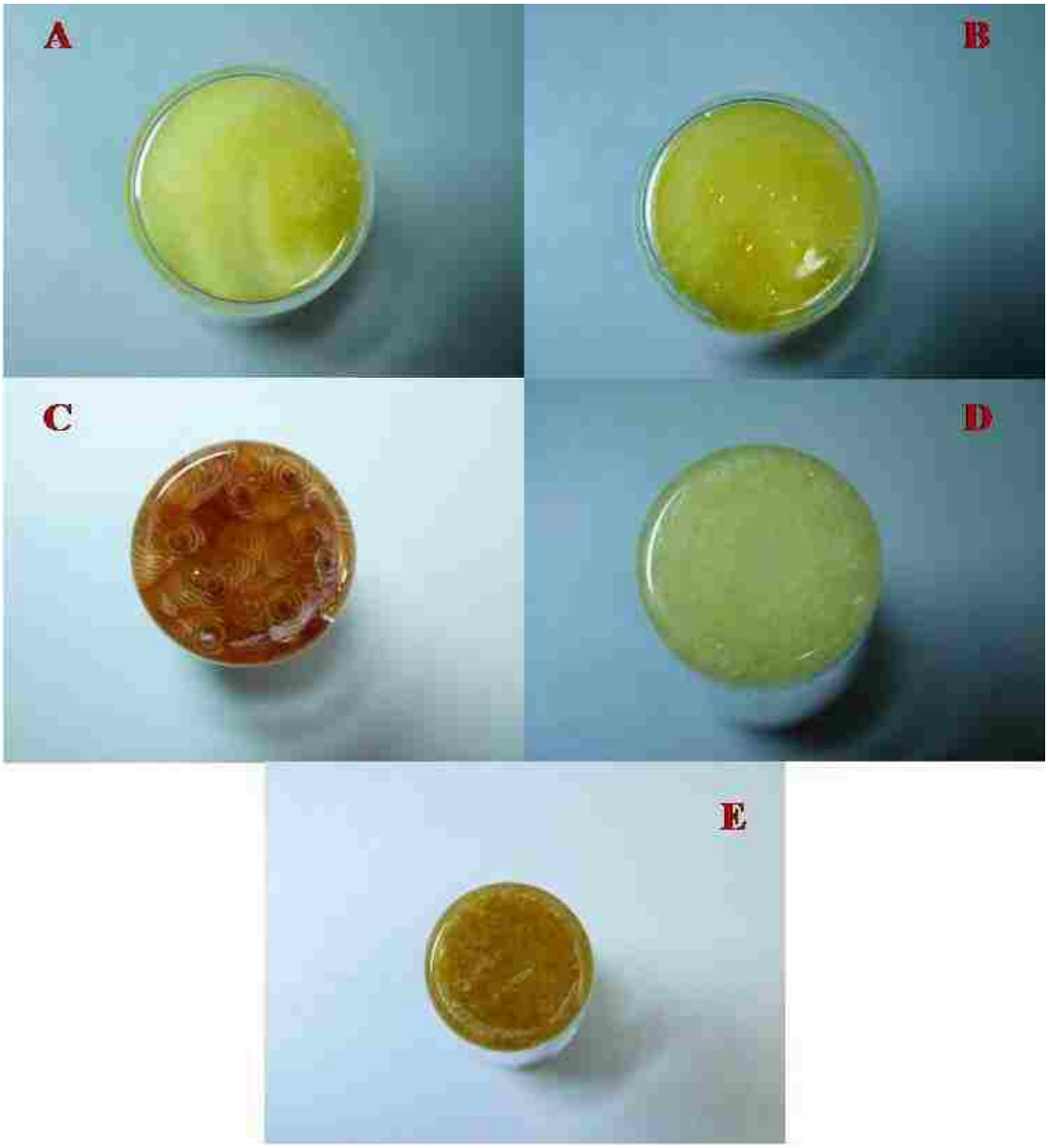

Figure 4.1 Images of patterns formed by solutions of gly6,6 in NMMO monohydrate: 2% (A), 5% (B), 10% (C), 15% (D), 20% (E). The diameter vial was 20 mm.

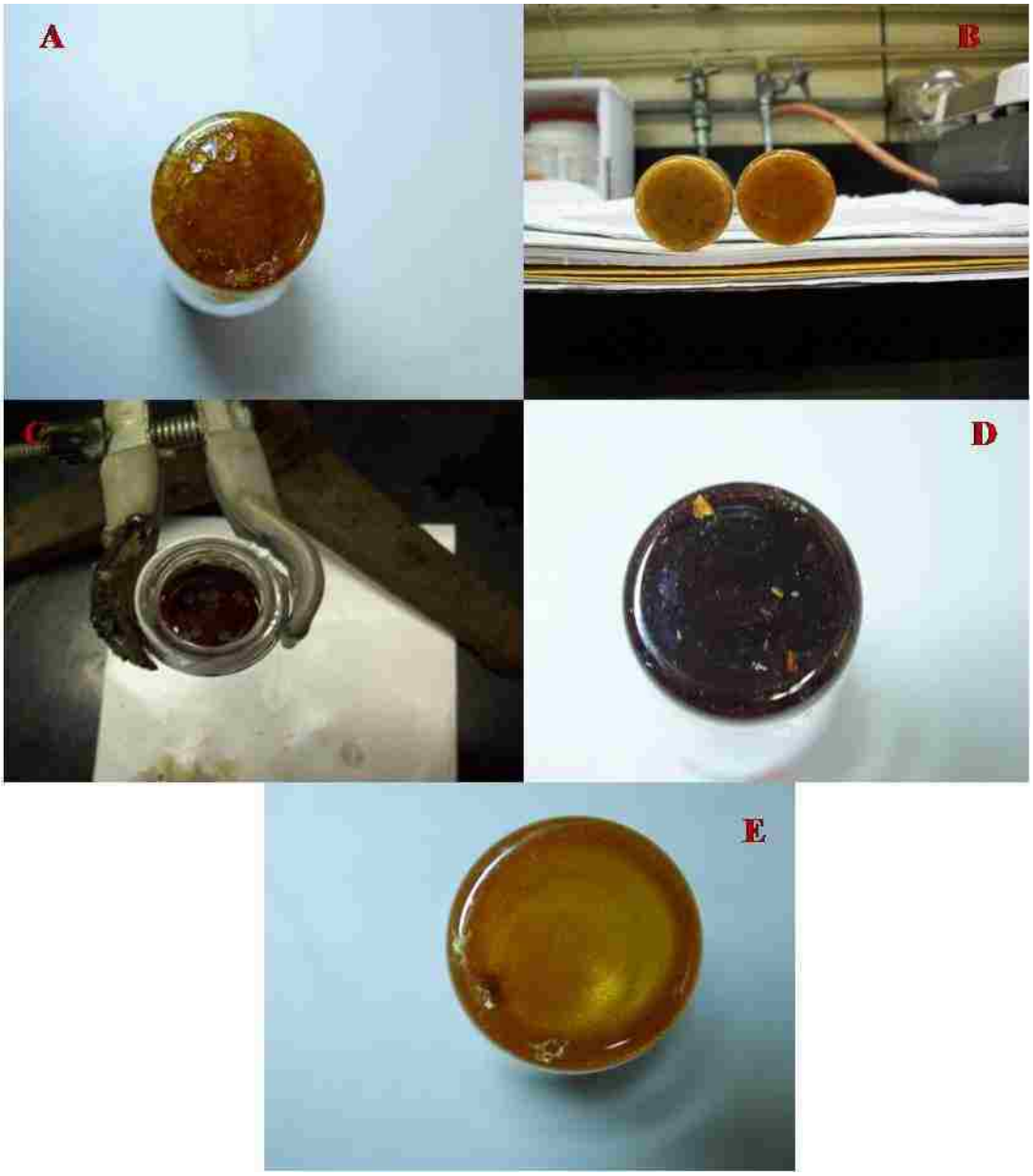

Figure 4.2 Images of morphologies recorded for glylons-6,6 solutions in NMMO monohydrate: 30% (A), 40% (B), 50% (C), 60% (D), 80% (E). The diameter of vial was 20mm.

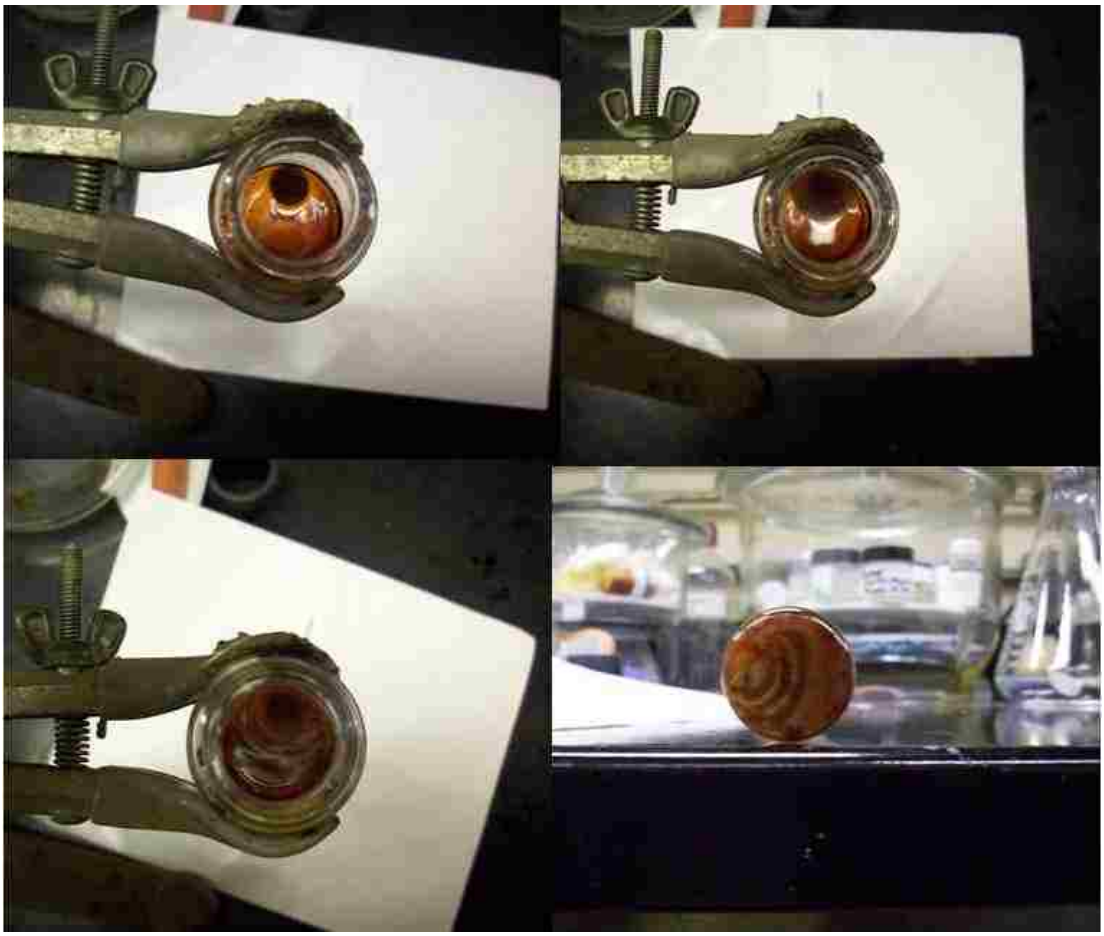

Figure 4.3 The growth of the single nucleation point in a 5% solution of glylon-6, 6 in NMMO x H_2O. The diameter of vial was 20 mm.

Figure 4.4 Nucleation and growth exhibited by a 15% solution of glylon-6,6 in NMMO x H_2O. The diameter of vial was 20mm.

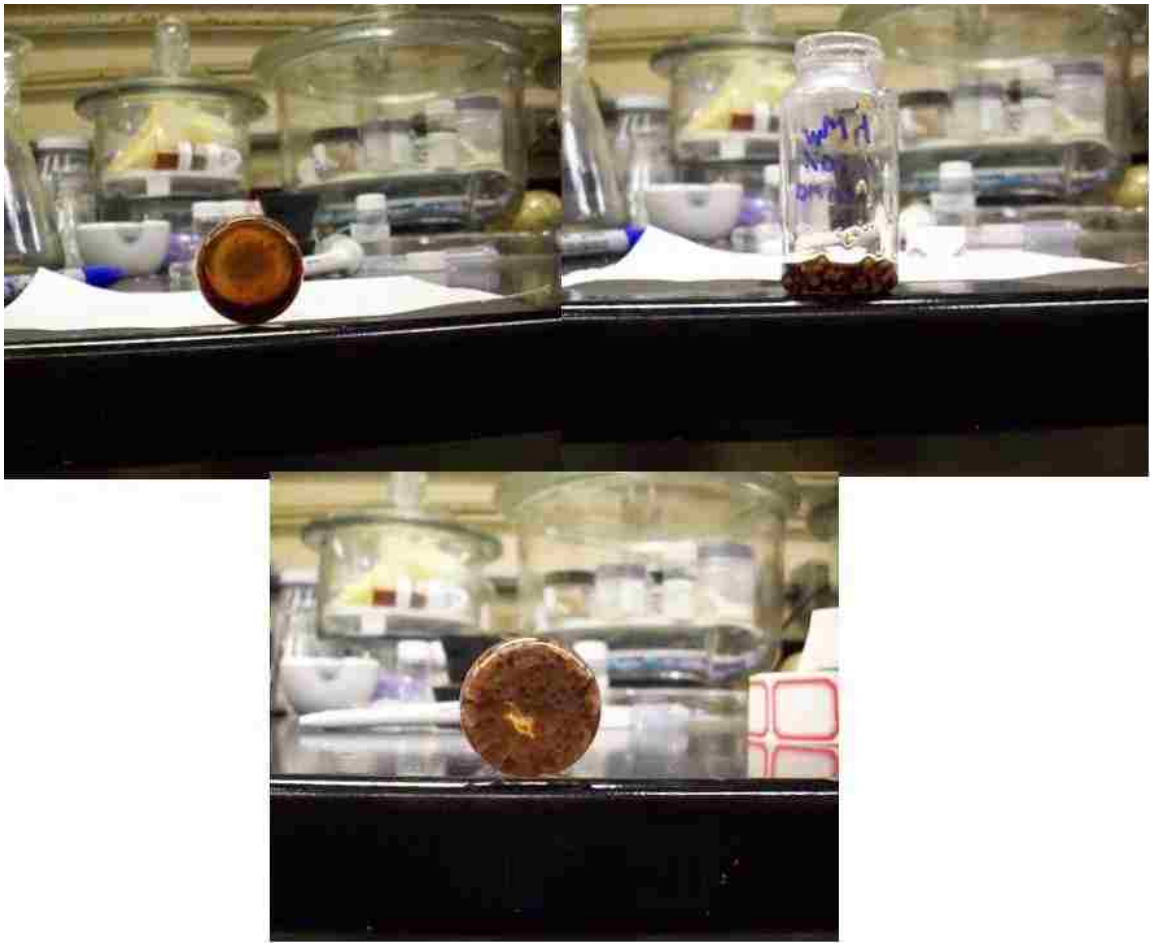

Figure 4.5 Nucleation and growth for a 20% solution of glylon-6,6 in NMMO x H_2O
The diameter of the vial was 20 mm.

4.3 Factors Influence on the Size and the Shape of the Spirals/ Tree Rings

The visual observation of these systems during their preparation led to a set of valuable concluding remarks regarding the range of factors that govern and play an important role in pattern formation.

4.3.1 Concentration

The study of the solutions revealed that the diameter of the rings decreases with the increase of concentration for the same diameter of the vial. 2% solution exhibited a single nucleation point due to less amount of polymer present in the mixture. The rings could grow relatively large in size on the whole bottom of the vial. Only two rings are visible for 2%. The next solution, 5%, shows more rings disposed on the vial's bottom. A single nucleation point it is visible in the picture but for the other samples, same concentration, two nucleations were involved. Higher amount of polymer brings more impurities (e.g. molecular defects). On this basis more nucleation points and growth fronts respectively can develop. Yet, the shape of the patterns and the ring thickness is the same. On the opposite side, 70% and 80% solutions couldn't exhibit spirals/ tree rings formation due to the high amount of the polymer considered for the same surface available. Probably the patterns nucleated but without growth because the depletition zone cannot occur. Consequently, the polymer chains cannot diffuse onto it. The large amount of the polymer in the system unbalanced the evolution of rings. The gly_60% nucleated after two weeks of refrigeration at 5°C.

4.3.2 Temperature

The solution formation required heat to melt and to mix the solvent and the polymer, both solid at room temperature, until a clear transparent mixture was obtained. The spirals/ tree rings patterns formation needed low tempetatures. As previously mentioned, the mixture was cooled down until the solutions began to nucleate. An interesting aspect was noticed: several samples of

gly-6, 6 and GalEt_hexaunpr were placed directly in the freezer during cooling process at a temperature of approximately -15ºC. The nucleation occurred faster when compared with the samples refrigerated at 5°C and with those cooled gradually at room temperature. Yet, the size of the patterns was visibly smaller probably due to the larger amount of heat withdrawn from the system in a shorter time that allowed the nucleation in more points.

4.3.3 Viscosity

The size of spirals/ tree rings was found to be highly dependent on the viscosity. The NMMO is a thick fluid at 80ºC (melting point) due to its high resistance to flow. The polymer powder added to the solvent increased its internal resistance. The 70 and 80% solution didn't show rings formation probably because of the thickness of the solution. The chains do not have the possibility to move and organize and the same situation is encoutered by the NMMO x H_2O molecules. The interactions between solvent and polymer molecules are "frozen". The solution's consistence is similar with gels. It is appearant that the forces between solvent and polymer before and after nucleation are highly dependent on the vicosity of the system.

4.3.4 Surface

The majority of the samples were prepared using 25 mm bottom large scintilation vials. It was apparent, after the observation of high concentration solutions behavior, that the area of the surface available for growth is very important in tree rings formation equation. Thus, several samples of low concentration were prepared increasing the size of the bottom vial. As expected the ring's diameter was increased not the thickness. More nucleation points were visible. Based on this observation a 80% sample was prepared and analysed in the same manner as mentioned above. The increase in surface favored the nucleation and the growth of visible organised paterns. Nonetheless, a dependence between the diameter of the rings and the size of the surface can be noted. Another interesting test was performed on different surfaces. Sets of rings grown

on a glass surface tend to adopt a planar axial disposition. The plastic surfaces favor a spatial tilted orientation of these patterns. This detail was noted by using confocal microscopy. Furthermore, the glass and plastic surfaces were modified by scratching various shapes. Even under these conditions tree rings maintained their morphology.

4. 4 Methods of Characterization

4.4.1 Optical Microscopy

The patterns formed by glylons derived from D-glucaric acid were investigated with an NIKON MICROPHOT FXA optical microscope. The images recorded with the optical microscop brought to light another interesting aspects not captured by the usual digital camera. Figure 4.6(A) shows clearly that each set of tree rings is enclosed in a polygonal shape, pentagonal or hexagonal. This was not noticed when NMMO or BMIMCl itself was heated and cooled. The crystallization pattern for the two solvents is branched, arborol like. It is appearent that interactions between the solvent and the polymer chains govern the appearance of such interesting patterns. The boundaries between neighbor sets of fringes are very straight, as illustrated in Figure 4.6(B). In Figure 4.6(C) one can see the way that sets of polymer fibrils are caught and coil around the nucleation (Figure 4.6(D)) point. The term fibril must be understood here as being a multitude of polymer chains caught together by intermolecular H-bonds. Figure 4.6(E) depicts better the organization of fibrils around the nucleation point. It is noteworthy that the rounded traiectory tends to be right-handed. This trend was not observed for GalEt_hexaunpr solutions in NMMO. The behavior of gly-6,6 solutions can be explain by taking in consideration the assimetry of glucose backbone. Naturally, the sugar's chirality allows coiling under the circumstances of free hydroxyl groups interaction through H-bonds. On the contrary, the galactose is a symmetric compound. The interactions needed to coil such structure needs to be stronger or the time they stress the backbone has to be longer.

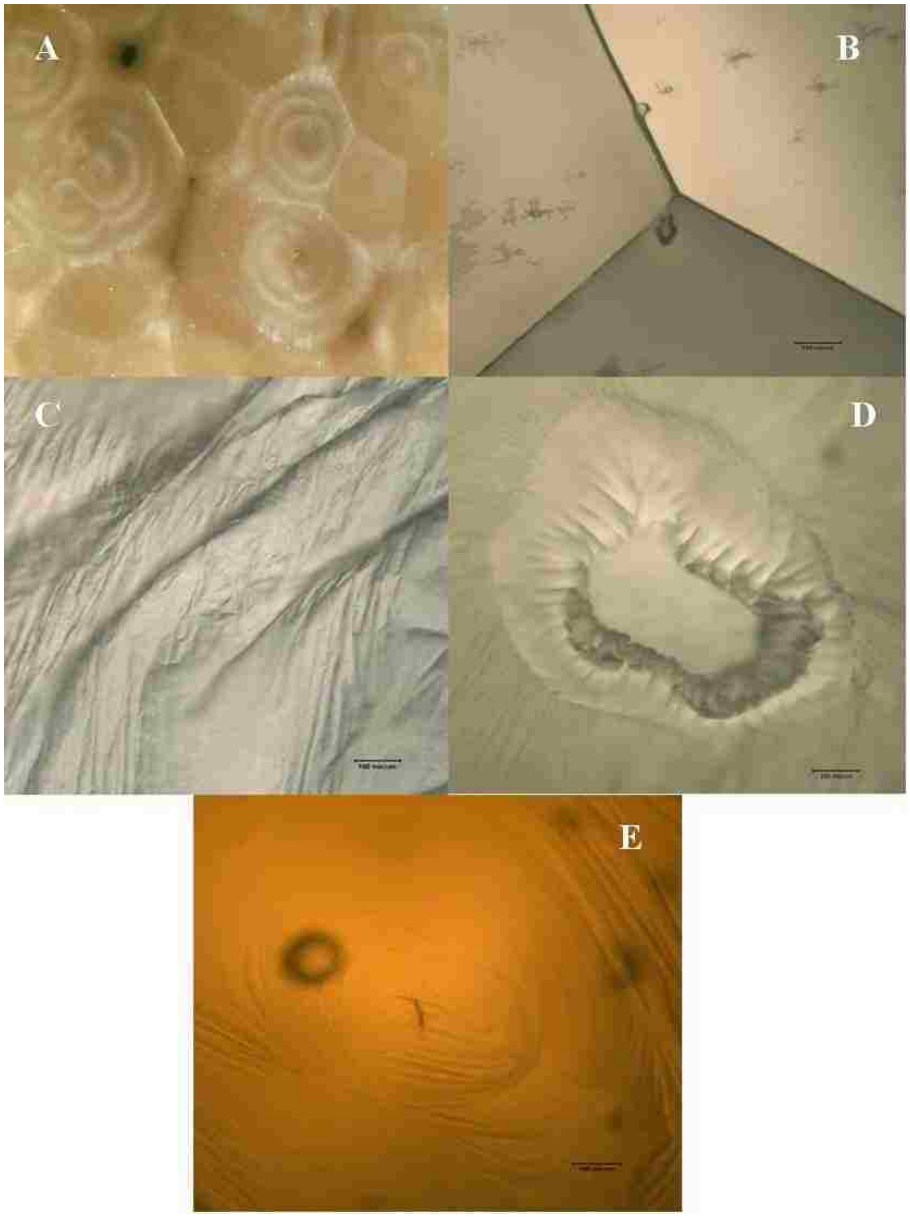

Figure 4.6 Microscopic image of tree rings (A), boundaries between sets of tree rings (B), fibrils organization (C), nucleation point (D), vicinity of the nucleation point. The dark spots are gas bubbles (air/nitrogen) caught in the mixture during sample preparation. Image A has the magnification 4×. The scale bar for the rest is 300 microns.

4.4.2. Polarized Light Microscopy (PLM)

An Olympus Polarizing Microscope was used to investigate the formation of liquid crystals under the crossed polarizers. The sample setting consisted in a glass slide, an *O*-ring and a glass cover. The microscope is equipped with a Canon camera to capture the images.

Polarized Light Microscopy is one of the most widely used techniques to investigate systems suspected to form liquid crystalls, LC. The glylons samples placed between crossed polarizers (90°C) exhibited anisotropy and are in the domain of LC organization. The sample were enclosed in plastic cuvettes or between two glass slides aparted by an *O*-ring. Figure 4.7 shows a 15% solution of glylon-6, 6 in NMMO. No order can be noticed for the solvent (Figure 4.8).

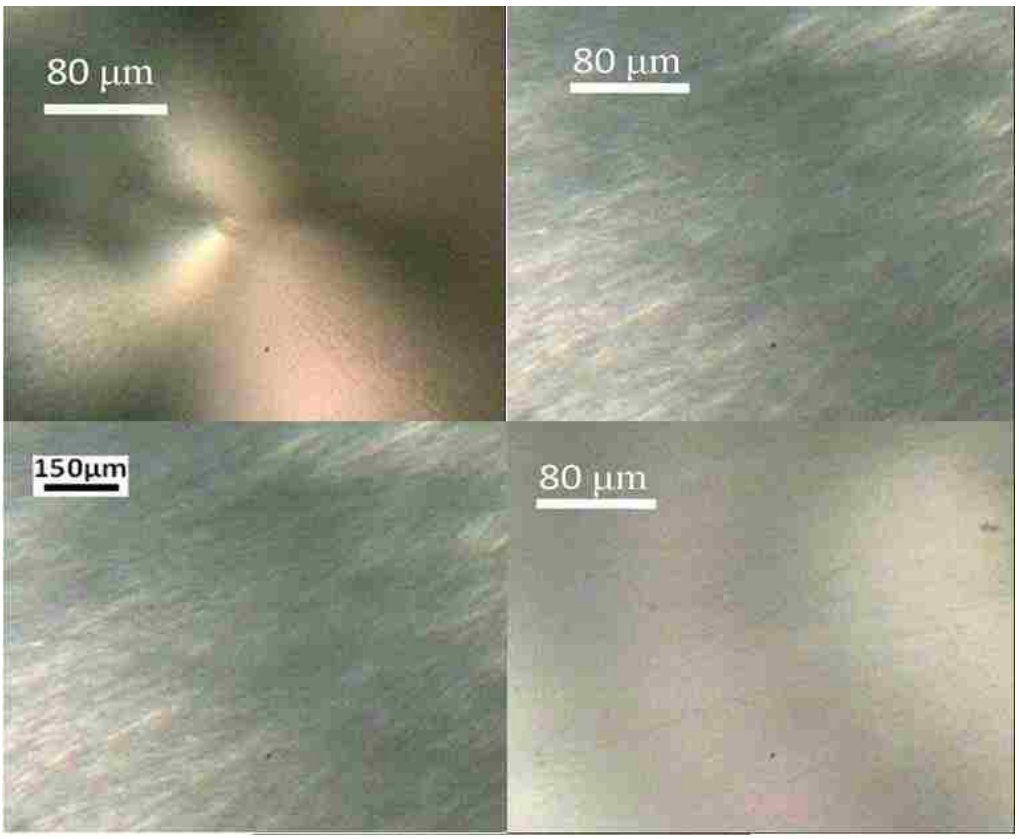

Figure 4.7 Polarized light micrograph of 15% gly-6,6 solution in NMMO monohydrate depicting a nucleation point (top left) and rings (top right, bottom left, right).

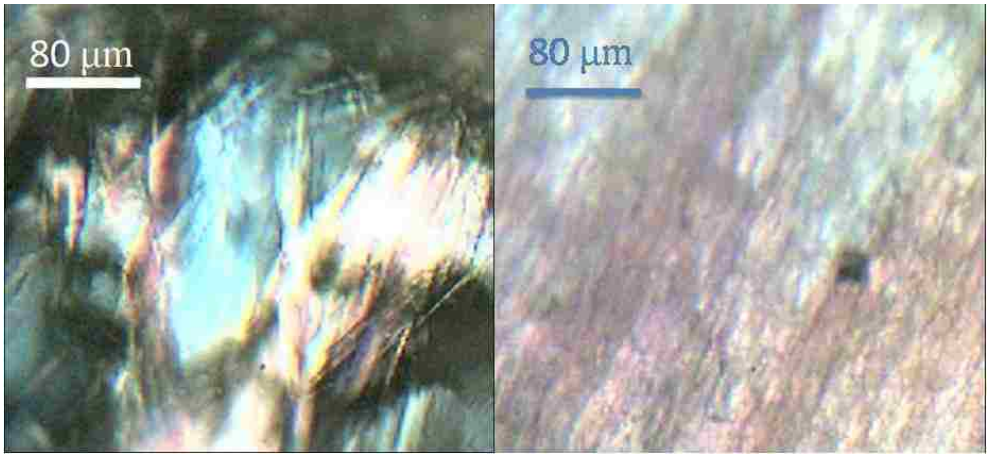

Figure 4.8 Image of NMMO monohyhrate between crossed polarizers. No order can be noted.

4.3.3 Confocal Microscopy (CM)

The means of confocal microscopy revealed two interesting aspects, as mentioned above. A Leica TCS SP2 confocal microscope was used to visualize solutions of gly-6, 6 and GalEt_hexaunpr. When the samples were placed between glass slides the patterns tend to adopt a planar arrangement (Figure 4.9) when compared with those from polycarbonate cuvettes that have a spatial distribution (Figure 4.10 and 4.11).

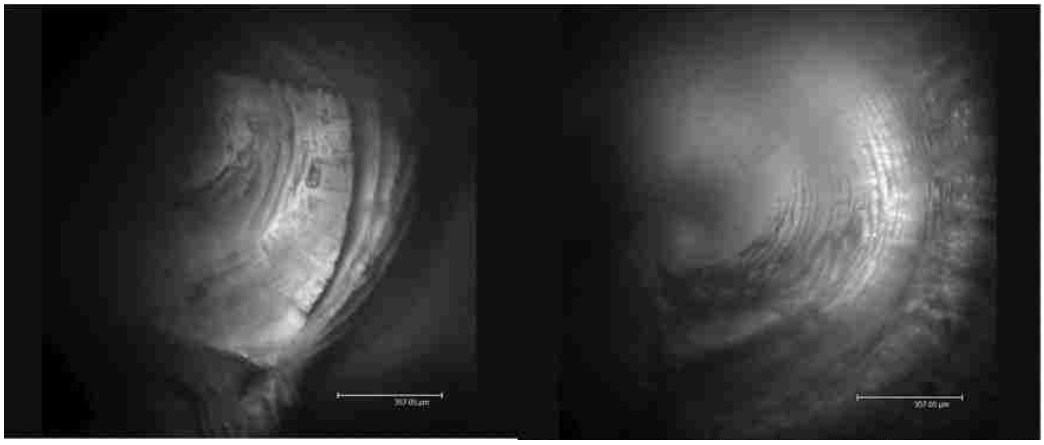

Figure 4.9 Confocal images of 15% solution of gly-6,6 in NMMO monohydrate. The sample was placed in a plastic cuvette. The scale bar represents 350 μm.

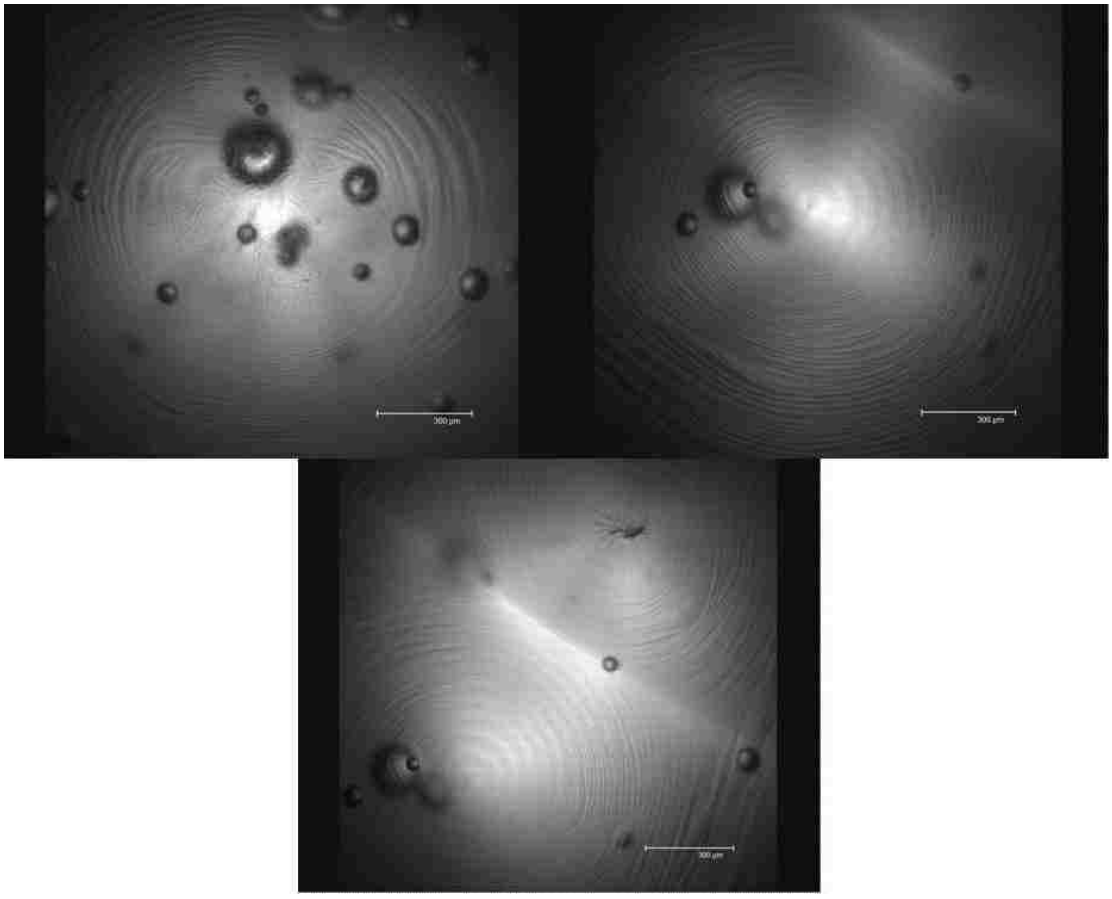

Figure 4.10 Confocal micrographs of tree rings pattern found in a 15% solution of gly-6,6. The solvent is NMMO monohydrate. The sample was placed between glass covers separates by an O-ring. The scale bar represents 300 μm.

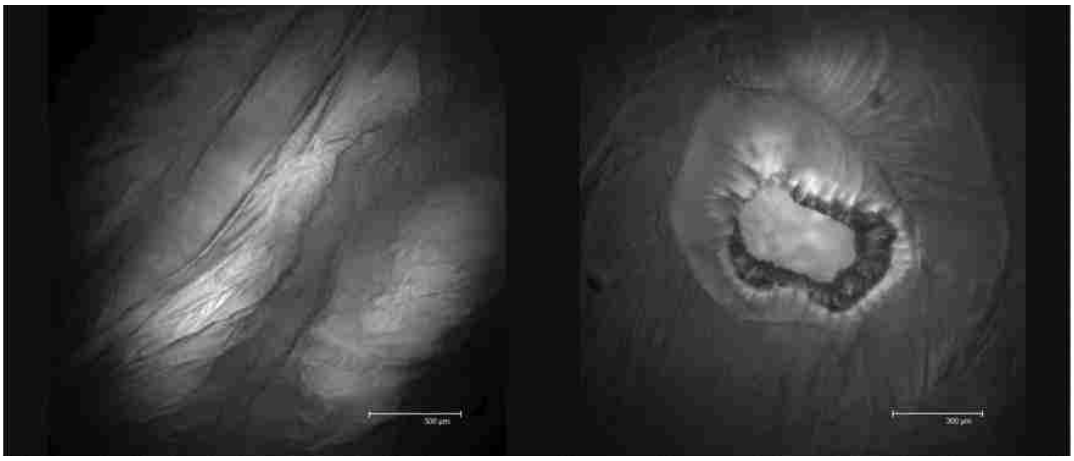

Figure 4.11 Confocal images of fibrils (left) and nucleation point (right) for a 15% solution of gly-6,6 in NMMO monohydrate. The sample was placed between two glass covers separated by an *O*-ring. The scale bar is 300 μm.

The difference is explained by the nature of interactions between solution system and hydrophylic or hydrophobic surfaces. As a physical body, the solution system is hydrophilic, consequently the growth front will be rejected by the hydrophobic plastic cuvette wall resulting in a "growing onto" tendency of polymer fibrils. On the other side, the glass surface attracts the new formed phase and the result is a "growing next to" behavior. Confocal microscopy gave useful information about the GalEt_hexaunpr solutions organization. The pattern morphology is different. Even the fibrils looks the same (Figure 4.12, top right) they exhibit completely different morphologies. They arrange in sets of "petals" (Figure 4.12 top left). The surface nature (hydrophobic or hydrophilic) do not exert an influence on fringes like in the case of the gly-6,6

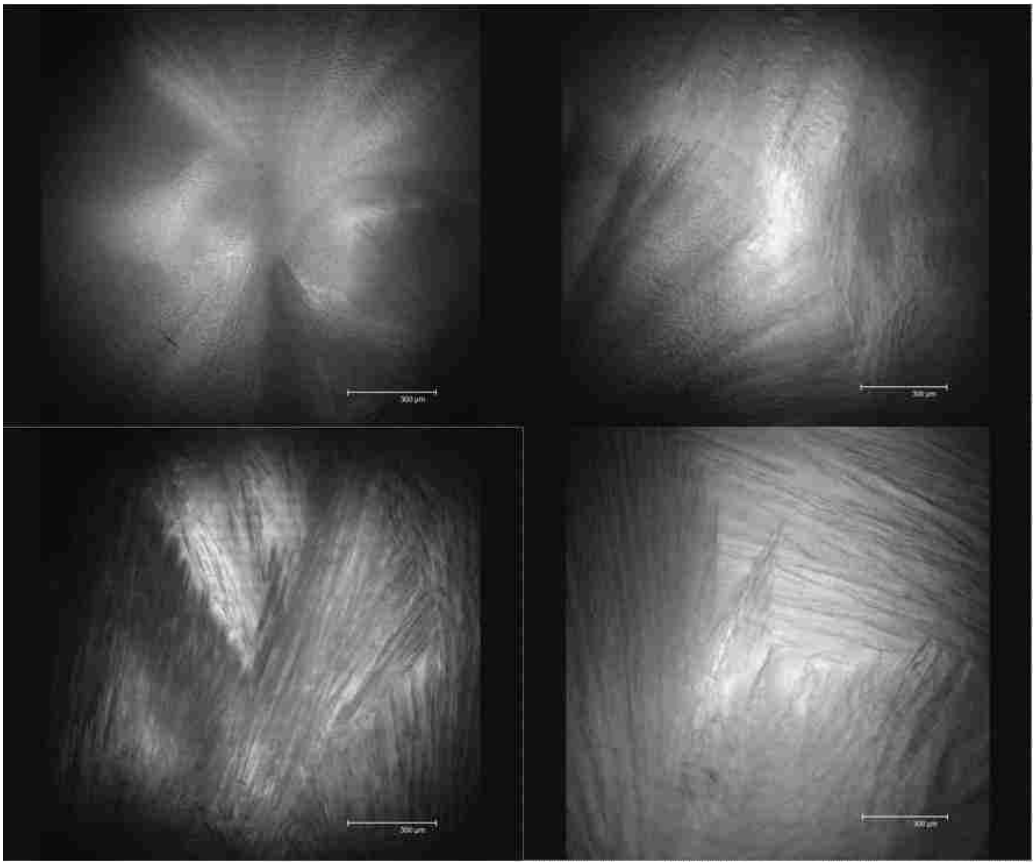

Figure 4.12 Confocal micrograms of a 15% solution of GalEt_hexaunpr in NMMO monohydrate depicting a nucleation point (top left), two sets of overlapped *picotees* (top right and bottom). The scale bar represents 300 μm.

solutions. The possible explanation is that the asymmetric glucose backbone coils and twists in the same time while the symmetric galactose only coils. The degree of ordering is influenced by the possible free paths that fringes can adopt. Certainly, in galactose solutions fibrils have an increased degree of freedom and can be influenced more easily by external forces (solvent and water influence as will be discussed in the paper "*Tree Rings*- organized resembling patterns formed upon cooling the glylon-6,6 solutions inn N-methyl-N-morpholine oxide and ionic liquids"). It can be concluded that for gly-6,6 solutions less energy must be withdrawn from the system to favor tree ring formation when compared with the GalEt_hexaunpr counterpart. Figure 4.13 reflects the morphology of NMMO crystals. No similarity with tree rings patterns can be observed.

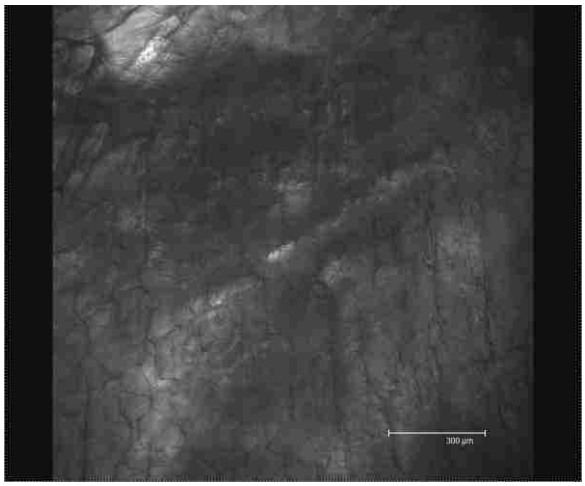

Figure 4.13 Confocal image of NMMO monohydrate. No tree ring organization is noticed. The scale bar represents 300 µm.

4.4.4 Small/Wide Angle Light Scattering (SAXS/WAXS)

SAXS/WAXS measurements were recorded at the Center for Advanced Microstructures and Devices, Louisiana State University. The SAXS beamline has a crystal monochromator with energy range from approximately 3 to 14 KeV. The scattering pattern was obtained by using a Gabriel multiwire detector having a 200 mm active diameter and a resolution of 200- 500 µm

FWHM in a 1024 x 1024 array. Presently the instrument operates at 1.3 GeV with the wiggler at 7 Tesla. Measurements were performed on a 15% gly-6,6 solution in NMMO (Figure 4.14). The scattering pattern for the neat polymer shows an amorphous structure (Figure 4.15). Circularly averaged scattering pattern images are also provided (Figure 4.16 and Figure 4.17). More investigation are necessary to elucidate the complex organization of these solutions.

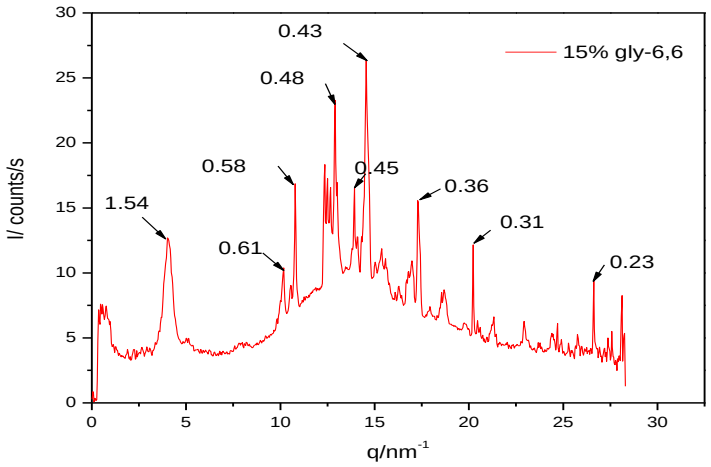

Figure 4.14 Circularly averaged scattering profile obtained by extraction from scattering pattern of a 15% solution gly-6,6. Time exposure is 4800 s

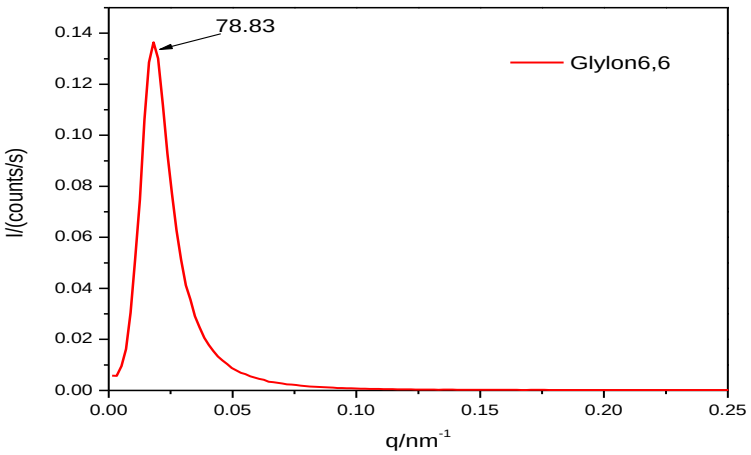

Figure 4.15 SAXS spectra of obtained by extraction from scattering pattern of glylon-6, 6 powder obtained from scattering pattern. Time exposure is 600s.

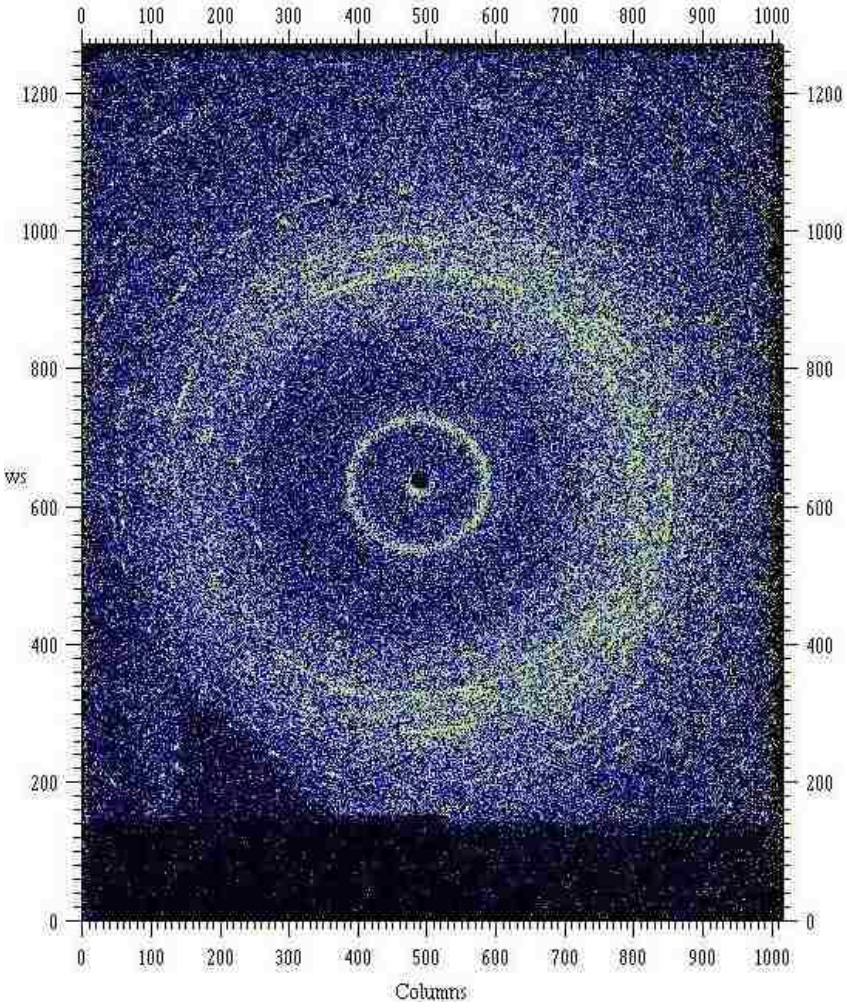

Figure 4.16 Circularly averaged scattering pattern of a 15% solution of gly-6, 6 in NMMO monohydrate

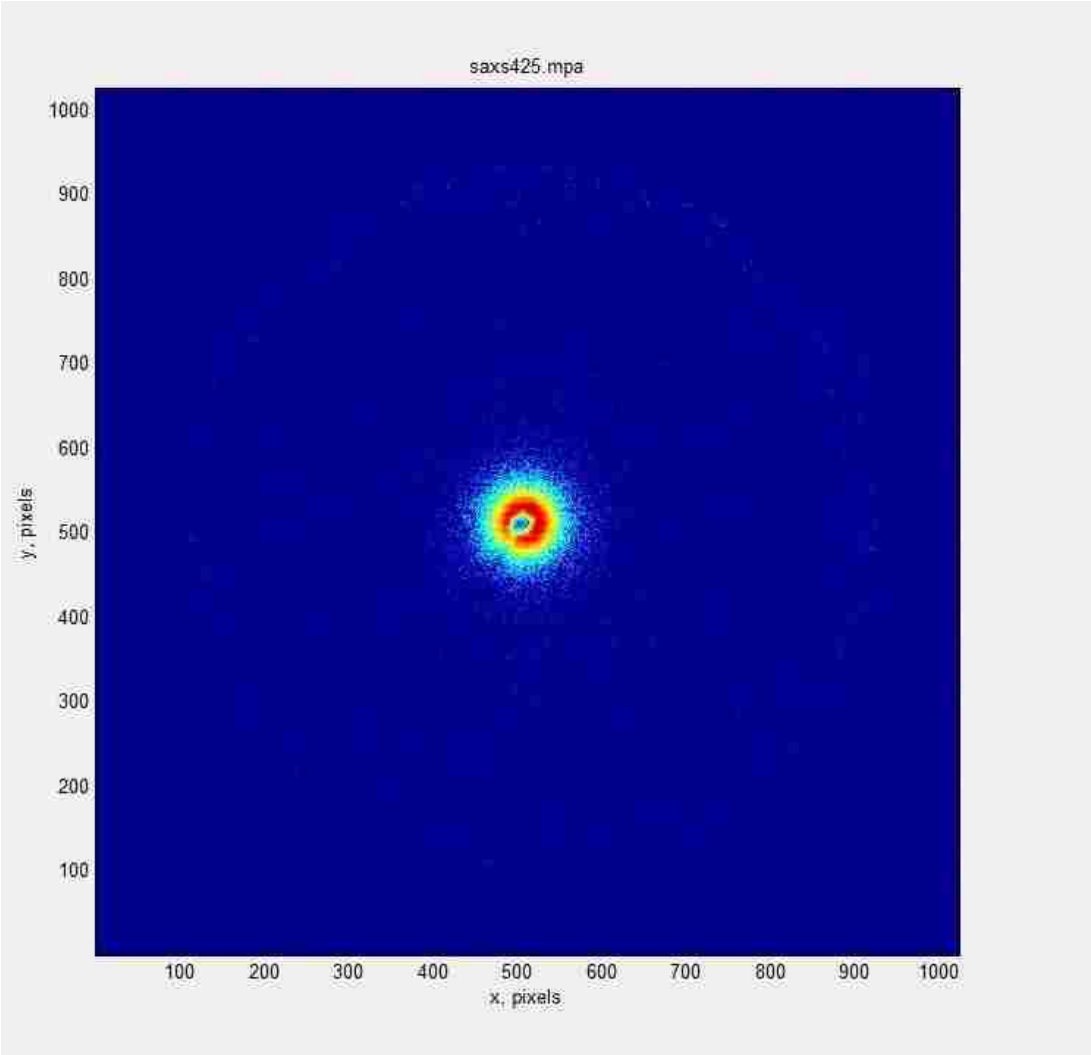

Figure 4.17 Circularly averaged scattering pattern of neat gly-6,6 in NMMO monohydrate

4.5 Characterization of Unprotected D-Galactaric Derivatives Solutions in Anionic Liquids (BMIMCl)

Solutions of both Gly-6,6 and GalEt_hexaunpr prepared in BMIMAc didn't exhibit any kind of organization even though were refrigerated at very low temperatures (<-15°C) for at least two weeks. The solutions in BMIMCl required refrigeration for two weeks (e.g, 10% solution shown in Figure 4.18) at a temperature of -15°C. These solutions are presently under investigation.

Figure 4.18 Patterns formed by a solution of GalEt_hexaunpr in BMIMCl. The concentration is 10%. The diameter of the vial was 20 mm.

4.6 Characterization of Unprotected Galactaric Derivatives Solutions in DMSO

Unprotected galactaric derivatives were found to form gels in DMSO (Figures 4.19 and 4.20). These systems are currently under investigation. The swelling properties of these gels can be exploited and new applicantions can be found.

Figure 4.19 Gel obtained form a 5% solution of GalEt_hexaunpr in DMSO

Figure 4.20 Gels obtained upon cooling from 5 and 10% solutions of GalEt_hexaunpr in DMSO

CHAPTER 5 SUMMARY AND CONCLUSIONS

Glylons are a new family of polymers with remarkable properties that have the potential to be highly functional materials. They have the advantage to be derived from renewable primary materials with respest to the impact on the environment. Future perspectives based on the availabilility of fossil fuels as sources for polymer synthesis should place a great deal of attention on the glylons, as renewable raw materials.

Several kinds of polymers from this family were synthesised. The attention was focused on monopotassium salt of D-glucaric and galactaric acid as starting materials. As expected, D-glucaric derivatives with free hydroxyl group named glylons-6, 6 exhibited low solubilities and low molecular weights. Attemps to increase the molecular weights led to limited success. The GPC curve for the polymer labeled gly6,6_hMw begins from lower values of elution volume when compared with the polymers that were not subjected to further treatments. The solubility impede to efficiently characterize these materials with the most common tecniques used in polymer synthesis.

FTIR data have confirmed the chemical shifts for the specific groups in good agreement with the data available for classic nylons. The presence of mixture's linear diester plus mono- and dilactones was confirmed by NMR spectroscopy accordingly with the observations provided by Professor Kiely's work.

The multitude of difficulties encountered along the characterization of these polymers led to idea to derivatize the compounds by blocking the pendant hydroxyl groups with acetal groups. Two starting reagents were used: D-glucaric monopotassium salt and galactaric (mucic) acid. As expected the derivatives exhibited better properties when compared with free hydroxyl groups counterparts. Yet, differences exist between the D-glucaric polymers (GluEt_prop, GluEt_hexa) and (GalEt_prop, GalEt_hexa). The comformations of D-glucose and galactose are responsible

for this properties. D-glucaric derivatives still have two hydroxyl groups capable to initiate H-bonding and to lower the solubility. On the other side, galactaric derivatives have all hydroxyls blocked reflected in the broad raw of solvents solubilities. The molecular weights are higher but not as high as expected. This was revealed by GPC coupled with MALDI-TOF mass spectroscopy. The polycondensation reaction proceeds with the occurrence of two competitive reactions: linear and propagation cyclization. Macrocycle formation limits the molecular weight that can be achieved.

Studies performed on stoichiometry showed that the best proportion of diacid to diamine is 1 to 0.95. Furthermore the MALDI-TOF spectra recorded for GalEt_prop1:95 and GalEt_hexa 1:95 revealed another important aspect: macrocycles are the dominant species for GalEt_hexa1:95 while for the GalEt_prop1:95 was the linear dominate.

Glylons- 6, 6 decompose right after the melting while the acetalated compounds show no decomposition up to 200°C. Acetalated D-glucaric acid and galactaric acid-based glylons are low crystaline polymers. The protected glylons have higher thermal stability when compared with unprotected counterparts. They have a high potential for adjusting the properties with respect to a respective application.

Solutions of glylons-6, 6 in NMMO monohydrate form organized patterns resembling tree rings. The mixtures are liquid crystalline systems with the great potential in electronics applications. The domains of the prepared solutions (2- 80%) were found to be highly dependent on concentration, viscosity, temperature, volume of the sample and the diameter of the vial. The formation of these patterns is explain by the occurrence of strong H-bonding initiated by the NMMO monohydrate. The morphologies of these solutions are under investigation. The same phenomena were observed for the solutions of unprotected galactaric derivatives in NMMO monohydrate, except the shape of the patterns. Due to their similarity with a flower they were

called *picotees*. Such kind of organization observed for glylons-6, 6 solutions in NMMO was noticed for the galactaric derivatives in anionic liquids more precisely in BMIMCl.

Mixtures of glylons-6, 6 with DMSO form gels. It was concluded that these polymers exhibit good swelling properties.

CHAPTER 6 RESEARCH IN PROGRESS AND FUTURE WORK

The main goal of future research will be to synthesize higher molecular weight glylons in order to be able to spun fibers. To this aim additional investigations should be performed. Several will be presented in the following.

6.1. Synthesis of Diamines from Sugars

Diamines used in the glylons synthesis are oil originated. To make the polymers entirely green the best idea is to obtain them from sugars.

6.2. Prevention of Macrocyclization Process

The polymerization of acetalated bis-galactaric and D-glucaric derivatives proceeds with formation of cyclic structures that evolve parallel with linear counterparts. The premature termination by cyclization limits the molecular weights that can be achieved. In order to obtain only linear polymer the best idea will be to use branched diamines or diamines having big pendant groups. A long, branched backbone will not allow cyclization due to the sterical hindrance induced by the attached groups.

6.3 Quantitative Analysis of the Tree Rings Morphology

The formation of the tree rings is very poorly understood at this stage. The microscopy, DSC and TGA results suggest that the water may be the key factor in the occurrence of such patterns. The goal will be to design an hyphotetical model to illustrate the interaction between the water and the solution system.

6.4 Preparation and Characterization of Glylons Molecular Composites

Glylons can be molecularly blended with other polymers (e.g., cellulose). They will generate new materials with enhanced properties. These materials will combine the strength and the hydrophilic properties of the glylons due to their polyamidic structure and sugar subunits, and the properties of natural cellulosic fibers.

6.5 Rheology of Glylons Solutions and Glylons Molecular Composites

Rheology is the best tool that investigates the basic textile properties of fibers such as tenacity, dimensional stability, elasticity and dyeability. The method can determine the domaine temperature and the concentration in which glylons and glylons composites can possibly form liquid crystalline systems.

6.6 Characterization of Glylons Solutions in NMMO x H_2O, DMSO and Ionic Liquids

Solutions of glylons in NMMO and anionic liquids show the tendency to form organized resembling tree ring patterns. Microscopic techniques such as Polarized Light, Confocal and Optical Microscopy were used to elucidate the formation of such fringes. SAXS/WAXS were poorly used to investigate the systems. One of the future goals will be to use the facilities provided by CAMD to better understand the spatial arrangement of the tree rings and the polygonal shapes that enclose them.

6.7 Computational Modelling

A challenging goal will be to model the formation of tree ring patterns based on the experiments performed so far.

6.8 Preparation and Characterization of Glylons Mixtures with Responsive Composite Nanoparticles

Mixtures of glylons with composite nanoparticles would have the potential to form liquid crystal systems with novel morphologies.

REFERENCES

(1) Kiely, D. E.; Ponder, G. *U.S. Patent 6,049,004*, Dec. 11, **1998**.

(2) Negulescu, I. I., Laine, R. Annual Report "Biomass Glucose Derived Fiber Forming Polyamides" LEQSF board of Regents Grant, ITRS Program, **2002**.

(3) Ogata, N.; Sanui, K.; Okouchi, K. *Polym. J.* **1973**, *5*, 186.

(4) Ogata, N.; Hosoda, Y. *Polym. J.* **1974**, *6*, 412.

(5) Ogata, N.; Sanui, K.; Asahara, T. *J. Polym. Sci. A-1* **1969**, *7*, 889.

(6) Ogata, N.; Hosoda, Y. *J. Polym. Sci., Polym. Lett.* **1974**, *12*, 355.

(7) Hashimoto, K.; Wibullucksanakul, S.; Matsuura, M.; Okada, M. *J. Polym. Sci.,Polym. Chem. Ed.* **1993**, *13*, 3141.

(8) Hashimoto, K.; Wibullucksanakul, S.; Ogata, M. *J. Polym. Sci., Polym. Chem. Ed.* **1995**, *33*, 1495.

(9) Ogata, N.; Sanui, K.; Nakamura, H.; Kuwahara, M. *J. Polym. Sci., Ed.* **1980**, *18*, 939.

(10) Ogata, N.; Hosoda, Y. *J. Polym. Sci., Polym. Chem. Ed.* **1975**, *13*, 1793.

(11) Ogata, N.; Sanui, K.; Nakamura, H.; Kuwahara, M. *J. Polym. Sci., Ed.* **1980**, *18*, 939.

(12) Hoagland P. D. *Carbohydr. Res.* **1981**, *98*, 203.

(13) Hoagland, P. D.; Pessen, H.; McDonald, G. G. *J. Carbohydr. Chem.* **1987**, *6*, 495.

(14) Pocker, Y.; Green, E. *J. Am. Chem. Soc.* **1976**, *98*, 6197.

(15) Tipson, R. S.; Clapp, M. A. *J. Org. Chem.***1953**, *18*, 952.

(16) Davey, C. L.; Kiely, D. E.; Harris-Manley, M. *Carbohydr. Res.* **2006**, *341*, 2688.

(17) Styron, S. D.; Kiely, D. E.; Ponder, G. *J. Carbohydr. Chem.* **2003**, *22*, 123.

(18) Morton, D. W.; Kiely, D. E. *J. Polym. Sci., Polym. Chem. Ed.* **2000**, *38*, 604.

(19) Kiely, D. E.; Chen, L.; Lin, T-H. *J.Polym. Sci., Polym. Chem. Ed.* **2000**, *38*, 594.

(20) Kiely, D. E.; Chen, L.; Lin, T-H. *J. Am. Chem. Soc.* **1994**, *116*, 571.

(21) Chen, L.; Kiely, D. E. *J. Org. Chem.* **1996**, *61*, 5847.

(22) Styron, S. D.; Kiely, D. E.; Ponder, G. *J. Carbohydr. Chem.* **2003**, *22*, 123.

(23) Viswanathan, A.; Kiely, D. E. *J. Carbohydr. Chem.* **2003**, *22*, 903.

(24) Carter, A.; Morton, D. W.; Kiely, D.E. *J. Polym. Sci., Polym. Chem. Ed.* **2000**, *38*, 3892.

(25) Styron, S. D.; French, A.D.; Friedrich, J. D.; Lake, C. H.; Kiely, D. E. *Carbohydr. Chem.* **2002**, *21*, 27.

(26) Chen, L.; Kiely, D. E. *J. Carbohydr.Chem.* **1994**, *13*, 585.

(27) Binkley, R. M.; Ambrose, M. G.; Heheman, D. G. *J. Org. Chem.* **1980**, *45*, 4387.

(28) Ambrose, M. G.; Binkley, R. W. *J. Org. Chem.* **1983**, *48*, 674.

(29) Binkley, R. W.; Koholic, D. J. *J. Carbohydr. Chem.* **1984**, *3*, 85.

(30) Binkley, R. W. *J. Carbohydr. Chem.* **1985**, *4*, 227.

(31) Binkley, R. W.; Sivik, M. R. *J. Org. Chem.***1986**, *51*, 2619.

(32) Binley, R. W.; Ambrose, M. G.; Heheman, D. G. *J. Carbohydr. Chem.* **1987**, *6*(2), 203.

(33) Satyamurthy, N.; Bida, G. T.; Padgett, H. C.; Bario, J. R. *J. Carbohydr. Chem.* **1985**, *4*, 489.

(34) Card, P. J. *J. Carbohydr. Chem.* **1985**, *4*, 451.

(35) Negulescu, I. I., Laine, R. Annual Report "Biomass Glucose Derived Fiber Forming Polyamides" LEQSF board of Regents Grant, ITRS Program, **2003**.

(36) Kiely, D. E.; Kramer, K. *U.S.Patent 7,314,906*, Dec. 10, **2003.**

(37) Sweeley, C. C..; Bentley, R.; Makita, M., Wells, W.W. *Gas Chromatography of Sugars* **1963**, *85*, 2497.

(38) Prömpers, G.; Keul, H.; Höcker, H. *Green Chemistry* **2006**, *8*, 467.

(39) Dyson, P. J.; Grossel, M.C. *J. Chem. Soc.* **1997**, 3465.

(40) Silverstein, R. M., Bassler, G. C., Morrill, T. C. "Spectrometric Identification of Organic Compounds", Fifth Edition: John Willey&Sons, Ink.

(41) Morton, D. W.; Kiely, D. E. *J. Polym. Sci., Polym. Chem. Ed.* **2000**, *38*, 604.

(42) Wetzel, S.J.; Guttman, M.C.; Girard, J.E.; *International Journal of Mass Spectrometry* **2004**, *238*, 215.

(43) Wetzel, S. J.; Guttman, C. M.; Flynn, K. M.; Filliben, J. J. *J. Am. Soc. Mass Spectro.* **2006**, *17*, 246.

(44) Wetzel, S.J.; Guttman, M.C.; Girard, J.E.; *International Journal of Mass Spectrometry* **2004**, *238*, 215.

(45) Haines, P.G. "Principles of Thermal Analysis and Calorimetry", Royal Society of

Chemistry: Cambridge CB4 0WF, UK, **2002**.

(47) Chen, L.; Kiely, D. E. *J. Carbohydr.Chem.* **1994**, *13*, 585.

(48) Ryschenkow, G.; Faivre, G. *J. Non-Cryst. Solids* **1988**, *87*, 221.

(49) Bisault, J.; Ryschenkow, G.; Faivre, G. *J. Cryst. Growth* **1991**, *110*, 889.

(50) Morse, H. G.; Waren, C. H.; Donnay, J. D. H. *J. Am. Sci* **1932**, *23 (5)*, 421.

(51) Magill, J. H.; Plazek, D. J. *J. Chem. Phys.* **1967**, *46*, 3757.

(52) Sperling, L. H. *Introduction to Physical Polymer Science* Wiley, New York, Chapter 6 **1992**.

(53) Magill, J. H. *J. Mater. Sci* **2001**, *36*, 3143.

(54) Hutter, J. L.; Bechhoefer, J. *Phys. Rev. E* **1999**, *59*, 4342.

(55) Hutter, J. L.; Bechhoefer, J. *J. Cryst. Growth* **2000**, *217*, 332.

(56) Phillips, P. J. *Handbook of Crystal Growth* Elsiever, Amsterdam, Vol. 2, Chapter 18, **1993**.

(57) Lotz, B.; Wittman, J. C. *J. Polym. Sci., Part B: Polym. Phys.* **1986**, *24*, 1541.

(58) Hosier, I. L.; Bassett, D. C.; Vaughan, A. S. *Macromolecules* **2000**, *33*, 8781.

(59) Norton, D. R.; Keller, A. *Polymer* **1985**, *26*, 704.

(60) Padden, F. J.; Keith, H. D. *J. Appl. Phys.* **1965**, *36*, 2987.

(61) Gránásy, L.; Pusztai, T.; Tegze, G.; Warren, J. A.; Douglas, J. F. *Phys. Rev.* **2005**, *72*, 011605-1.

(62) Keith, H. D.; Padden, J. F. *J. Polym. Sci.* **1958**, *31*, 415.

(63) Schuur, G. *J. Polym. Sci.* **1953**, *11*, 385.

(64) Schram, A. *Kolloid-Z.* **1957**, *151*, 18.

(65) Keith, H. D.; Padden, F. G. *J. Appl. Phys.* **1963**, *34*, 2409.

(66) Gránásy, L.; Pusztai, T.; Tegze, G.; Warren, J. A.; Douglas, J. F. *Phys. Rev.* **2005**, *72*, 011605-1.

(67) Wang, Y.; Chan, C-M.; Li, L.; Ng, K-M. *Langmuir* **2006**, *22*, 7384.

(68) Gazzano, M.; Focarete, M. L.; Riekel, C.; Scandola, M. *Biomacromolecules* **2004**, *5*, 553.

(69) Abe, H.; Kikkawa, Y. I.; Doi, Y. *Biomacromolecules* **2001**, *2*, 1007.

(70) Pan, P.; Liang, Z.; Zhu, B.; Dong, T.; Inoue, Y. *Macromol.* **2009**, *42*, 3374.

(71) Murray, S. B.; Neville, A. C. *Int. J. Biol. Macromol.* **1998**, *22*, 137.

(72) Teramoto, Y.; Nishio, Y. *Biomacromolecules* **2004**, *5*, 397.

VITA

Cornelia Rosu was born in Romania in Vatra Dornei city. She is the daughter of Pavel and Leontina Rosu.

Cornelia attended the "Al. I. Cuza" University, Iasi, Romania, from October 1991 to June 1996 and obtained a Bachelor of Science degree with a concentration in general chemistry and physics. Her favorite topics as an undergraduate student were plasma, optics and spectroscopy, electrochemistry, physical chemistry and psychology. Her thesis regarded nuclear magnetic resonance characterization, under the guideness of Professor Constantin Ghirvu, her advisor. Cornelia worked in education as schoolmaster (1996-1998) and high school teacher (1999- 2007). She taught chemistry and physics. She was the manager of the school between 2002 and 2003. Her responsibility was to train the teachers in teaching skills and to write programs to attract funds for the school.

Cornelia was accepted in 2007 by the Louisiana State University Graduate School as a doctoral student in the chemistry department. She joined Professor Paul Russo's group and she is coadvised by Professor William Daly and Professor Ioan Negulescu. Her present investigations regard glylons, new polymers used along with classic nylons. During the doctoral studies she wants to do more by writing this master thesis as an intermediate step and a good practise for the doctoral thesis. As a graduate student Cornelia worked for the last two years as a teaching assistant in the Department of Chemistry. Cornelia is looking forward to obtaining the Master of Science degree from Louisiana State University in May 2010 and to step on to another challenging program for her degree of doctor of philosophy thesis.